

Nonperturbative renormalization group approach to frustrated magnets

B. Delamotte* and D. Mouhanna†

*Laboratoire de Physique Théorique et Hautes Energies,
CNRS UMR 7589 Universités Paris VI-Pierre et Marie Curie - Paris VII-Denis Diderot,
2 Place Jussieu, 75251 Paris Cedex 05, France.*

M. Tissier‡

*Laboratoire de Physique Théorique des Liquides, CNRS UMR 7600 Université
Paris VI-Pierre et Marie Curie, 4 Place Jussieu, 75252 Paris Cedex 05, France.*

(Dated: August 6, 2018)

This article is devoted to the study of the critical properties of classical XY and Heisenberg frustrated magnets in three dimensions. We first analyze the experimental and numerical situations. We show that the unusual behaviors encountered in these systems, typically *nonuniversal scaling*, are hardly compatible with the hypothesis of a second order phase transition. Moreover, the fact that the scaling laws are significantly violated and that the anomalous dimension is negative in many cases provides strong indications that the transitions in frustrated magnets are most probably of very weak first order. We then review the various perturbative and early nonperturbative approaches used to investigate these systems. We argue that none of them provides a completely satisfactory description of the three-dimensional critical behavior. We then recall the principles of the nonperturbative approach — the effective average action method — that we have used to investigate the physics of frustrated magnets. First, we recall the treatment of the unfrustrated — $O(N)$ — case with this method. This allows to introduce its technical aspects. Then, we show how this method unables to clarify most of the problems encountered in the previous theoretical descriptions of frustrated magnets. Firstly, we get an explanation of the long-standing mismatch between different perturbative approaches which consists in a nonperturbative mechanism of annihilation of fixed points between two and three dimensions. Secondly, we get a coherent picture of the physics of frustrated magnets in qualitative and (semi-) quantitative agreement with the numerical and experimental results. The central feature that emerges from our approach is the existence of scaling behaviors *without* fixed or pseudo-fixed point and that relies on a slowing-down of the renormalization group flow in a *whole* region in the coupling constants space. This phenomenon allows to explain the occurrence of *generic* weak first order behaviors and to understand the absence of universality in the critical behavior of frustrated magnets.

PACS numbers: 75.10.Hk,64.60.-i,11.10.Hi

*Electronic address: delamotte@lpthe.jussieu.fr

‡Electronic address: tissier@lptl.jussieu.fr

†Electronic address: mouhanna@lpthe.jussieu.fr

Contents

I. Introduction	3
II. The STA model and generalization	5
A. The lattice model, its continuum limit and symmetries	5
B. The Heisenberg case	6
C. The XY case	8
D. Generalization	8
III. Experimental and numerical situations	8
A. Preliminaries	8
B. The XY systems	9
1. The experimental situation	9
2. The numerical situation	10
3. Summary	11
4. Conclusion: five possible scenarios	12

C. The Heisenberg systems	12
1. The experimental situation	12
2. The numerical situation	13
3. Summary	14
4. Conclusion	14
D. The $N = 6$ STA	15
IV. A brief chronological survey of the theoretical approaches	15
V. The perturbative situation	16
A. The Nonlinear Sigma ($NL\sigma$) model approach	17
B. The Ginzburg-Landau-Wilson (GLW) model approach	19
1. The RG flow	19
2. The three and five-loop results in $d = 4 - \epsilon$	19
3. The improved three and five-loop results	19
4. The three-loop results in $d = 3$	20
5. The large- N results	20
6. The six-loop results in $d = 3$	20
7. Critical remarks	21
8. The six-loop results in $d = 3$ re-examined	21
C. Conclusion	22
VI. The Effective Average Action Method	22
A. Block spin in the continuum	22
B. The Polchinski equation	23
1. Derivative expansion	24
C. The effective average action method	25
1. Construction	25
2. The equation	27
3. Properties	27
4. Truncations	28
D. The $O(N)$ model	29
1. Definition of the coupling constants	29
2. The t -derivation	30
3. The renormalization group flow	31
4. The weak-coupling expansion around $d = 4$	33
5. The low-temperature expansion around $d = 2$	33
6. The large- N analysis	34
7. The critical exponents in three dimensions	34
8. The XY and multicritical Ising models in two dimensions	34
9. A difficulty related to the field expansion	35
E. Conclusion	35
VII. The $O(N) \times O(2)$ model	35
A. Truncation procedure	35
1. The spectrum	36
B. The flow equations	38
1. Definition of the coupling constants	38
2. The t -derivation and the flow equations	38
VIII. Tests of the method and first results	39
A. The weak-coupling expansion around $d = 4$	39
B. The low-temperature expansion around $d = 2$	39
C. The large- N expansion in $d = 3$	40
D. The determination of $N_c(d)$	40
E. The critical exponents for $N = 6$	41
F. Conclusion	41
IX. The physics in $d = 3$	41

A. The search of fixed points for $N < N_c(d)$	41
B. The physics in $d = 3$ just below $N_c(d)$: scaling with a pseudo-fixed point and minimum of the flow	41
C. Scaling with or without pseudo-fixed point: the Heisenberg and XY cases	42
D. The integration of the RG flow for Heisenberg and XY systems	43
1. Three difficulties	43
2. The Heisenberg case	44
3. The XY case	45
4. Comments	46
X. Possible tests of our scenario	46
XI. Consequences for perturbation theories	46
A. The $NL\sigma$ model approach	47
B. The GLW model approach vs the NPRG approach	48
XII. Conclusion and prospects	48
Acknowledgments	49
A. The positivity of the anomalous dimension	49
B. The invariants of the symmetry group	49
C. The threshold functions	50
1. Definitions	50
2. Substitution rules	51
3. Universal values of the threshold functions	52
4. Threshold functions from the θ cut-off	52
D. The minimum of the RG flow	52
E. The discontinuous character of the phase transition	53
References	54

I. INTRODUCTION

Understanding phase transitions and, specifically, critical phenomena has been one of the central issues of statistical mechanics during these last decades [1] and the field theoretical renormalization group (RG) approach to these phenomena has been one of the great successes of theoretical physics. This is so true that it is generally believed that, apart from specific problems — disordered and glassy systems for instance —, an almost complete understanding of the physics occurring at a phase transition has been reached. This is certainly due to the fact that it is indeed the case for all the systems belonging to the so-called Wilson-Fisher universality classes of d -dimensional systems whose symmetry breaking scheme is given by $O(N) \rightarrow O(N-1)$. In fact, although they have become the archetype of systems displaying critical phenomena well described by perturbative field theoretical approaches, these $O(N)$ symmetric systems turn out to be exceptions rather than the rule. For most systems a quantitative and, even sometimes, a qualitative description of the critical physics is either still lacking or very difficult to obtain by perturbative RG methods. This is

the case, for instance, in the Potts model [2, 3], in magnetic systems with disorder [4], in superconductors [5, 6], in Josephson junction arrays [7], in He_3 [8, 9], in smectic liquid crystals [10], in electroweak phase transitions [11, 12] and in frustrated magnets like helimagnets or geometrically frustrated magnets (triangular for instance) which are our main purpose in this article (see [13] for a review).

Actually, it should not be surprising that a qualitative difference exists between the critical behaviors of systems belonging to the $O(N)$ universality class and the others: among the systems where the order parameter has N real components, $O(N)$ corresponds to the maximal symmetry and, thus, to the simplest situation. Think, for instance, at a unit-norm constraint imposed on the microscopic degrees of freedom ($\vec{S}^2 = 1$): the maximal symmetry compatible with it is indeed $O(N)$. From a perturbative point of view, this means that the Ginzburg-Landau-Wilson (GLW) Hamiltonian of an $O(N)$ symmetric model involves only one (marginal) interaction term — $(\vec{\phi}^2)^2$ — and, thus, only one coupling constant. As a consequence, the perturbative RG flow of the critical theory takes place in a one-dimensional space of cou-

pling constant and is thus simple. In particular, only one nontrivial perturbative fixed point can exist [14]. On the contrary, the Hamiltonian of systems having a N -dimensional order parameter and displaying a symmetry group G smaller than $O(N)$ involves also terms that *explicitly* break $O(N)$. It thus contains several interaction terms and, therefore, several coupling constants. The RG flow then takes place in a multi-dimensional space and is thus far less simple: it can, in particular, involve fluctuation-induced first order transitions — runaway in a region of instability — and several fixed points with different symmetries. Universality itself is not guaranteed in these systems since the basins of attraction of the fixed points can be highly nontrivial.

Of particular interest for us, it is generically observed in these systems that, by varying N and/or d , the critical physics changes qualitatively: low dimensions ($d \rightarrow 2$) and large number of spin components ($N \rightarrow \infty$) favor smooth fluctuations and, thus, second order phase transitions, while larger dimensions ($d \rightarrow 4$) and small N ($N \sim 1$) favor larger fluctuations and thus first order transitions [206]. Therefore, in many systems — and notably in frustrated systems — the critical behavior changes qualitatively *i)* for the physically interesting values of N — $N \sim 1$ — when the dimension varies between $d = 2$ and $d = 4$ *ii)* at fixed dimension when the number N of components varies between $N = \infty$ and $N \sim 1$. Thus, the different perturbative approaches are in the worst possible position: it is quite difficult to obtain definite conclusions in $d = 3$ and for $N \sim 1$ from extrapolations of perturbative results even if they are valid in the domains where they have been established: $d = 2$ for the Nonlinear Sigma (NL σ) model, $d = 4$ for the GLW model and for large N in a $1/N$ expansion. This is one of the reasons why, after more than twenty five years of considerable efforts, the situation is still not clear for most three-dimensional systems that do not belong to the $O(N)/O(N - 1)$ universality classes.

Let us now discuss two concrete problems encountered in the perturbative RG studies performed on the three-dimensional systems we are interested in. First, the computational difficulties encountered in perturbation theory are non negligible. Within the NL σ model approach, the series are generally considered as useless due to the lack of Borel-summability (see however [15]). Within the GLW approach, the perturbative computations almost always call for resummation procedures. In general, these procedures are not as easy as they are in the $O(N)/O(N - 1)$ models. The series are either not proven to be Borel summable or are even suspected to be non Borel summable. This is the root of a lot of difficulties encountered in this approach (see [16, 17, 18, 19, 20, 21, 22]; for a review in the case of the diluted Ising model, see [23], for the presence of non analyticities in perturbative series, see [24, 25, 26, 27] and, for a general review, see [28]). The second point is more conceptual: although it is generically possible to perform a perturbative expansion of the critical theory around $d = 2$ — within the

NL σ model approach — and around $d = 4$ — within the GLW approach — it has not been possible to relate these two expansions within the usual field theoretical approach (except for large enough N where the $1/N$ expansion allows to recover, at leading orders, the perturbative results obtained in the NL σ and GLW approaches). From this point of view, even high-order perturbative calculations performed in the GLW model do not help since the perturbative expansion cannot be extrapolated down to $d = 2$ for $N \geq 2$. For instance, the critical exponent ν diverges in $d = 2$ when it is calculated as a power series in $\epsilon = 4 - d$. This fact, which is not crucial for systems whose critical behavior does not change qualitatively between $d = 2$ and $d = 4$ (e.g. the $O(N)/O(N - 1)$ models) forbids for the others to obtain a completely coherent picture of the physics between $d = 2$ and $d = 4$. Most of the time one of the perturbative approach — usually the NL σ one — is dismissed without real justifications and the other is blindly trusted. Since all the RG equations are smooth in N and d , it is not clear if and also, why, this procedure is legitimate. It would, of course, be much more satisfactory to have a unified approach not linked to a particular value of d or N and that allows to interpolate between both approaches.

All these drawbacks of the usual perturbative RG methods call for a nonperturbative approach. Such an approach is, in fact, already known and its foundations go back to Kadanoff and Wilson with the idea of block spin and effective, scale-dependent theory [1, 29]. It is sometimes called the exact renormalization group method but we prefer to call it the nonperturbative renormalization group (NPRG) method (for contributions of different authors to the early attempts to use NPRG, see [30, 31, 32, 33], for an exhaustive bibliography of the subject, see [34]). This idea has been turned into an efficient computational tool during the last ten years, mainly by Ellwanger [35, 36, 37, 38, 39], Morris [40, 41] and Wetterich [42, 43, 44, 45]. It has allowed to determine the critical exponents of the $O(N)$ models with high precision without having recourse to resummation techniques [45, 46, 47, 48, 49, 50]. It has also allowed, for the first time [51], to relate, for any N , the results of the $O(N)/O(N - 1)$ model obtained near $d = 4$ and $d = 2$, a fact of major importance for our purpose. Also important for the present purpose, it has allowed to tackle with genuinely nonperturbative situations. For instance, the Berezinskii-Kosterlitz-Thouless phase transition [52, 53] has been recovered directly from a study of the GLW model, *i.e.* *without* introducing explicitly the vortices [54, 55]. To cite just a few other successes of this method, let us mention low-energy Quantum Chromodynamics [45], the abelian Higgs model relevant for superconductivity [56], the study of the Gross-Neveu model in three dimensions [57, 58], phase transitions in He₃ [59], the study of cubic anisotropy in all dimensions as well as the randomly diluted Ising model [60], the two-dimensional Ising multicritical points [61], etc.

In this article, we study by means of NPRG methods

one of the most famous systems exhibiting the changes of critical behavior previously described: it is the system consisting of XY or Heisenberg spins on the triangular lattice (stacked triangular in $d = 3$) with antiferromagnetic nearest neighbor interaction (Section II). This system is the archetype of frustrated spin systems and is supposed to be in the same universality class as another set of frustrated magnets: the helimagnets. Almost all these systems have been intensively studied both numerically and experimentally these last twenty five years (see Section III). However, their behavior remains unclear and displays quite unconventional features. For instance, almost all experiments exhibit scaling laws around the transition temperature — which suggests a second order phase transition — but with critical exponents that depend on the particular material studied, on microscopic details, etc, which is incompatible with the standard phenomenology of a second order phase transition. In some experiments or numerical simulations, the scaling laws are sometimes significantly violated while the anomalous dimension η is found negative, a fact forbidden by first principles if the theory is ϕ^4 GLW-like (see the following). The theoretical situation in these systems is also not clear from the perturbative point of view (Sections IV and V): first, independently of the experimental context, the results obtained within the usual perturbative approaches — in dimensions $d = 2 + \epsilon$ and $d = 4 - \epsilon$ — conflict. Second, neither the low-temperature expansion around $d = 2$ nor high-order weak-coupling calculations performed around $d = 4$ or directly in $d = 3$ succeed in reproducing satisfactorily the phenomenology. We show, in this article, that the NPRG approach (Section VI) to frustrated systems (Section VII) clarifies almost entirely the situation. First, it allows to smoothly interpolate between $d = 2$ and $d = 4$ and to clarify the mismatch between these approaches. In particular, a mechanism of annihilation of fixed points, already identified for a long time around $4 - \epsilon$ dimensions for $N \sim 21.8$ is shown to operate around two dimensions for $N \sim 3$ *nonperturbatively* with respect to the low-temperature approach of the $N\mathbb{L}\sigma$ model [62, 63]. This explains the irrelevance in $d = 3$ of the $O(4)$ fixed point obtained within a low-temperature approach in $d = 2 + \epsilon$. Second, our approach provides a description of the physics in $d = 3$, in terms of weakly first order behaviors, compatible with the phenomenology (Sections VIII and IX). In this respect, an important feature of our work is that it explains the occurrence of scaling in frustrated magnets *without* fixed or pseudo-fixed [64, 65, 66] point. This phenomenon relies on a slowing-down of the RG flow in a whole region in coupling constants space. This allows to explain one of the most puzzling aspect of the critical physics of these systems, *i.e.* the occurrence of scaling *without* universality. We discuss (Section X) possible experimental and numerical tests of our scenario. We then comment (Section XI) the consequences of our work for the perturbative approaches that have been used to investigate the physics of frustrated magnets. Finally, we give our conclusions

(Section XII).

II. THE STA MODEL AND GENERALIZATION

A. The lattice model, its continuum limit and symmetries

We now describe the archetype of frustrated spin systems, the Stacked Triangular Antiferromagnets (STA). This system is composed of two-dimensional triangular lattices which are piled-up in the third direction. At each lattice site, there is a magnetic ion whose spin is described by a classical vector. The interaction between the spins is given by the usual lattice Hamiltonian:

$$H = \sum_{\langle ij \rangle} J_{ij} \vec{S}_i \cdot \vec{S}_j \quad (1)$$

where, depending on the anisotropies, the \vec{S}_i are two or three-component vectors and the sum runs on all pairs of nearest neighbor spins. The coupling constants J_{ij} equals J_{\perp} for a pair of sites inside a plane and J_{\parallel} between planes.

The interactions between nearest neighbor spins within a plane is antiferromagnetic, *i.e.* $J_{\perp} > 0$. This induces frustration in the system and, in the ground state, gives rise to the famous 120° structure of the spins, see Fig. 1a. This nontrivial magnetic structure is invariant

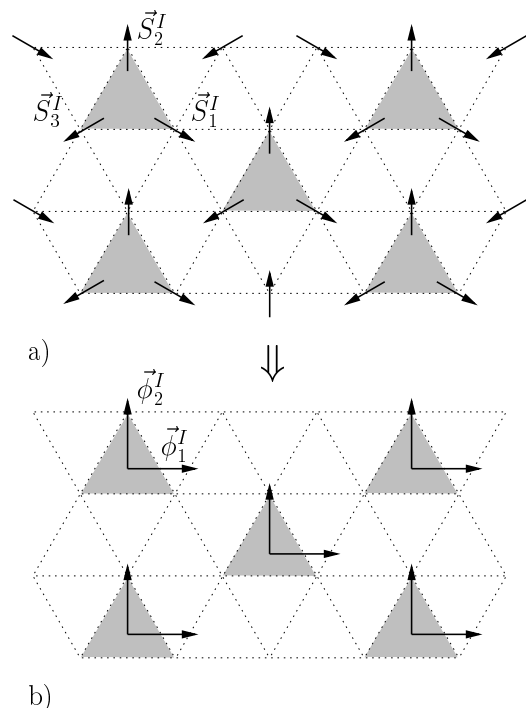


FIG. 1: The ground state configurations a) of the spins on the triangular lattice and b) of the order parameter made of two orthonormal vectors. The plaquettes, which constitute the magnetic cell, are indexed by I and are shaded.

under translations of length $\sqrt{3}$ times the initial lattice spacing. The magnetic cell, indexed by I , which is replicated all over the system, is a plaquette of three spins \vec{S}_1^I , \vec{S}_2^I and \vec{S}_3^I , see Fig. 1a.

Note that the nearest-neighbor out-of-plane interaction J_{\parallel} is, depending on the compounds, ferro- or antiferromagnetic, but the two cases can be treated simultaneously since no extra frustration appears through this interaction. Finally, interactions between more distant spins (next-to-nearest neighbors, etc) also exist but are neglected in the following since they are supposed to be irrelevant.

There have been numerous derivations of the long distance effective field theory supposed to describe the critical physics of this system [67, 68, 69, 70]. We here sketch the derivation which is the most appropriate for our purpose. The Hamiltonian (1) has the usual rotational symmetry acting on the spin components: $O(2)$ or $O(3)$ for XY or Heisenberg spins, respectively. To identify the order parameter, it is also necessary to consider the symmetry of the magnetic cell. For the triangular lattice, this is the C_{3v} group that interchanges the spins inside a plaquette [207].

The identification of the order parameter is close in spirit to what is done in the nonfrustrated case, *e.g.* for the antiferromagnets on a square lattice. At zero temperature, the sum of the three spins for a given plaquette I :

$$\vec{\Sigma}^I = \vec{S}_1^I + \vec{S}_2^I + \vec{S}_3^I \quad (2)$$

is vanishing (Let us note that $\vec{\Sigma}^I$ is analogous to the local magnetization of nonfrustrated antiferromagnets — $\vec{\Sigma}^I = \vec{S}_1^I + \vec{S}_2^I$ in this last case — that also vanishes in the ground state). In average, this is also the case at any finite temperature so that the thermal average of:

$$\vec{\Sigma} = \sum_I \vec{\Sigma}^I, \quad (3)$$

where the sum runs on all plaquettes, cannot be an order parameter: the associated modes are never critical. We therefore replace $\vec{\Sigma}^I$ by its average value:

$$\vec{\Sigma}^I \rightarrow \langle \vec{\Sigma}^I \rangle = \vec{0} \quad (4)$$

which is equivalent to freezing the fluctuations of the spins inside each plaquette. The constraint $\vec{\Sigma}^I = \vec{0}$ is called the “local rigidity constraint”. Having eliminated $\vec{\Sigma}$, we keep only two vectors per plaquette ($\vec{\phi}_1^I, \vec{\phi}_2^I$) which represent the local order parameter. For $\vec{\phi}_2^I$, we choose one of the spins of the plaquette, see Figs. 1a and b. For the other, $\vec{\phi}_1^I$, we choose the linear combination of the spins which is orthogonal to $\vec{\phi}_2^I$ and of unit norm, see Fig. 1b. The local order parameter thus obeys on each plaquette:

$$\vec{\phi}_i^I \cdot \vec{\phi}_j^I = \delta_{ij} \quad \text{with} \quad i, j \in \{1, 2\}. \quad (5)$$

The dihedral ($\vec{\phi}_1^I, \vec{\phi}_2^I$) plays a role analogous to the staggered magnetization in the nonfrustrated case.

As usual, once the model is reformulated in terms of its order parameter, the effective interaction — from plaquette to plaquette — becomes ferromagnetic, see Fig. 1b. By taking the dihedral ($\vec{\phi}_1^I, \vec{\phi}_2^I$) on the center of the plaquette I , we indeed find that it interacts ferromagnetically with the dihedral ($\vec{\phi}_1^J, \vec{\phi}_2^J$) defined on the center of the plaquette J — the plaquettes I and J being nearest neighbours — such that $\vec{\phi}_1^I$ interacts only with $\vec{\phi}_1^J$ and $\vec{\phi}_2^I$ only with $\vec{\phi}_2^J$. A more detailed analysis shows that the two vectors $\vec{\phi}_1^I$ and $\vec{\phi}_2^I$ play symmetric roles [68]. As a consequence, the effective Hamiltonian reads:

$$H = -J \sum_{\langle I, J \rangle} \left(\vec{\phi}_1^I \cdot \vec{\phi}_1^J + \vec{\phi}_2^I \cdot \vec{\phi}_2^J \right) \quad (6)$$

with the same coupling constant $J > 0$ for the $\vec{\phi}_1^I$'s and for the $\vec{\phi}_2^I$'s. Moreover, since the anisotropies resulting from the stacked structure of the lattice are supposed to be irrelevant, we take the same coupling constant for the interactions inside a plane and between the planes. The continuum limit is now trivial and proceeds as in the usual ferromagnetic case. The effective Hamiltonian in the continuum thus writes, up to constants:

$$H = - \int d^d \mathbf{x} \left((\partial \vec{\phi}_1(\mathbf{x}))^2 + (\partial \vec{\phi}_2(\mathbf{x}))^2 \right) \quad (7)$$

with the constraint that $\vec{\phi}_1$ and $\vec{\phi}_2$ are orthonormal. This model is called the Stiefel $V_{N,2}$ model with $N = 2$ in the XY case and $N = 3$ in the Heisenberg case. In $V_{N,2}$ the index 2 means that we are considering *two* orthonormal vectors $\vec{\phi}_1$ and $\vec{\phi}_2$.

It is convenient to gather the vectors $\vec{\phi}_1$ and $\vec{\phi}_2$ into a rectangular matrix:

$$\Phi = (\vec{\phi}_1, \vec{\phi}_2) \quad (8)$$

and to rewrite H as:

$$H = - \int d^d \mathbf{x} \text{Tr} (\partial^t \Phi(\mathbf{x}) \cdot \partial \Phi(\mathbf{x})) \quad (9)$$

where $({}^t \Phi)_{ij} = \Phi_{ji}$.

In the following two sections, we consider successively the case of Heisenberg and XY spins.

B. The Heisenberg case

In this case, H is invariant under the usual left $O(3)$ rotation and inversion group acting on the spins:

$$\Phi' = R\Phi, \quad R \in O(3). \quad (10)$$

It is also invariant under a right $O(2)$:

$$\Phi' = \Phi U, \quad U \in O(2). \quad (11)$$

This last symmetry encodes the fact that $\vec{\phi}_1$ and $\vec{\phi}_2$ play the same role which, itself, is reminiscent of the C_{3v} symmetry of the triangular plaquette. The system is thus symmetric under $G = O(3) \times O(2)$. In the low-temperature phase, a typical ground state configuration is given by (see Fig. 1b):

$$\Phi_0 \propto \begin{pmatrix} 1 & 0 \\ 0 & 1 \\ 0 & 0 \end{pmatrix}. \quad (12)$$

It is symmetric under the diagonal group — $O(2)_{\text{diag}}$ — built from the right $O(2)$ and from a particular left $O(2)$ in $O(3)$:

$$\Phi_0 = \begin{pmatrix} \epsilon \cos \theta & -\sin \theta & 0 \\ \epsilon \sin \theta & \cos \theta & 0 \\ 0 & 0 & 1 \end{pmatrix} \Phi_0 \begin{pmatrix} \epsilon \cos \theta & \epsilon \sin \theta \\ -\sin \theta & \cos \theta \end{pmatrix} \quad (13)$$

where $\epsilon = \pm 1$ encodes the \mathbb{Z}_2 part of $O(2)_{\text{diag}}$. Apart from the previous \mathbb{Z}_2 contained in the $O(2)_{\text{diag}}$, another \mathbb{Z}_2 is also left unbroken. It is the combination of a \mathbb{Z}_2 included into the right $O(2)$ of G , Eq. (11), and of a rotation of π around the x -axis contained in the rotation group $SO(3)$ of G . Thus, G is spontaneously broken down to $H = \mathbb{Z}_2 \times O(2)_{\text{diag}}$. As a consequence, the symmetry breaking scheme reads:

$$G = O(3) \times O(2) \rightarrow H = \mathbb{Z}_2 \times O(2)_{\text{diag}} \quad (14)$$

which is often referred to, once all the \mathbb{Z}_2 groups have been cancelled, as the $SO(3) \times SO(2)/SO(2)$ model.

Here appears the main feature of frustrated magnets: the $SO(3)$ group is *fully* broken in the low-temperature phase whereas it is only broken down to $SO(2)$ in non-frustrated magnets. This has two important consequences that are at the very origin of the nontrivial critical behavior encountered in frustrated magnets.

First, there are three Goldstone modes in the broken phase instead of two in the nonfrustrated case. This implies a physics of spin waves different from that of the $O(3)/O(2)$ model. Second, the order parameter space $SO(3)$ having a nontrivial first homotopy group [71]:

$$\pi_1(SO(3)) = \mathbb{Z}_2 \quad (15)$$

there exist stable nontrivial topological configurations called vortices. Because of the \mathbb{Z}_2 homotopy group, only one kind of vortex exists, contrarily to the well-known case of XY ferromagnets where there are infinitely many different kinds of vortices, each one being indexed by an integer, the winding number.

It has been established firstly by Kawamura and Miyashita [72] that the existence of vortices is important at finite temperature in two dimensions. This has been largely confirmed by subsequent works studying the temperature dependence of thermodynamical quantities such as the correlation length, the spin-stiffness, etc [73, 74, 75, 76, 77, 78]. Actually, although this has not

been directly established, they certainly also play an important role for the critical physics of the STA in three dimensions. A simple argument allows to argue to that end: let us go back on the lattice and introduce, on each plaquette I , together with $\vec{\phi}_1^I$ and $\vec{\phi}_2^I$, a third vector $\vec{\phi}_3^I$ defined by:

$$\vec{\phi}_3^I = \vec{\phi}_1^I \wedge \vec{\phi}_2^I. \quad (16)$$

Let us then gather them into a 3×3 matrix:

$$\Phi^I = \begin{pmatrix} \vec{\phi}_1^I \\ \vec{\phi}_2^I \\ \vec{\phi}_3^I \end{pmatrix}. \quad (17)$$

Since $(\vec{\phi}_1^I, \vec{\phi}_2^I, \vec{\phi}_3^I)$ are three orthonormal vectors, one has ${}^t\Phi^I \Phi^I = \mathbb{1}$ and, therefore, Φ^I is a $SO(3)$ matrix. This allows to rewrite the Hamiltonian (6) on the lattice as:

$$H = - \sum_{\langle I, J \rangle} \text{Tr} (\mathcal{P} {}^t\Phi^I \cdot \Phi^J) \quad (18)$$

where \mathcal{P} is a diagonal matrix of coupling constants that characterizes the interaction between the $\vec{\phi}_1^I$'s, between the $\vec{\phi}_2^I$'s and between the $\vec{\phi}_3^I$'s. One deduces from the microscopic derivation that $\mathcal{P} = \text{diag}(J, J, 0)$, *i.e.* that the interaction is the same between the $\vec{\phi}_1^I$'s and between the $\vec{\phi}_2^I$'s and that there is no interaction between the $\vec{\phi}_3^I$'s. However, for the present purpose, we consider, without loss of generality, the case where the interaction is nonvanishing and identical between all vectors. One thus has $\mathcal{P} = J\mathbb{1}$. Now, we use the decomposition of a rotation matrix Φ^I of $SO(3)$ in terms of a four-component *unit* vector $\widetilde{S}^I = (S_0^I, S_1^I, S_2^I, S_3^I)$:

$$\Phi_{kl}^I = 2 \left(S_k^I S_l^I - \frac{1}{4} \delta_{kl} \right) + 2\epsilon_{klm} S_0^I S_m^I + 2 \left(S_0^{I^2} - \frac{1}{4} \right) \delta_{kl}. \quad (19)$$

In terms of the vector \widetilde{S}^I , the Hamiltonian (18) writes:

$$H = -4J \sum_{\langle I, J \rangle} \left(\widetilde{S}^I \cdot \widetilde{S}^J \right)^2 \quad (20)$$

which is the Hamiltonian for *four*-component nonfrustrated spins with a particularity that each vector \widetilde{S}^I appears quadratically. Therefore, the Hamiltonian (20) is invariant under a global $O(4)$ group and under a *local* — gauge — \mathbb{Z}_2 group that changes \widetilde{S}^I to $-\widetilde{S}^I$. It corresponds to the $RP^3 = SO(4)/(SO(3) \times \mathbb{Z}_2)$ model. Note that, had we kept the microscopical coupling constants: $\mathcal{P} = \text{diag}(J, J, 0)$, the Hamiltonian (20) would be supplemented by terms breaking the $SO(4)$ global symmetry and leaving untouched the \mathbb{Z}_2 local symmetry which is the important point for our purpose (see [78] for details). For three-component spins, an analogous Hamiltonian — the RP^2 model — had been introduced by Maier and Saupé [79] and by Lebwohl and Lasher [80] to investigate the isotropic-nematic transition in liquid crystals. An extensive study of the RP^2 model, as well as a detailed

investigation of the role of vortices in this transition, has been performed by Lammert *et al.* [81, 82]. These authors have shown, in particular, that these nontrivial topological configurations favor the first order character of the transition. In the case of four-component spins, no such detailed analysis has been performed. However, the $RP^N = SO(N)/(SO(N-1) \times \mathbb{Z}_2)$ models that generalizes Hamiltonian (20) to N -component spins have been numerically studied in [83] for $2 \leq N \leq 4$. These systems have been shown to undergo a first order phase transition. Since the only difference between the RP^N and the $O(N)/O(N-1)$ — or, equivalently, $SO(N)/SO(N-1)$ — models lies in their topological properties, one is naturally led to attribute the origin of the first order character of the phase transition in the RP^N models to the \mathbb{Z}_2 vortices. Finally, since the Hamiltonian (18), relevant to STA, can be mapped onto the Hamiltonian (20) — up to the $O(4)$ -breaking terms — one can expect that the topological configurations also favor first order phase transitions in frustrated magnets in three dimensions.

C. The XY case

In the XY case, the Hamiltonian (9) is still invariant under a right $O(2)$ group, see Eq. (11), while the left symmetry group becomes $O(2)$. In the low-temperature phase, the rotational symmetry is broken and, since the spins are constrained to be in a plane, the permutation symmetry between $\vec{\phi}_1$ and $\vec{\phi}_2$ is also broken. As a consequence, the symmetry breaking scheme is:

$$G = O(2) \times O(2) \rightarrow H = O(2)_{\text{diag}}. \quad (21)$$

This symmetry-breaking scheme is usually referred to as $SO(2) \times \mathbb{Z}_2 \rightarrow \mathbb{1}$. The \mathbb{Z}_2 degrees of freedom are known as chirality variables [70, 72, 84, 85].

In this case, there also exist topological defects since:

$$\pi_1(SO(2)) = \mathbb{Z}. \quad (22)$$

These defects are identical to those of the ferromagnetic XY model that drive the famous Berezinskii-Kosterlitz-Thouless transition in two dimensions [52, 53]. However, in the frustrated case, they very likely interact non trivially with the chirality degrees of freedom which are critical in $d = 3$ at the same temperature as the spin wave degrees of freedom. This is apparent from the fact that one observes a unique phase transition and not two distinct Ising-like and XY-like transitions [86]. As a consequence, one can expect, in the frustrated case, a physics different and probably more complicated than in the non-frustrated $O(2)$ model that undergoes a standard second order phase transition in three dimensions.

D. Generalization

For reasons that will become clear, we consider the generalization of Hamiltonian (1) to N -component spins. It

is straightforward to extend the previous considerations to this case. One finds the symmetry breaking scheme:

$$G = O(N) \times O(2) \rightarrow H = O(N-2) \times O(2)_{\text{diag}}. \quad (23)$$

In the following, we shall drop the “diag” index for simplicity. Note that the previous Heisenberg and XY cases are recovered trivially provided that we identify $O(0)$ with the trivial group $\mathbb{1}$ and $O(1)$ with \mathbb{Z}_2 .

We now give a review of the experimental and numerical results for both the XY and Heisenberg systems. We will argue that a critical analysis of these results is crucial to understand that, up to now, the critical behavior of these systems is still unexplained.

III. EXPERIMENTAL AND NUMERICAL SITUATIONS

A. Preliminaries

In this section, we analyze the experimental and numerical results relevant to the physics of frustrated magnets. Our aim is to show that these data are hardly compatible with a second order phase transition since, in particular, they show that frustrated magnets display scaling *without* universality. Moreover, we show that there are even some direct indications for weak first order behaviors in these systems. We recall that a phase transition is said to be weakly of first order when, at the transition, the jump of the order parameter is small and the correlation length is large. Thus, scaling behaviors can be observed on a large range of temperatures so that these transitions look like second order phase transitions except very close to the critical temperature where scaling aborts.

We emphasize that, by itself, the analysis of the experimental and numerical results would not be sufficient to firmly conclude on the first order nature of the transitions. It has to be seen as one of the pieces of the argumentation that, together with a theoretical analysis, will lead to a coherent picture of the critical physics of frustrated systems.

To perform this analysis we need, in our discussion, to compare experimental results among themselves, as well as with numerical and theoretical calculations. Let us explain how we extract average values and error bars out of a set of experimental determinations of critical exponents. In the experimental literature, only one error bar is quoted, which merges the systematic and statistical errors. Our first — minimal — hypothesis is that error bars have a purely statistical origin (no systematic error). Under this assumption, we can trivially compute the (weighted) average values of the exponents together with their error bars. This is the meaning of the numbers we give in the following when we deal with average values of the critical exponents. It is clear that this hypothesis is too simple to be realistic since the experimental systematic errors cannot be neglected. Thus, the values we

compute, especially the error bars, should be taken with caution. We however show in the course of this article that our conclusions are robust to a possible underestimation of the error bars in our calculations, see Section VB 7.

Let us also notice that a possible source of error in the estimation of the critical exponents themselves could be the existence of corrections to scaling that could bias all the results. As we now argue, we can however expect that these effects are not dramatic. Let us consider the well-documented case of the ferromagnetic Ising model in $d = 3$. Most of the time corrections to scaling are not considered in the determination of the critical exponents and the associated error bars. When they are taken into account, they induce a tiny change in the critical exponents, *i.e.* at most of few percents (see for instance [87] and [88] for a review). It is therefore reasonable to think that neglecting corrections to scaling induce an error of few percents on the critical exponents while this probably leads to largely underestimated error bars when those are announced to be of the order of 1% [208].

In the case of frustrated magnets, if we make the assumption that the corrections to scaling are comparable with those found in the ferromagnetic Ising model and bear in mind that the error bars quoted in the literature are of the order of 5 – 10% (see Tables I, II and IV), we are led to the conclusion that corrections to scaling are significant neither for the exponents nor for the error bars.

B. The XY systems

Let us first discuss the XY case since the experimental situation is richer than in the Heisenberg case. Also, the symptoms of the existence of a problem in the interpretation of the results are clearer than in this latter case for reasons that shall be explained in this article and particularly in Section IX.

1. The experimental situation

Two classes of materials are supposed to be described by the Hamiltonian (9). The first one is made of ABX_3 hexagonal perovskites — where A is an alkali metal, B a transition metal and X a halogen atom — which are physical realizations of XY STA. The most studied ones are $CsMnBr_3$, $CsCuCl_3$, $CsNiCl_3$ and $CsMnI_3$ (see [89] for a review and [90] for $RbMnBr_3$). We have excluded this material since the measurement of its specific heat presents a shoulderlike anomaly near T_c which renders the determination of α and β doubtful). The second one is made of rare earth helimagnets: Ho, Dy, Tb. For most materials, the transitions are found continuous but *not* with the same critical exponents. For $CsCuCl_3$, the transition is found to be weakly of first order, *i.e.* with small

discontinuities. The results are summarized in Tables I and II.

Compound	Ref.	α	β	γ	ν
$CsMnBr_3$	[86]		0.21(1)		
	[91]		0.24(2)		
	[92]		0.21(2)	1.01(8)	0.54(3)
	[93]		0.25(1)		
	[94]		0.22(2)		
	[95]	0.39(9)			
	[96]	0.40(5)			
	[97]	0.44(5)			1.10(5)
$CsNiCl_3$	[98]	0.37(8)			
	[98]	0.37(6)			
	[99]	0.342(5)			
	[100]		0.243 (5)		
$CsMnI_3$	[98]	0.34(6)			
$CsCuCl_3$	[101]		0.23-0.25(2)		
	[90]	0.35(5)	1 st order		

TABLE I: The critical exponents of the XY STA.

Compound	Ref.	α	β	γ	ν
Tb	[102]	0.20(3)			
	[103]		0.23(4)		
	[104]		0.21(2)		
	[105]				0.53
	[106]	1 st order			
Ho	[107]	0.27(2)			
	[95]	0.10-0.22			
	[108]		0.30(10)	1.24(15)	0.54(4)
	[108]		0.37(10)		
	[109]		0.39(3)		
	[110]		0.39(2)		
	[111]		0.39(4)		
	[112]		0.39(4)		
	[112]		0.41(4)		
	[113]			1.14(10)	0.57(4)
[114]		0.38(1)			
Dy	[115]		0.335(10)		
	[116]		$0.39^{+0.04}_{-0.02}$		
	[110]		0.38(2)		
	[109]		0.39(1)		
	[113]			1.05(7)	0.57(5)
	[117]	0.24(2)			

TABLE II: The critical exponents of the XY helimagnets.

We highlight four striking characteristics [118] of these data. Their consequences for the physics of frustrated magnets will be discussed in more details in the following.

i) There are two groups of incompatible exponents. In the following discussion, we mainly use the exponent β to analyze the results since, as seen in Tables I and II, it is by far the most precisely measured exponent. Clearly, there are two groups of materials, each of which being characterized by a set of exponents, β in particular.

In the first one — that we call group 1 — made up of:

$$\text{group 1 : CsMnBr}_3, \text{CsNiCl}_3, \text{CsMnI}_3, \text{Tb} \quad (24)$$

one has:

$$\beta \sim 0.237(4) . \quad (25)$$

Note that, as far as we know, there is no determination of the exponent β for CsMnI_3 that, being given its composition, has been included in the group 1 of materials. Anyway, our conclusions are not affected by this fact.

In the second — group 2 — made up of

$$\text{group 2 : Ho, Dy} \quad (26)$$

one has:

$$\beta \sim 0.389(7) . \quad (27)$$

These exponents are clearly incompatible. Actually, we find for the average exponents of CsMnBr_3 alone — the most and best studied material of group 1 —:

$$\beta = 0.228(6), \nu = 0.555(21), \alpha = 0.416(33), \gamma = 1.075(42) . \quad (28)$$

If we consider all the materials of group 1 (except Tb for which the results are not fully under control, but perhaps β) we find:

$$\beta = 0.237(4), \nu = 0.555(21), \alpha = 0.344(5), \gamma = 1.075(42) . \quad (29)$$

For materials of group 2 (Ho and Dy) we find:

$$\beta = 0.389(7), \nu = 0.558(25), \gamma = 1.10(5) . \quad (30)$$

We do not give a value for α which is poorly determined.

Let us indicate that the exponents vary much from compound to compound in group 1. Although less accurately determined than β , α is only marginally compatible between CsNiCl_3 and CsMnBr_3 . Note moreover that, even for the same material, the data are not fully compatible among themselves: β in CsMnBr_3 shows a somewhat too large dispersion.

ii) The anomalous dimension η is negative for group 1 which is impossible. If we assume that the transition is of second order for group 1, we can use the scaling relations to compute η . In particular, the precise determination of β allows to use $\eta = 2\beta/\nu - 1$ to determine rather accurately η . The exponent ν itself can be obtained directly from the experiments or deduced using the scaling relation:

$$\nu = (2 - \alpha)/3 . \quad (31)$$

The large number of experiments devoted to the determination of α allows a precise determination of ν . By using the scaling relation Eq. (31), we find $\nu = 0.528(11)$ if we consider the experimental results for CsMnBr_3 alone

and $\nu = 0.552(2)$ if we consider CsMnBr_3 , CsNiCl_3 and CsMnI_3 . By using the relation $\eta = 2\beta/\nu - 1$ together with Eq. (31) or the relation $\eta = 6\beta/(2 - \alpha) - 1$ and by considering the data of CsMnBr_3 alone or the data of the materials of group 1 (except Tb for which it is not sure that the data are reliable) we can obtain four determinations of η . In the four cases, we find η negative by at least 4.1 standard deviations and the probability to find it positive always less than 10^{-5} . In fact, the most precise determination is obtained by combining all the data of group 1, Eq. (29), and by using the relation $\eta = 6\beta/(2 - \alpha) - 1$. In this case, we obtain $\eta = -0.141(14)$ and thus a (almost) vanishing probability to find it positive. Note also that, although β and ν are less accurately known in Tb — for which experiments are anyway delicate —, η is also found negative.

However, we stress that η *cannot* be negative in a true second order phase transition. This is a general result, based on first principles of field theory, that η is always positive if the theory describing the transition is a unitary GLW ϕ^4 -like model [119] as it is the case here (see Appendix A).

iii) For group 2, the scaling relation $\gamma + 2\beta - 3\nu = 0$ is violated. From Eq. (30) it is possible to check the scaling relations. We find $\gamma + 2\beta - 3\nu = 0.202(92)$ and thus a violation by 2.2 standard deviations.

iv) CsCuCl_3 undergoes a weak first order phase transition. Until recently, CsCuCl_3 was believed to undergo a second order phase transition with exponents compatible with those of group 1, see Table I. It has been finally found to display a weak first order phase transition [90].

2. The numerical situation

Monte Carlo simulations have been performed on five different kinds of XY systems. The first one is the STA itself [120, 121, 122, 123, 124, 125, 126]. The second model is the STAR (where R stands for rigidity) which consists in a STA for which the local rigidity constraint — Eq. (4) — has been imposed on each plaquette at all temperatures [127]. The third model is the Stiefel $V_{2,2}$ model whose Hamiltonian is given by Eq. (6) [127, 128]. This is a hard spin, discretized version of the $NL\sigma$ model relevant to frustrated magnets. Note that, for this last model, the triangular structure is irrelevant since the interaction is ferromagnetic; a cubic lattice can be chosen. Also a soft spin, discretized version of the GLW model has recently been studied by Itakura [126] who also re-studied the STA model for large sizes. Finally, a helimagnetic system defined on a body-centered-tetragonal (BCT) lattice — the “BCT model” — has been investigated [129].

Here, we emphasize that the local rigidity constraint — Eq. (4) — as well as the manipulations that lead to the STAR, Stiefel $V_{2,2}$, GLW and BCT models only affect the *massive* — noncritical — modes. Thus, all the STA, STAR, Stiefel $V_{2,2}$, GLW and BCT models have the

same *critical* modes, the same symmetries and the same order parameter. Therefore, one could expect a common critical behavior for all these systems.

Let us comment the results of the simulations given in Table III. Note that, due to the its novel character, we shall comment the recent work of Itakura [126] separately.

System	Ref.	α	β	γ	ν	η
STA	[120, 123]	0.34(6)	0.253(10)	1.13(5)	0.54(2)	-0.09(8)
	[124]	0.46(10)	0.24(2)	1.03(4)	0.50(1)	-0.06(4)
	[125]	0.43(10)			0.48(2)	
STA	[126]	1 st order				
STAR	[127]	1 st order				
$V_{2,2}$	[127]	1 st order				
BCT	[129]	1 st order				
GLW	[126]	1 st order				

TABLE III: Monte Carlo critical exponents of XY systems. Note that the exponent η is computed from $\gamma/\nu = 2 - \eta$.

i) For STA, scaling laws are found with exponents compatible with those of group 1. Let us however notice that, similarly to what happens for the materials of group 1 there exists, in the numerical simulations of STA, a rather large dispersion of the results. For instance, the two extreme values of ν differ by 2.1 standard deviations.

Let us make two other remarks. First, the good agreement between the numerical results for STA and the experimental ones for materials of group 1 has been repeatedly interpreted in the literature as a proof of the existence of a second order transition and even as an evidence of the existence of the chiral fixed point of the GLW model [70]. We emphasize here that the fact that a Monte Carlo simulation reproduces experimental results only means that the Hamiltonian of the simulated system is a good approximation of the microscopic Hamiltonian describing the physics of real materials. However, this neither explains nor proves anything else — and *certainly not* the existence of a second order phase transition — since Monte Carlo simulations suffer from problems analogous to those encountered in experiments: a weakly first order phase transition is very difficult to identify and to distinguish from a second order one.

Let us now come to our second remark. In a beautiful experiment, Plakhty *et al.* [86] have measured the so-called chiral critical exponents β_c and γ_c [120] in CsMnBr_3 . They have found values compatible with those found numerically in STA [120]. Let us emphasize, again, that this agreement simply means that the parameters characterizing the numerical simulations are not too far from those associated to the experiments. By no means it implies — or gives a new indication of the existence of — a second order transition. Let us notice that β_c has also been measured in Ho [114]. The value found completely disagrees with the result found in STA and in CsMnBr_3 .

ii) The anomalous dimension η is negative for STA. As shown in [127], η is found negative using the two scaling

relations $\eta = 2\beta/\nu - 1$ and $\eta = 2 - \gamma/\nu$ for the two simulations where these calculations can be performed.

iii) The simulations performed on STAR, $V_{2,2}$ and BCT models give first order transitions. Therefore, the modifications in the microscopic details which change STA into STAR, $V_{2,2}$ and BCT affect drastically the scaling behavior.

iv) In a remarkable work, Itakura has recently performed Monte Carlo and Monte Carlo RG approaches of the STA and its GLW model version that has led to a clear first order behavior [126]. Itakura has performed standard Monte Carlo simulations of the STA involving sizes up to $126 \times 144 \times 126$ leading to clear first order transitions. In particular, for these lattice sizes, the double-peak of the probability distribution of the energy at the transition is clearly identified. Itakura has also used an improved Monte Carlo RG simulation of the STA and its GLW model version. One advantage of this approach compared with previous RG Monte Carlo studies is that it allows to reach the asymptotic critical behavior using systems of moderately large lattice sizes. Within this approach, Itakura has found several evidences for a first order behavior with, notably, a runaway behavior of the RG flow and the absence of any nontrivial fixed point.

3. Summary

We now summarize the results of our analysis of both experiments and numerical simulations for XY frustrated magnets.

1) Scaling laws are found in STA and helimagnetic materials on a rather wide range of temperature. This is also the case within all — but an important one [126] — numerical simulations of the STA.

2) There are two groups of systems that differ by their critical exponents. The first one includes the group 1 of materials and the numerical STA model. The second one corresponds to the group 2 of materials. One also observes variations of critical exponents inside a given group of exponents.

3) The anomalous dimension η is negative for the materials of group 1 and for the numerical STA model. This is very significant from the experimental results, less from the numerical ones.

4) For group 2, the scaling relations are violated by 2.2 standard deviations.

5) CsCuCl_3 is found to undergo a weak first order transition.

6) STAR, $V_{2,2}$ and BCT models undergo strong first order transitions.

7) Recent Monte Carlo and Monte Carlo RG approaches of STA and the soft spin discretized version of the GLW model give clear indications of first order behaviors.

4. Conclusion: five possible scenarios

Let us now propose five possible scenarios to explain the phenomenology of XY frustrated systems.

Scenario I.

This scenario is — together with the second one — the most often invoked: the critical behavior of frustrated magnets, when they display scaling, is controlled by a *unique* fixed point of the RG flow which is associated to a *new universality class* [67, 68, 70, 122, 123, 130]. Although, from point 1) above, XY frustrated magnets appear to display rather generic scaling behaviors, the examination of the experimental and numerical data provides clear indications against this first scenario. Indeed, from point 2), there is a manifest lack of universality in the scaling behavior of frustrated magnets. Also several points, from 3) to 7), strongly militate in favor of first order behaviors.

Scenario II.

In the second scenario, the two sets of exponents corresponding to groups 1 and 2 are, in fact, associated with two true second order phase transitions from which result two distinct universality classes. This scenario is ruled out by the fact — see point 3) — that the anomalous dimension η is negative for group 1 and for the numerical STA model. Thus, provided *i*) the quoted error bars in the literature are reliable, *ii*) our hypothesis of a purely statistical origin of the errors does not completely bias our analysis and *iii*) corrections to scaling do not alter drastically all the results, we are led to the conclusion that the behavior of the materials of group 1 and of the numerical STA model *cannot* be explained by the existence of a fixed point in the GLW model. In the simplest hypothesis, these systems must undergo first order phase transitions. This last hypothesis seems to be confirmed by several other facts. Firstly, CsCuCl₃, whose exponents are close to those of group 1 has been finally found to undergo first order phase transitions, see point 5) of the summary. Secondly, point 6), numerical models very close to STA — STAR, $V_{2,2}$ and BCT — also undergo first order phase transitions. Finally, the hypothesis of a first order phase transition for STA itself is corroborated by the fact, point 7), that recent Monte Carlo and Monte Carlo RG simulations of this system predict a first order phase transition [126].

Scenario III.

In the third scenario, materials of group 2 undergo a second order phase transition — η is found positive there — while those of group 1 as well as the numerical STA model all undergo weakly first order phase transitions. Within this scenario, the critical exponents of materials of group 1 should be considered as *effective* or *pseudo*-critical exponents, characterizing the *pseudo*-scaling observed, valid for temperatures far enough from the critical temperature. There is no direct and definitive argument against this scenario. Of course, violation of the scaling relations for materials of group 2, point 4), makes doubtful a second order behavior. However, this violation is

too small to definitely reject it. Actually, the drawback with this third scenario is its lack of naturalness. Indeed, it implies a very specific fine-tuning of the microscopical coupling constants — *i.e.* of the initial conditions of the RG flow — for materials of group 1. Their representative points in the coupling constant space must lie outside the basin of attraction of the fixed point governing the critical behavior of materials of group 2 but very close to its border so that the transitions are weakly of first order.

Scenario IV.

In the fourth scenario, all frustrated magnets undergo first order phase transitions that almost generically appear to be weak or very weak and are characterized by pseudo-scaling and pseudo-critical exponents. This fourth scenario, compared with the third one, could thus seem even more unnatural. This is true, but only within the usual explanation of weak first order phase transitions where the weakness of the first order transition is obtained by fine-tuning of parameters. Actually, we shall provide arguments in favor of the present scenario and shall show that the genericity of pseudo-scaling has, in fact, a natural explanation relying neither on the existence of a fixed point nor on a fine-tuning of parameters.

Scenario V.

Finally, one can imagine several variants of these scenarios. For instance, we have adopted the standard position that consists in associating a unique set of critical exponents to a fixed point. On the contrary, Calabrese *et al.* [131, 132] have suggested that a unique fixed point could lead to a whole spectrum of critical exponents. This scenario, which would explain the occurrence of a spreading of critical exponents in the experimental and numerical contexts, will be discussed in details in the following.

We now review the experimental and numerical results obtained for the Heisenberg systems.

C. The Heisenberg systems

1. The experimental situation

Contrarily to the XY case, there is no Heisenberg helimagnets (see however [67]). Therefore there remain, *a priori*, only the Heisenberg STA materials. In fact, the A/B phase transition of He₃ can be described by the same GLW Hamiltonian as the Heisenberg STA [8, 9]. It is thus a candidate. Unfortunately, the narrowness of the critical region of this transition does not allow a reliable study of the critical behavior of this system and there are no available data about it.

Three classes of Heisenberg STA materials have been studied. First, systems like VCl₂, VBr₂, Cu(HCOO)₂2CO(ND₂)₂2D₂O and Fe[S₂CN(C₂H₅)₂]₂Cl which are generically quasi-XY except in a particular range of temperature where their anisotropies are irrelevant. Second, those which become isotropic thanks to a magnetic field that exactly counterbalances the anisotropies. This is the case of CsNiCl₃ and CsMnI₃

at their multicritical point. Finally, those which become isotropic because they have been prepared in a fine-tuned stoichiometry such that the Ising-like and XY-like anisotropies cancel each other to form an isotropic material. This is the case of $\text{CsMn}(\text{Br}_{0.19}\text{I}_{0.81})_3$.

Let us comment the experimental results summarized in Table IV.

Compound	Ref.	α	β	γ	ν
VCl ₂	[133]		0.20(2)	1.05(3)	0.62(5)
VBr ₂	[134]	0.30(5)			
A	[135]		0.22(2)		
B	[87, 136, 137] [138]	0.244(5)	0.24(1)	1.16(3)	
CsNiCl ₃	[98, 139] [99] [100]	0.25(8) 0.23(4)	0.28(3)		
CsMnI ₃	[98]	0.28(6)			
C	[140] [141] [142]	0.23(7)	0.29(1) 0.28(2)	[0.75(4)]	[0.42(3)]

TABLE IV: The critical exponents of the Heisenberg STA. The abbreviations A, B and C stand for $\text{Cu}(\text{HCOO})_2\text{2CO}(\text{ND}_2)_2\text{2D}_2\text{O}$, $\text{Fe}[\text{S}_2\text{CN}(\text{C}_2\text{H}_5)_2]_2\text{Cl}$ and $\text{CsMn}(\text{Br}_{0.19}\text{I}_{0.81})_3$ respectively. The data in brackets are suspected to be incorrect. They are given for completeness.

i) As in the XY case, the Heisenberg materials fall into two groups. The group 1, made up of:

$$\begin{aligned} \text{group 1 : } & \text{Cu}(\text{HCOO})_2\text{2CO}(\text{ND}_2)_2\text{2D}_2\text{O}, \\ & \text{Fe}[\text{S}_2\text{CN}(\text{C}_2\text{H}_5)_2]_2\text{Cl}, \\ & \text{VCl}_2, \text{VBr}_2 \end{aligned} \quad (32)$$

is characterized by:

$$\beta = 0.230(8) \quad (33)$$

while for group 2, made up of:

$$\text{CsNiCl}_3, \text{CsMnI}_3, \text{CsMn}(\text{Br}_{0.19}, \text{I}_{0.81})_3 \quad (34)$$

one finds:

$$\beta = 0.287(8) . \quad (35)$$

Note that, strictly speaking, the values of β for VBr₂ and for CsMnI₃ are not known and, thus, our classification is somewhat improper. It seems however logical to suppose that VBr₂ is close to VCl₂ and CsMnI₃ close to CsNiCl₃. Anyway, it will be clear in the following that our analysis is almost insensitive to this point.

For group 1, the average values of the critical exponents are given by:

$$\beta = 0.230(8), \alpha = 0.272(35), \nu = 0.62(5), \gamma = 1.105(21) . \quad (36)$$

A very severe difficulty in the study of the materials of group 1 is their two-dimensional character and Ising-like

anisotropies. The temperature range where the systems behave effectively as three-dimensional Heisenberg systems is narrow. This is the case of VCl₂ where this range is less than two decades and where, closer to the critical temperature, the system becomes Ising-like. For this group of materials the exponent β is very small and the authors of [133] have noticed that such small values have also been found in materials where dimensional cross-over is suspected. Thus, it is not clear whether the whole set of results really corresponds to a three-dimensional Heisenberg STA.

For group 2, the experimental situation seems to be better under control. The average values of the critical exponents are given by:

$$\beta = 0.287(9), \alpha = 0.243(3), \nu = 0.585(9), \gamma = 1.181(33) \quad (37)$$

where the scaling relations have been used to compute ν and γ . Note that the values of ν and γ thus obtained differ significantly from those of $\text{CsMn}(\text{Br}_{0.19}\text{I}_{0.81})_3$ whose critical behavior has been claimed to be perturbed by disorder (see however [209]).

ii) For group 1, the anomalous dimension η is significantly negative. Using the two exponents that have been measured at least twice in group 1 — β and γ — we can compute the anomalous dimension from the scaling relation $\eta = (4\beta - \gamma)/(2\beta + \gamma)$. We find $\eta = -0.118(25)$ which is thus negative by 4.8 standard deviations.

iii) For group 2, the anomalous dimension η is marginally negative. Using the critical exponents given in Eq. (37), one obtains, for the anomalous dimension: $\eta = -0.018(33)$. Thus η is found negative but not significantly, contrarily to what happens in group 1.

iv) For group 1, the scaling relations $\gamma + 2\beta - 2 + \alpha = 0 = 2\beta + \gamma - 3\nu$ are violated. Indeed, $\gamma + 2\beta - 2 + \alpha = -0.135(56)$ and $2\beta + \gamma - 3\nu = -0.29(15)$. Of course, none of these violations is completely significant in itself because of the lack of experimental data. However, since they are both independently violated it remains only a very small probability that the scaling relations are actually satisfied.

2. The numerical situation

In the Heisenberg case, as in the XY case, five different kinds of systems: STA, STAR, Stiefel ($V_{3,2}$ in this case), BCT and GLW models have been studied. The results of the simulations are given in Table V.

Let us comment them. Again, we put aside the work of Itakura [126].

i) For the STA, scaling laws are found with an exponent β close to that of group 2. The average values for the exponents of STA are:

$$\beta = 0.288(6), \gamma = 1.185(3), \nu = 0.587(5) . \quad (38)$$

β is thus extremely close to the experimental value of group 2 while ν and γ are extremely close to the ex-

System	Ref.	α	β	γ	ν	η
STA	[120, 130]	0.240(80)	0.300(20)	1.170(70)	0.590(20)	0.020(180)
	[143]	0.242(24)	0.285(11)	1.185(3)	0.586(8)	-0.033(19)
	[144]	0.245(27)	0.289(15)	1.176(26)	0.585(9)	-0.011(14)
	[145]	0.230(30)	0.280(15)		0.590(10)	0.000(40)
	[146]				0.589(7)	
STA	[126]	1 st order				
STAR	[147]	0.488(30)	0.221(9)	1.074(29)	0.504(10)	-0.131(13)
V _{3,2}	[147]	0.479(24)	0.193(4)	1.136(23)	0.507(8)	-0.240(10)
	[128]	0.460(30)		1.100(100)	0.515(10)	-0.100(50)
V _{3,2}	[126]	1 st order				
BCT	[148]	0.287(30)	0.247(10)	1.217(32)	0.571(10)	-0.131(18)
GLW	[126]	1 st order				

TABLE V: Monte Carlo critical exponents of the Heisenberg systems. η is computed by $\gamma/\nu = 2 - \eta$ and, apart in [120] and [128], α is computed by $3\nu = 2 - \alpha$.

perimental values deduced from the scaling relations, Eq. (37). The scaling relation $\gamma + 2\beta - 3\nu = 0$ is very well verified since $\gamma + 2\beta - 3\nu = 10^{-4} \pm 6 \cdot 10^{-2}$.

ii) *For the STA, η is negative.* Using the values of β/ν and γ/ν obtained directly in the simulations, one can compute the average value of η : $-0.0182(89)$. The probability of it to be positive is 0.02 and is thus small although not vanishing.

iii) *For the STAR, V_{3,2} and BCT models, the values of β are all incompatible with that of STA (three standard deviations at least) and are all incompatible among each others.* This has been interpreted as an indication of very weak first order phase transitions [147]. This is to be compared with the XY case, where the transitions for STAR and the V_{2,2} model are strongly of first order.

iv) *For the BCT, STAR and V_{3,2} models, η is always found significantly negative,* see Table V where η has been calculated from γ/ν .

v) *The Monte Carlo and Monte Carlo RG approaches of the STA, V_{3,2} and GLW model performed by Itakura has led to clear first order behaviors* [126]. For Heisenberg STA, contrarily to the XY case, even for the largest lattice sizes — $84 \times 96 \times 84$ — the double-peak of the probability distribution of the energy is not observed. However, the V_{3,2} model displays a clear double-peak. Moreover, for the STA and the V_{3,2} model, the RG flow clearly does not exhibit any fixed point. Instead, a run-away of the RG flow toward the region of instability is found which indicates first order transitions. The transitions are thus — weakly — of first order. The transition is also weaker of first order for Heisenberg than for XY spins.

3. Summary

We now summarize the experimental and numerical situations for frustrated magnets with Heisenberg spins. Here, the experimental situation is much poorer than in the XY case and is still unclear on many aspects. On the

contrary, the numerical results are numerous and more precise than in the XY case.

1) Scaling laws are found in STA materials on a rather wide range of temperatures as well as in all Monte Carlo simulations — apart that based on Monte Carlo RG.

2) There are two groups of materials that do not have the same exponents. The exponent β of the numerical STA model agrees very well with that of group 2.

3) The anomalous dimension is manifestly negative for group 1 and marginally negative for group 2. For the numerical STA model, η is found negative although not completely significantly. For STAR, V_{3,2} and BCT, η is found significantly negative.

4) For group 1, the scaling relations are violated.

5) STAR, V_{3,2} and BCT exhibit scaling behaviors without universality. Also, the results are incompatible with that of the numerical STA model.

6) A Monte Carlo RG approach of the STA, V_{3,2} and GLW models has led to clear first order behaviors.

4. Conclusion

Let us now draw some conclusions about the Heisenberg case. The experimental and numerical data reveal the same problems as those encountered in the XY case: the different materials split into two groups, the anomalous dimension is found negative in many materials and in most numerical simulations, the scaling relations are violated in some materials and there is no universality in the exponents found in the simulations. The same kind of conclusion as in the XY case follows (see Section III B 4) : the first scenario, that of an explanation based on the existence of a unique fixed point appears unlikely. There are also signs of first order behaviors but less significantly than in the XY case. Thus, at this stage, it is impossible from the experimental and numerical data alone to discriminate between the different scenarios II, III, IV and V. It is therefore important to gain insight from the theoretical side.

Before discussing this, let us mention another interesting numerical result.

D. The $N = 6$ STA

Let us quote a simulation of the STA with six-component spins that has been performed by Loison *et al.* [22]. The results are given in Table VI. Six-component spins were chosen since it was expected that the transition was of second order. Loison *et al.* have clearly identified scaling laws at the transition with a positive anomalous dimension. Let us emphasize that, even if the transition is actually of first order, as suggested by the recent results of Calabrese *et al.* [132], it should be extremely weakly of first order — see the following. Thus, scaling laws should hold for all temperatures but those very close to T_c . In this respect, the exponents for $N = 6$ are therefore very trustable so that reproducing them is a challenge for the theoretical approaches.

System	α	β	γ	ν
$N = 6$ STA	-0.100(33)	0.359(14)	1.383(36)	0.700(11)

TABLE VI: Monte Carlo critical exponents for six-component spins in the STA system [22].

Note that using the results of Loison *et al.* and the relation $\eta = 2 - \gamma/\nu$, one finds $\eta = 0.025(20)$.

IV. A BRIEF CHRONOLOGICAL SURVEY OF THE THEORETICAL APPROACHES

Let us briefly review the most important theoretical developments concerning this subject.

The first microscopic derivation and RG study — at one- and two-loop order in $d = 4 - \epsilon$ — of the effective GLW model relevant for the STA — see below — was performed for He_3 by Jones *et al.* in 1976 [8] and by Bailin *et al.* in 1977 [9]. The model was re-derived and re-studied in the context of helimagnets (for general N) by several groups including Bak *et al.* (1976) [149], Garel and Pfeuty (1976) [67] and Barak and Walker (1982) [150]. It was established at that time that, around $d = 4$, the transitions for Heisenberg spin systems had to be of first order. More precisely, these authors found that there exists a critical value $N_c(d)$ of the number N of spin components above which the transition is of second order and below which it is of first order. They found [8, 9] :

$$\begin{aligned}
 N_c(d = 4 - \epsilon) &= 4(3 + \sqrt{6}) - 4 \left(3 + \frac{7}{\sqrt{6}} \right) \epsilon + O(\epsilon^2) \\
 &\sim 21.8 - 23.4\epsilon + O(\epsilon^2)
 \end{aligned}
 \tag{39}$$

with $\epsilon = 4 - d$. A first large- N expansion was also studied, in particular for $d = 3$, by Bailin *et al.* in 1977 [9].

A group theoretical derivation of the GLW model relevant to the XY STA was performed by Yosefin and Domany [68] in 1985. They found the same Hamiltonian as for helimagnets. Between 1985 and 1988 Kawamura [70, 122, 123, 130] have performed this analysis for N -component STA. He has shown that the Hamiltonian is the same as for He_3 or helimagnets, the RG analysis giving obviously the same results. This author has also extrapolated the two-loop result for $N_c(d)$ of Eq. (39) in $d = 3$ and found $N_c(d = 3) < 2$. This led him to conjecture the existence of a second order phase transition for frustrated magnets associated with a new universality class. However, as well-known, this direct extrapolation cannot be reliable since it is notorious that the perturbative series must be resummed.

In 1988, Dombre and Read [69] derived, in the quantum case, the Nonlinear Sigma ($\text{NL}\sigma$) model relevant to frustrated magnets. In 1990, Azaria *et al.* studied the classical version of this $\text{NL}\sigma$ model around $d = 2$. They found a fixed point of the RG flow in a two-loop calculation for any $N \geq 3$ [151]. For $N = 3$, they found the phenomenon of enlarged symmetry: at the fixed point the symmetry becomes $SO(3) \times SO(3) \sim SO(4)$ instead of $SO(3) \times SO(2)$. Thus, their conclusion was that, if the transition is of second order, it is characterized by $O(4)/O(3)$ critical exponents — at least for ν . Another possibility proposed by these authors was that the transition could be also mean-field tricritical or of first order. However, *none* of the experimental or numerical results are compatible with the $O(4)/O(3)$ or mean-field tricritical exponents. Note finally that these authors supposed that, if tricritical, the behavior at the transition should be mean-field tricritical in $d = 3$, something which is mandatory only for $O(N)/O(N - 1)$ models, but not for more complex models.

The first nonperturbative approach to frustrated magnets was performed by Zumbach in 1993 [64, 65, 66]. He wrote down the NPRG equations for the GLW models suited to the description of these systems. He studied them within the Local Potential Approximation (LPA) of the Wilson-Polchinski equation — analogous to the Wegner-Houghton approximation [30] — and found $N_c(d = 3) \sim 4.7$. Since he found no fixed point for $N = 2$ and $N = 3$ he claimed that the transition is of first order in these cases. In the case $N = 3$, there is a minimum in the RG flow, a pseudo-fixed point, that fakes a true fixed point (see below for details). The transition was thus conjectured to be *weakly* of first order with pseudo-scaling characterized by pseudo-critical exponents. Note that, within the LPA, all derivative terms in the Hamiltonian are neglected so that the anomalous dimension is vanishing. This has two important consequences. First, the pseudo-critical exponents found by Zumbach were not very reliable and thus difficult to compare with the experimental and numerical results. Second, this approach neglects terms — the so-called current-term (see below) — that are fundamental within the perturbative approach of the $\text{NL}\sigma$ model performed around two di-

mensions. Thus, within Zumbach's approach, it was *not* possible to match with these results. Finally note that, in the $N = 2$ case, *no* minimum in the RG flow was found and, thus, no pseudo-critical exponent was obtained, in contradiction with the scaling behaviors observed in the experimental and numerical contexts.

Then, three-loop calculations have been performed by Antonenko *et al.* in 1994 and 1995 on the GLW model. In $d = 3$ this has led, after Padé-Borel resummation, to $N_c(d = 3) = 3.91$ [152]. In $d = 4 - \epsilon$, they have determined the three-loop contribution $-7.1 \epsilon^2$ to $N_c(d = 4 - \epsilon)$, see Eq. (39). This has led to $N_c(d = 3) = 3.39$ [153]. These authors have mentioned that, contrarily to the $O(N)$ models, their three-loop results were not well converged.

In 1996, Jolicœur and David studied a generalization of the Stiefel model that involves N vectors with N components [154]. They showed within a mean field approximation and a one-loop calculation performed in $d = 2 + \epsilon$ that a first order line should appear in a nontrivial dimension above two. It should isolate the chiral fixed point in the metastability region in such a way that this point should no longer play any role. Above this dimension, the transition should therefore be of first order.

Then, in 2000-2002, using the technique of the effective average action, including derivative terms, the present authors performed a nonperturbative study of frustrated magnets for any dimension between two and four [62, 63, 118]. They recovered *all* known perturbative results at one-loop in two and four dimensions as well as for $N \rightarrow \infty$. They determined $N_c(d)$ for all d and found $N_c(d = 3) = 5.1$. Accordingly, for $N = 6$, they found a second order phase transition. Their exponents were in very good agreement with those found numerically. For $N = 3$ [63], they recovered Zumbach's results — presence of a minimum in the RG flow — and improved his approach: they found pseudo-critical exponents in good agreement with *some* experimental realizations of frustrated magnets. *However*, regarding the spreading of the experimental and numerical data, the recourse to a minimum, leading to a *unique* set of pseudo-critical exponents, was clearly not the end of the story. During the study of the $N = 2$ case [118], the present authors realized that the property of pseudo-scaling and even more, generic pseudo-scaling, does not rely on the concept of minimum of the flow. Pseudo-scaling appears as a consequence of the existence of a *whole region* in the flow diagram in which the flow is slow. This allowed them to account for the *nonuniversal scaling* that occurs in XY as well as in Heisenberg frustrated magnets. The present article accounts for these last developments.

In 2001, Pelissetto *et al.* [155] derived the six-loop series for the GLW model. They used sophisticated resummation methods in order to find the fixed points and to determine the critical exponents of the model. For $N \gtrsim 7$, they found a fixed point of the same nature as the one obtained at large- N and in the $4 - \epsilon$ expansion. Thus, a second order phase transition is expected in this

case. For $5 \lesssim N \lesssim 7$, they considered that their resummed series were not well converged, the number of fixed points depending strongly of the number of loops considered. This led them to interpret this result as an indication that $N_c(d = 3) \sim 6$. Finally and surprisingly, for $N \lesssim 5$ and, in particular, for the physically relevant cases $N = 2$ and $N = 3$, they found stable fixed points. Thus, a second order phase transition was also predicted in these cases. However, the critical exponents found were far from all experimental and numerical data (see the following). Moreover, regarding again the spreading of these data, an interpretation in terms of a unique set of exponents was clearly insufficient.

In another work [156], assuming that $N_c(d = 2) = 2$, Pelissetto *et al.* have reformulated the three-loop version of the series of Eq. (39) — see below — to make it compatible with this last guess. The series seemed to have better convergence properties — see however below — and allowed Pelissetto *et al.* to compute $N_c(d)$. They found $N_c(d = 3) = 5.3$, in good agreement with the value — $N_c(d = 3) = 5.1$ — obtained from the NPRG approach [63, 157].

Recent re-investigations of the five and six-loop perturbative series [131, 132] have led Calabrese *et al.* (see also [158]) to conjecture that the fixed point found by Pelissetto *et al.* — that corresponds to a *focus* fixed point — could explain the existence of the spreading of critical exponents encountered in frustrated magnets. Indeed, they observed that, due to the specific structure of the fixed point, the critical exponents display strong variations along the RG trajectories that could explain the lack of universality observed experimentally and numerically. They have also given estimates of the critical number of spin components for which there is a change of the order of the phase transition. They have found that there is a first order phase transition in the whole domain $5.7(3) < N < 6.4(4)$ and a second order phase transition for the other values of N and, in particular, for $N = 2$ and $N = 3$.

Finally, a very recent computation of the five-loop β function of the GLW model in a $4 - \epsilon$ expansion has led to a novel estimation of $N_c(d)$. Calabrese and Parrucini [159] have found the value $N_c(d = 3) = 6.1(6)$ which is compatible with the value $N_c(d = 3) = 6.4(4)$ found within the six-loop computation performed in three dimensions [131, 132].

Since several aspects of the recent perturbative and nonperturbative approaches differ, in particular in their interpretations of the origin of the nonuniversal scaling found in frustrated magnets, we postpone the detailed discussion of these last developments of both methods to the following sections.

V. THE PERTURBATIVE SITUATION

Let us discuss in more details the perturbative approaches that have been used to investigate frustrated

magnets.

There are essentially two different methods to analyze the critical behavior of the system described by the Hamiltonian (9). They correspond to two different methods to deal with the constraints obeyed by the microscopic degrees of freedom, Eq. (5). They lead to the NL σ and GLW models that have been both perturbatively analyzed around their respective critical dimension as well as, for the GLW model, directly in three dimensions. Let us review the results of these approaches.

A. The Nonlinear Sigma (NL σ) model approach

The idea underlying the construction of this model is to consider the system in its low-temperature — symmetry broken — phase and to take into account small fluctuations of the fields around the direction of the order parameter. The corresponding treatment is thus, by construction, a low-temperature expansion. Its actual validity is in fact less stringent than that: it is sufficient that the system is *locally* ordered and that the temperature is small. This explains why this approach is valid even in two dimensions for systems obeying the Mermin-Wagner theorem. Note that this approach applies — a priori (see Section II B and the discussion at the end of this section) — only for $N \geq 3$. Indeed, in the $N = 2$ case, the low-temperature expansion of the NL σ model leads to a trivial result, *i.e.* the theory is perturbatively free. This result is however not reliable since there exist topological as well as Ising-like degrees of freedom in the XY frustrated case (see Section II). These degrees of freedom, that are completely missed within the low-temperature perturbative approach, drastically affect the physics at finite temperature as in the famous Berezinskii-Kosterlitz-Thouless phase transition [52, 53].

Within the NL σ model approach, the partition function of the $SO(3) \times SO(2)$ -symmetric model follows from the Hamiltonian Eq. (7) together with the constraints of Eq. (5) [69]:

$$\begin{aligned} \mathcal{Z} = & \int \mathcal{D}\vec{\phi}_1 \mathcal{D}\vec{\phi}_2 \prod_{i \leq j} \delta(\vec{\phi}_i \cdot \vec{\phi}_j - \delta_{ij}) \cdot \\ & \cdot \exp\left(-\frac{1}{2T} \int d^d \mathbf{x} \left((\partial\vec{\phi}_1)^2 + (\partial\vec{\phi}_2)^2 \right)\right). \end{aligned} \quad (40)$$

The delta-functionals allow the integration of the three massive modes among the six degrees of freedom of $\vec{\phi}_1$ and $\vec{\phi}_2$. Therefore, only the three — Goldstone — modes $\vec{\pi}$ remain, in terms of which the partition function writes [151, 160, 161]:

$$Z = \int_{|\vec{\pi}| \leq 1} D\vec{\pi} \exp\left(-\frac{1}{2T} \int d^d \mathbf{x} g_{ij}(\pi) \partial\pi^i \partial\pi^j\right). \quad (41)$$

The Eq. (41), where $g_{ij}(\pi)$ embodies the interaction, is the suitable expression for a low-temperature expansion of the $SO(3) \times SO(2)/SO(2)$ NL σ model.

The low-temperature expansion of such NL σ models has been studied in general but rather abstract terms by Friedan [160]. The specific study of the $SO(3) \times SO(2)/SO(2)$ model and its generalization to N -component spins — the $O(N) \times O(2)/(O(N-2) \times O(2))$ model — has been performed by Azaria *et al.* [151, 161] (see also [156]). The RG analysis requires to consider the most general Hamiltonian invariant under $O(N) \times O(2)$ and renormalizable around $d = 2$. This Hamiltonian involves not only the usual kinetic terms for $\vec{\phi}_1$ and $\vec{\phi}_2$, Eq. (40), but also a nontrivial derivative term, called the “current-term”, which reads:

$$\int d^d \mathbf{x} \left(\vec{\phi}_1 \cdot \partial\vec{\phi}_2 - \vec{\phi}_2 \cdot \partial\vec{\phi}_1 \right)^2. \quad (42)$$

This term must be included in the model since it has the right symmetry, is power-counting renormalizable around $d = 2$ and is thus generated during the RG flow. The correct NL σ model — in the sense of stability under RG transformations — is given by (for any $N \geq 3$) [151]:

$$\begin{aligned} H = & \int d^d \mathbf{x} \left(\frac{\eta_1}{2} \left((\partial\vec{\phi}_1)^2 + (\partial\vec{\phi}_2)^2 \right) + \right. \\ & \left. + \left(\frac{\eta_2}{8} - \frac{\eta_1}{4} \right) \left(\vec{\phi}_1 \cdot \partial\vec{\phi}_2 - \vec{\phi}_2 \cdot \partial\vec{\phi}_1 \right)^2 \right) \end{aligned} \quad (43)$$

where we have chosen to reparametrize the coupling constants in a way convenient for what follows. Now, the Hamiltonian of the naïve continuum limit Eq. (40) is just the initial condition of the RG flow corresponding to $\eta_1 = \eta_2/2 = 1/T$. Note that we have included the temperature in the coupling constants.

For the special case $N = 3$, it is convenient to rewrite the model differently. We define, as in Eq. (16), a third vector $\vec{\phi}_3$ by:

$$\vec{\phi}_3 = \vec{\phi}_1 \wedge \vec{\phi}_2. \quad (44)$$

With this expression, it is easy to verify that the current-term, Eq. (42), is nothing but a linear combination of the kinetic terms of $\vec{\phi}_1$, $\vec{\phi}_2$ and $\vec{\phi}_3$:

$$\begin{aligned} \int d^d \mathbf{x} \left(\vec{\phi}_1 \cdot \partial\vec{\phi}_2 - \vec{\phi}_2 \cdot \partial\vec{\phi}_1 \right)^2 = \\ 2 \int d^d \mathbf{x} \left((\partial\vec{\phi}_1)^2 + (\partial\vec{\phi}_2)^2 - (\partial\vec{\phi}_3)^2 \right). \end{aligned} \quad (45)$$

One can then gather the three vectors $\vec{\phi}_1$, $\vec{\phi}_2$ and $\vec{\phi}_3$ into a 3×3 matrix:

$$\Phi = \begin{pmatrix} \vec{\phi}_1 & \vec{\phi}_2 & \vec{\phi}_3 \end{pmatrix}. \quad (46)$$

Since $(\vec{\phi}_1, \vec{\phi}_2, \vec{\phi}_3)$ are three orthonormal vectors, one has ${}^t \Phi \Phi = \mathbb{1}$ and Φ is therefore a $SO(3)$ matrix.

The partition function thus reads:

$$\mathcal{Z} = \int \mathcal{D}\Phi \delta(t\Phi\Phi - \mathbb{1}) e^{-\int d^d\mathbf{x} \text{Tr}(\mathcal{P} \partial^t\Phi \partial\Phi)} \quad (47)$$

where \mathcal{P} is a diagonal matrix of coupling constants: $\mathcal{P} = \text{diag}(p_1 = p_2 = \eta_2/4, p_3 = \eta_1/2 - \eta_2/4)$.

It is easy to check on Eq. (47) that the model is invariant under the right transformation:

$$\Phi \rightarrow \Phi.V \quad (48)$$

with V being the subset of $SO(3)$ matrices that commute with \mathcal{P} . When $p_3 \neq p_1$, *i.e.* $\eta_1 \neq \eta_2$, V is isomorphic to $SO(2)$. When \mathcal{P} is proportional to the identity, V is isomorphic to the whole $SO(3)$ group. In this last case, the high-temperature symmetry group is $G = SO(3) \times SO(3) \sim SO(4)$. Note that this identity has to be understood at the level of the Lie algebras since $SO(3) \times SO(3)$ and $SO(4)$ are locally isomorphic but differ globally and have different topological properties. This fact will be important in the following.

The RG equations for the $O(N) \times O(2)/(O(N-2) \times O(2))$ model have been computed at two-loop order in $d = 2 + \epsilon$ [151, 161]. We recall here the one-loop result that will be useful in the following:

$$\begin{cases} \beta_{\eta_1} = -(d-2)\eta_1 + N - 2 - \frac{\eta_2}{2\eta_1} \\ \beta_{\eta_2} = -(d-2)\eta_2 + \frac{N-2}{2} \left(\frac{\eta_2}{\eta_1}\right)^2 \end{cases} \quad (49)$$

A fixed point is found for any $N \geq 3$. For $N = 3$, it corresponds to $p_1^* = p_3^*$, *i.e.* $\eta_1^* = \eta_2^*$ and, thus, to an enlarged symmetry $SO(3) \times SO(3)/SO(3) \sim SO(4)/SO(3)$. This fixed point has only one direction of instability — the direction of the temperature — and thus corresponds to a second order phase transition. Surprisingly, the critical behavior is thus predicted to be governed by the usual ferromagnetic Wilson-Fisher fixed point with the subtlety that it corresponds to *four-component* spins. Note that this precisely corresponds to the particular case considered in Section II B. Another subtlety is that since, here, the order parameter is a matrix instead of a vector — it is a $SO(4)$ tensor — the anomalous dimension is different from the usual anomalous dimension of the four-component vector model. Only the exponent ν is independent of the nature of the order parameter and is thus identical to the usual value of ν of the Wilson-Fisher $N = 4$ universality class [151, 161].

In fact, it is easy to convince oneself that the fixed point found exists to all order of perturbation theory. Actually, the crucial fact is that, in $d = 2 + \epsilon$, the *perturbative* β functions of a $NL\sigma$ model associated with the symmetry breaking scheme $G \rightarrow H$ only depend on the *local geometrical* structure of the manifold G/H which is itself determined by the Lie algebras of G and H [151, 161]. Since the Lie algebras of $SO(3) \times SO(3)$ and of $SO(4)$

are identical, the perturbative β function for the — remaining — coupling constant of the model with $p_1 = p_3$ is identical at all orders to the perturbative β function of the usual $SO(4)/SO(3)$ $NL\sigma$ model. The existence of a fixed point for the $SO(3) \times SO(3)/SO(3)$ $NL\sigma$ model at all order of perturbation theory follows from the fact that its existence makes no doubt for the $SO(4)/SO(3)$ $NL\sigma$ model.

At the time of the first investigation of the $O(N) \times O(2)/(O(N-2) \times O(2))$ $NL\sigma$ model, the most natural position was to extend this equivalence *beyond* perturbation theory and to assume that the $SO(3) \times SO(3)/SO(3)$ fixed point exists everywhere between two and four dimensions, as it is the case for the $SO(4)/SO(3)$ fixed point. This was, in particular, the position advocated by Azaria *et al.* [151, 161]. The outstanding fact is that although the $SO(4)$ behavior has indeed been seen numerically in $d = 2$ [74, 78], it actually does not exist far from two dimensions. This is clear since *no* such fixed point is found in $d = 4 - \epsilon$ and since, as already emphasized, the $SO(4)$ behavior is not seen in any numerical or experimental data in $d = 3$. It is thus extremely probable that either the fixed point disappears in a nontrivial dimension smaller than 3 or it survives in $d = 3$ while being no longer the usual $N = 4$ fixed point. Note that, in the first case, its $SO(4)$ nature can also change before it disappears. Anyway, this fixed point must disappear below $d = 4$. The situation is thus more involved than in the “usual” $SO(4)/SO(3)$ model. There must exist nonperturbative reasons explaining the disappearance of the fixed point and/or the loss of its $SO(4)$ character.

Actually, it is clear that the perturbative low-temperature expansion performed on the $NL\sigma$ model misses several nonanalytic terms in T — typically terms that behave as $\exp(-1/T)$ — that could be responsible for the disappearance of the fixed point and/or its change of nature. There are, at least, two origins for such terms.

1) The first one consists in the nontrivial topological configurations — see the discussion in Section II B following Eq. (15) — that are completely neglected in the low-temperature expansion of the $NL\sigma$ models. Indeed this expansion relies, by construction, on the local geometrical properties of the manifold G/H and is insensitive to its global — topological — structure. Thus it ignores vortex-like configurations that likely play an important role in three dimensions.

2) The second origin of nonanalytic corrections to the low-temperature β function is more technical. The low-temperature expansion is performed in terms of the Goldstone — or pseudo-Goldstone in $d = 2$ — modes that are represented by fields constrained to have a modulus less than one, see Eq. (41). This inequality cannot be taken into account in the perturbative treatment [162] and is thus relaxed, leading to neglect terms of order $\exp(-1/T)$. All these terms are negligible for the critical behavior when the critical temperature is very small, which is the case near $d = 2$. However, they become important when $T_c \sim 1$ which is typically the case in

$d = 3$.

Only a nonperturbative treatment can take into account these nonanalytic terms and thus allows to follow, when the dimension is increased, the fate of the $O(4)$ fixed point.

B. The Ginzburg-Landau-Wilson (GLW) model approach

The GLW model for the $O(N) \times O(2) / (O(N-2) \times O(2))$ model can be deduced from a generalization of Eq. (40) to N -component vectors, by replacing the functional delta-constraint by the most general potential that favors the field configurations obeying the initial constraint. For convenience, we choose to parametrize it by:

$$\prod_{i \leq j} \delta(\vec{\phi}_i \cdot \vec{\phi}_j - \delta_{ij}) \rightarrow e^{-U} \quad (50)$$

with:

$$U = \int d^d \mathbf{x} \left(\frac{r}{2} (\vec{\phi}_1^2 + \vec{\phi}_2^2) + \frac{\lambda + \mu}{16} (\vec{\phi}_1^2 + \vec{\phi}_2^2)^2 - \frac{\mu}{4} (\vec{\phi}_1^2 \vec{\phi}_2^2 - (\vec{\phi}_1 \cdot \vec{\phi}_2)^2) \right) \quad (51)$$

where, as usual, r is proportional to the reduced temperature while λ and μ are ϕ^4 -like coupling constants.

All field-dependent terms in Eq. (51) can be rewritten in terms of the rectangular matrix Φ defined in Eq. (8). The corresponding Hamiltonian then reads:

$$H = \int d^d \mathbf{x} \left(\frac{1}{2} \text{Tr} (\partial^t \Phi \partial \Phi) + \frac{r}{2} \rho + \frac{\lambda}{16} \rho^2 + \frac{\mu}{4} \tau \right) \quad (52)$$

with $\rho = \text{Tr} ({}^t \Phi \Phi)$ and $\tau = \frac{1}{2} \text{Tr} ({}^t \Phi \Phi - \mathbb{1} \rho / 2)^2$ being the only $O(N) \times O(2)$ independent invariants that can be built out the fields, see Appendix B. Note that minimizing the term in front of μ corresponds to imposing ${}^t \Phi \Phi \propto \mathbb{1}$, *i.e.* to imposing that $\vec{\phi}_1$ and $\vec{\phi}_2$ are orthogonal and of the same norm in agreement with the characteristics of the ground state of frustrated magnets, see Fig. 1b.

1. The RG flow

The RG equations for the coupling constants entering in Hamiltonian (52) have been computed in the $\epsilon = 4 - d$ -expansion up to five-loop order [159] and in a weak-coupling expansion in $d = 3$ up to six-loop order [155]. We recall here only the one-loop result of the ϵ -expansion to discuss qualitatively the flow diagram:

$$\begin{cases} \beta_\lambda = -\epsilon \lambda + \frac{1}{16\pi^2} (4\lambda\mu + 4\mu^2 + \lambda^2(N+4)) \\ \beta_\mu = -\epsilon \mu + \frac{1}{16\pi^2} (6\lambda\mu + N\mu^2). \end{cases} \quad (53)$$

As well known, for any $N > N_c(d = 4 - \epsilon) = 21.8 + O(\epsilon)$ there exist four fixed points: the Gaussian — G — the vector $O(2N)$ — V — and two others, called the chiral — C_+ — and anti-chiral — C_- — fixed points. Among these fixed points one, C_+ , is stable and governs the critical properties of the system and the others are unstable (see Fig. 2a). When, at a given dimension d close to four, N is decreased, C_+ and C_- move closer together, coalesce at $N_c(d)$ and then disappear (see Fig. 2b). More precisely, for $N < N_c(d)$, the roots of the β functions acquire an imaginary part. Since no stable fixed point exists below $N_c(d)$ and since the flow drives the system in a region of instability, it is believed that the transition is of first order. Note that for $N < N'_c(d = 4 - \epsilon) = 2.2 + O(\epsilon)$, C_+ and C_- reappear but not in the physically relevant region to frustrated magnets.

For completeness we give the exponent ν at one-loop:

$$\nu = \frac{1}{2} + \epsilon \left(\frac{(N-3)(N+4)\sqrt{48-24N+N^2}}{8(144-24N+4N^2+N^3)} + \frac{N(48+N+N^2)}{8(144-24N+4N^2+N^3)} \right) \quad (54)$$

and recall that the anomalous dimension vanishes at this order. Note that the square root becomes complex for $2.2 < N < 21.8$, which is reminiscent of the critical values $N_c(d)$ and $N'_c(d)$ of the number of spin components, see above.

2. The three and five-loop results in $d = 4 - \epsilon$

In $4 - \epsilon$ dimensions, the critical value $N_c(d)$ has been computed at three-loop order [153] and, very recently, at five-loop order [159]:

$$N_c(d = 4 - \epsilon) = 21.80 - 23.43\epsilon + 7.09\epsilon^2 - 0.03\epsilon^3 + 4.26\epsilon^4 + O(\epsilon^5). \quad (55)$$

In fact, as it is often the case within this kind of expansion, the series are not well behaved and it is difficult to obtain reliable results even after resummation [22, 153, 159]. We however indicate the value found at three-loop order [153]: $N_c(d = 3) = 3.39$ and at five-loop order [159]: $N_c(d = 3) = 5.45$.

3. The improved three and five-loop results

It has been conjectured by Pelissetto *et al.* [156] that $N_c(d = 2) = 2$, a result which is however somewhat controversial [159]. It is possible to use this nonperturbative information to reformulate the series obtained within the $4 - \epsilon$ expansion. Imposing the constraint $N_c(d = 2) = 2$ to the three-loop series, Pelissetto *et al.* have obtained [156]:

$$N_c(d = 4 - \epsilon) = 2 + (2 - \epsilon)(9.90 - 6.77\epsilon + 0.16\epsilon^2) + O(\epsilon^3). \quad (56)$$

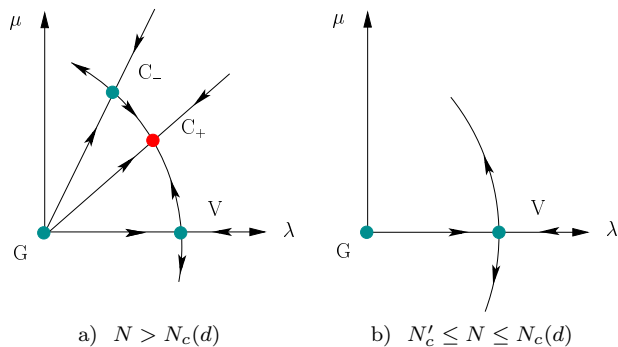


FIG. 2: Flow diagram for a) N above $N_c(d)$ and b) N below $N_c(d)$. The fixed points C_+ and C_- that exist above $N_c(d)$ coalesce at $N_c(d)$ and then disappear. G and V are the Gaussian and vector $O(2N)$ fixed points.

Reformulated in this way, the coefficients of the series decrease rapidly. It is thus reasonable to use this expression to estimate $N_c(d=3)$. Pelissetto *et al.* have thus obtained [156]: $N_c(d=3) = 5.3(2)$ where the error bar indicates how $N_c(d=3)$ varies from two to three loops. However, Calabrese and Parruccini have shown that, extended to five loops, the same series behaves badly [159]:

$$N_c(d=4-\epsilon) = 2 + (2-\epsilon)(9.90 - 6.77\epsilon + 0.16\epsilon^2 + 0.06\epsilon^3 + 2.16\epsilon^4) + O(\epsilon^5). \quad (57)$$

Using different kinds of tricks, notably the inverse of the series, they have obtained, from the five-loop series, the value $N_c(d=3) = 6.1(6)$.

From this approach one is strongly tempted to conclude that, in the physical cases $N=2$ and $N=3$, the transitions are of first order, even if it is impossible to conclude about the strong or weak character of this transition.

4. The three-loop results in $d=3$

A weak-coupling analysis has been performed directly in $d=3$ at three-loop order in [152]. This leads to $N_c(d=3) = 3.91$. However, as already emphasized, this result is not well converged.

5. The large- N results

The large- N expansion was first performed by Bailin *et al.* [9]. It was then re-examined by Kawamura [70] and Pelissetto *et al.* [156]. A fixed point is found within this expansion in all dimensions between 2 and 4. The exponents ν and η have been computed up to order $1/N^2$

in $d=3$ [156]:

$$\begin{cases} \nu = 1 - \frac{16}{\pi^2} \frac{1}{N} - \left(\frac{56}{\pi^2} - \frac{640}{3\pi^4} \right) \frac{1}{N^2} + O(1/N^3) \\ \eta = \frac{4}{\pi^2} \frac{1}{N} - \frac{64}{3\pi^4} \frac{1}{N^2} + O(1/N^3). \end{cases} \quad (58)$$

Around $d=4$ and $d=2$ the perturbative results of, respectively, the GLW and NL σ models are recovered once the limit $N \rightarrow \infty$ has been performed. This suggests that, at least for sufficiently large N , the two models belong indeed to the same universality class in all dimensions. However, within this approach, no $N_c(d)$ line is found (see however [156]). It is thus impossible to extrapolate to finite N the results obtained in this approach.

6. The six-loop results in $d=3$

In three dimensions, a six-loop computation has been performed by Pelissetto *et al.* [155] and re-examined by Calabrese *et al.* [131, 132], see below. The results are the following:

- 1) For N sufficiently large — $N > 6.4(4)$ — there exist four fixed points, one stable and three unstable, in agreement with the usual picture given above, see Fig. 2a. The transition is thus of second order.
- 2) For $5.7(3) < N < 6.4(4)$, there is no nontrivial fixed point and the transition is expected to be of first order.
- 3) For $N < 5.7(3)$ and, in particular, for $N=2$ and $N=3$ a *stable fixed point* is found and a second order phase transition is expected.

According to Pelissetto *et al.* [155, 156], the fixed points found for $N=2$ and $N=3$ should be non analytically connected with those found in the $1/N$ and $4-\epsilon$ approaches. Therefore, it should be impossible to obtain them by following smoothly those obtained at large- N or close to $d=4$.

The critical exponents obtained by Pelissetto *et al.* are given in Table VII. Note that the error bars are about ten times larger here than in the ferromagnetic $O(N)$ models [28, 162] computed by the same method. This is an indication that the resummed perturbative series are converging much slower than in the vectorial case.

Let us now discuss these results.

System	Ref.	α	β	γ	ν
XY	[155]	0.29(9)	0.31(2)	1.10(4)	0.57(3)
Heis.	[155]	0.35(9)	0.30(2)	1.06(5)	0.55(3)

TABLE VII: The six-loop perturbative results in $d=3$.

The XY case. First, one should indicate that the exponents γ and ν computed from the six-loop approach compare reasonably well with the data of group 1. However, as already mentioned, the value of η found by the scaling relations must be positive when there exists a fixed point.

One finds, with the data of Table VII, $\eta \sim 0.08$ which is significantly positive. Let us recall that this is *not* the case for the experiments performed on the materials of group 1 and for the numerical simulations performed on STA. Note, moreover, that the value of β found within the six-loop calculation, is very far — around four theoretical error bars — from the average experimental ones which are $\beta = 0.228(6)$ for CsMnBr₃ alone, $\beta = 0.237(4)$ for the whole group 1 and far from the numerical values obtained for STA $\beta = 0.24 - 0.25$. Thus, contrarily to what is asserted in [155], it seems extremely improbable that the exponents found at six loops could fit with those of group 1 and those of the numerical STA model. Actually, this is also the case for the materials of group 2 for which the average β equals 0.389(7).

The Heisenberg case. First, one notes that the agreement between the γ and ν exponents obtained from the six-loop approach and from the experimental or numerical data is not as good as it is in the XY case. Concerning η , one finds, with the data of Table VII, $\eta \sim 0.08$. This has to be compared with the value of η obtained *i*) for the materials of group 1, which is significantly negative — $\eta = -0.118(25)$ — *ii*) for materials of group 2, which is marginally negative — $\eta = -0.018(33)$ — and *iii*) in the simulations of the STA which is also negative although not completely significantly: $\eta = -0.0182(89)$. The negativity of η is an indication of a mismatch between the six-loop results and the data for the Heisenberg systems even if it cannot be used as a definitive argument against a second order phase transition. The exponent γ obtained from the numerical simulations of the Heisenberg STA model provides a further information. The average value of this exponent — $\gamma = 1.185(3)$ — is rather far — 2.5 theoretical error bars — from the six-loop results [210].

From the previous analysis one can conclude that, as such, the fixed point obtained within the six-loop approach turns out to be *not* directly relevant to the phenomenology of XY materials or simulated systems. This seems to exclude the scenarios I, II and III that all assume that, at least, a certain number of compounds or systems are well described by a fixed point.

7. Critical remarks

As we mentioned at the beginning of our analysis of the experimental results, see Section III A, we have made an assumption on the nature of the experimental errors which is not realistic: the systematic errors cannot be neglected. We now come back on this point and show that the conclusions we have drawn from our analysis persist without this assumption.

Let us consider the XY case, where the symptoms of a mismatch between the theoretical and experimental results are the clearest. We concentrate on the materials of group 1 and on the exponent β which is the best measured, see Table I. With our assumption, we have found

$\beta = 0.228(6)$. Let us suppose that, contrarily to our assumption, the systematic error is large and dominates the total error. Let us take:

$$\beta = 0.23(2) \quad (59)$$

so that all experimental and numerical results lie in the interval of values, see Tables I and III. This estimate has to be compared with the six-loop result:

$$\beta = 0.31(2) \quad (60)$$

where, in this case, the authors indicate that they have been very conservative in the estimation of the error bar [155]. Although it is difficult to get fully unambiguous conclusions out of these numbers, it is clear that the agreement between them is not satisfactory. The same considerations on group 2 of XY materials lead to suppose:

$$\beta = 0.39(2) \quad (61)$$

which, again, is far from being in agreement with the six-loop result Eq. (60).

It is also possible to test the negativity of the anomalous dimension η with our new assumption. In the same spirit, one estimates $\nu = 0.555(30)$. We find, in this case:

$$-0.28 \leq \eta \leq -0.048 . \quad (62)$$

Thus, η is again found negative even in the most extreme hypothesis.

We thus conclude that, although it is — up to now — impossible to estimate rigorously the confidence level of our analysis of the experimental data since only one error bar is given in the literature, it appears to be very difficult to reconcile the experimental and numerical data with the six-loop results.

8. The six-loop results in $d = 3$ re-examined

In order to cope with the discrepancy between the six-loop results obtained by Pelissetto *et al.* and the experimental and numerical data, Calabrese *et al.* have reconsidered the resummed six-loop series [131, 132, 158]. They claim that they can account for the unusual properties of the critical exponents for XY and Heisenberg frustrated systems in $d = 3$ — negative anomalous dimension and weak universality — by the fact that the RG trajectories around the stable — focus — fixed point found by Pelissetto *et al.* are spiral-like. By integrating the resummed β functions for the two coupling constants of the GLW model and computing the effective exponents η and ν along the RG trajectories, they have found that these exponents display large variations in a transient regime. These authors argue that the scaling properties

of the system are governed, over several decades of temperatures, by the preasymptotic regime so that the effective exponents observed experimentally can differ significantly from their asymptotic values, *i.e.* those defined at the fixed point.

Let us underline here several drawbacks of the scenario of Calabrese *et al.* .

First, it is based on the existence of stable fixed points that are not related to any already known fixed point. In particular, the fixed points found for $N = 2$ and $N = 3$ within this computation in $d = 3$ are, according to Pelissetto *et al.* and Calabrese *et al.* *non analytically* related to those found in the large- N as well as in the $4 - \epsilon$ expansions. This means that there is no way to check their existence using these perturbative methods. This is specifically problematic in the context of frustrated magnets where the properties of the fixed points appear to be very unusual: *i)* the existence of the stable fixed points strongly depends on the order of perturbation — they are not present at three-loop order and only show up, as far as we know, at five-loop order *ii)* the location of the fixed points, as N and d are varied, seems to have, in the (N, d) plane, a very particular structure since, in three dimensions, they only exist when N is below *another* critical value of N — which is found to be equal to $5.7(3)$.

Second, it is very difficult, in the computation of Calabrese *et al.* , to relate — even in principle — the initial conditions of the RG flow to the microscopic characteristics of real systems. This would require to handle the infinity of coupling constants entering into the microscopic Hamiltonian obtained from the Hubbard-Stratonovitch transformation. This is impossible, at least within the usual perturbation theory.

Third, it is very difficult to account, in this framework, for the first order behavior deduced from several numerical simulations of XY and Heisenberg systems [126, 127]. We have also already noticed that XY-systems have a stronger tendency to undergo first order transitions than Heisenberg systems. However, there is no natural explanation for this phenomenon in the scenario of Calabrese *et al.* .

Fourth, in this scenario, it is also very difficult to explain why there is no physical system characterized by the asymptotic critical exponents, *i.e.* those corresponding to the fixed point found by Pelissetto *et al.*. This seems to require very unnatural experimental circumstances such that the initial conditions of the flow corresponding to the physical realizations of frustrated magnets are such that their long distance properties are *never* controlled by the nontrivial fixed point.

Finally, there is no possible explanation of the breakdown of the $NL\sigma$ model predictions.

C. Conclusion

XY and Heisenberg frustrated systems exhibit the kind of problems we have described in the introduction: the perturbative results obtained within a low-temperature expansion around two dimensions, within a weak-coupling expansion around four dimensions or within a large- N expansion fail to describe their critical physics in three dimensions. Moreover, these different perturbative predictions are in contradiction with each other. Contrarily to the $O(N)$ nonfrustrated case, there is no possible smooth interpolation of these results between two and four dimensions and, at fixed dimension, between $N = \infty$ and $N = 2, 3$. More surprisingly and, again in contradiction with what happens in the $O(N)$ nonfrustrated case, high-order calculations performed directly in $d = 3$ also fail to reproduce the phenomenology, at least when they are interpreted in the usual way. This situation reveals the difficulties of the conventional approaches to tackle with the physics of frustrated magnets. Only new interpretations or methods can allow to shed light on the problems encountered here. We have presented the solution proposed by Calabrese *et al.* on the basis of a high-order perturbative calculation and underlined its difficulties. We now present the nonperturbative method we have used to explain the unusual behavior of frustrated magnets. This is the subject of the next sections. We start by a methodological introduction to this method and then apply it to the frustrated systems.

VI. THE EFFECTIVE AVERAGE ACTION METHOD

We now present the NPRG method we use: the effective average action method [42, 43, 44, 51, 163]. The content of this section is neither original nor exhaustive. There exist several well-documented reviews on the subject [34, 45, 164]. Our aim here is only to provide some of the physical ideas underlying this method — notably the block spin concept and its formulation in the continuum — as well as its technical implementation on the simple example of the $O(N)$ model.

A. Block spin in the continuum

The effective average action method, as well as many other NPRG techniques, is based on the well known concept of “block spin” [29, 165]: when dealing with any strongly correlated system, it is fruitful to integrate out the fluctuations step by step and, more precisely, scale by scale. In practice, one first gathers the initial — microscopic — degrees of freedom into small “blocks”. It is then possible, at least formally, to integrate out, in the partition function of the system, the internal fluctuations of the blocks. This “decimation” is followed by a rescaling of length-scales, coupling constants and fields. In this

way, starting from a “bare” GLW Hamiltonian, one gets an effective Hamiltonian for the block degrees of freedom, *i.e.* for the low-energy modes. By iterating this procedure, one generates a sequence of — scale-dependent — effective Hamiltonians, parametrized by a running scale k , that all share the same long-distance physics. This sequence defines a RG flow. At a fixed point of this flow the system displays scale invariance. This allows to obtain the critical quantities through an analysis of the neighborhood of the fixed point in the flow of effective Hamiltonians [1].

To illustrate how this concept of block spin is implemented concretely in the continuum, we consider the case of an Ising-like system, initially defined on a lattice which, in the continuum, is described by a scalar field $\zeta(\mathbf{x})$. If the lattice spacing is given by a , the corresponding continuum field theory is characterized by an overall momentum cut-off Λ of order a^{-1} . The partition function writes:

$$\mathcal{Z} = \int \mathcal{D}\zeta e^{-\frac{1}{2}\zeta \cdot C_\Lambda^{-1} \cdot \zeta} - H_\Lambda^{\text{int}}[\zeta] \quad (63)$$

where $H_\Lambda^{\text{int}}[\zeta]$ stands for the interacting part of the GLW Hamiltonian and:

$$\zeta \cdot C_\Lambda^{-1} \cdot \zeta = \int \frac{d^d \mathbf{q}}{(2\pi)^d} \zeta(\mathbf{q}) C_\Lambda^{-1}(\mathbf{q}) \zeta(-\mathbf{q}) \quad (64)$$

corresponds to the cut-off kinetic part. In Eq. (63) and (64), $C_\Lambda(\mathbf{q})$ is an ultra-violet (*UV*) cut-off propagator that prevents the propagation of unphysical modes with momentum higher than Λ . One writes it:

$$C_\Lambda(\mathbf{q}) = \frac{F_{k=\Lambda}(\mathbf{q}^2)}{\mathbf{q}^2} \quad (65)$$

where $F_k(\mathbf{q}^2)$ is a function of the ratio $z = \mathbf{q}^2/k^2$ that rapidly decreases when $z \rightarrow \infty$. One also imposes to $F_k(\mathbf{q}^2)$ to be unity at the origin: $F_k(\mathbf{q}^2 = 0) = 1$. A typical example of function F is: $F_k(\mathbf{q}^2) = e^{-(\mathbf{q}/k)^2}$ but other forms can obviously be considered.

In Fourier space, the idea of block spin is specified by separating the low- and high-momentum modes of the spin-field ζ :

$$\zeta(\mathbf{q}) = \zeta_>(\mathbf{q}) + \zeta_<(\mathbf{q}) . \quad (66)$$

The fields $\zeta_>(\mathbf{q})$ and $\zeta_<(\mathbf{q})$ being unconstrained, the separation between high- and low-momentum modes is actually realized through their respective propagator. We thus write:

$$C_\Lambda(\mathbf{q}) = C_k(\mathbf{q}) + (C_\Lambda(\mathbf{q}) - C_k(\mathbf{q})) \doteq C_<(\mathbf{q}) + C_>(\mathbf{q}) \quad (67)$$

where k is the typical scale that separates the high- and low-momenta. In Eq. (67), $C_>(\mathbf{q})$ (resp. $C_<(\mathbf{q})$) propagates $\zeta_>$ (resp. $\zeta_<$), the high- (resp. low-) momentum degrees of freedom of the field ζ . This comes from a property of the Gaussian integral that can be easily seen on

a one-dimensional integral:

$$\int dz \exp\left(-\frac{z^2}{2(\alpha + \beta)} + f(z)\right) \propto \int dx dy \exp\left(-\frac{x^2}{2\alpha} - \frac{y^2}{2\beta} + f(x+y)\right) . \quad (68)$$

This result is easily obtained by changing, in the right hand side of Eq. (68), the integration variables x, y , into $z = x + y$ and $t = x - y$ and by integrating on t .

Thus from Eqs. (63), (66), (67) and (68) one gets:

$$\mathcal{Z} = \int \mathcal{D}\zeta_< \mathcal{D}\zeta_> \exp\left(-\frac{1}{2}\zeta_< \cdot C_<^{-1} \cdot \zeta_< - \frac{1}{2}\zeta_> \cdot C_>^{-1} \cdot \zeta_> - H_\Lambda^{\text{int}}[\zeta_< + \zeta_>]\right) . \quad (69)$$

The effective Hamiltonian $H_k^{\text{int}}[\zeta_<]$ for the low-momentum degrees of freedom $\zeta_<$ is defined through the integration over the high-momentum degrees of freedom in Eq. (69):

$$e^{-H_k^{\text{int}}[\zeta_<]} \doteq \int \mathcal{D}\zeta_> \exp\left(-\frac{1}{2}\zeta_> \cdot C_>^{-1} \cdot \zeta_> - H_\Lambda^{\text{int}}[\zeta_< + \zeta_>]\right) . \quad (70)$$

Integrating out the internal degrees of freedom of a block spin between the scales a and $a' > a$ corresponds, in this language, to the integration of the modes $\zeta_>$ with momenta between $k = a^{-1}$ and $k' = a'^{-1}$. The Equation (70) implements the block spin procedure in the continuum which is the starting point of any NPRG approach.

B. The Polchinski equation

The effective Hamiltonian $H_k^{\text{int}}[\zeta_<]$ follows an exact equation describing its infinitesimal evolution when the running scale k is lowered. To establish this equation we rewrite Eq. (70) as:

$$\begin{aligned} e^{-H_k^{\text{int}}[\zeta_<]} &= \\ &= \int \mathcal{D}\zeta \exp\left(-\frac{1}{2}(\zeta - \zeta_<) \cdot C_>^{-1} \cdot (\zeta - \zeta_<) - H_\Lambda^{\text{int}}[\zeta]\right) \\ &= \exp\left(\frac{1}{2} \frac{\delta}{\delta \zeta_<} \cdot C_> \cdot \frac{\delta}{\delta \zeta_<}\right) e^{-H_\Lambda^{\text{int}}[\zeta_<]} . \end{aligned} \quad (71)$$

This last functional relation can be inferred from the one-dimensional identity:

$$\int dx \exp\left(-\frac{(x-y)^2}{2\gamma} - f(x)\right) \propto e^{\frac{\gamma}{2} \frac{\partial^2}{\partial y^2}} e^{-f(y)} . \quad (72)$$

By differentiating each side of Eq. (71) with respect to k we obtain:

$$\begin{aligned}
-(\partial_k H_k^{\text{int}}) e^{-H_k^{\text{int}}} &= \\
&= \frac{1}{2} \left(\frac{\delta}{\delta \zeta_{<}} \cdot \partial_k C_{>} \cdot \frac{\delta}{\delta \zeta_{<}} \right) e^{-H_k^{\text{int}}} \\
&= \frac{1}{2} \left(\frac{\delta H_k^{\text{int}}}{\delta \zeta_{<}} \cdot \partial_k C_{>} \cdot \frac{\delta H_k^{\text{int}}}{\delta \zeta_{<}} - \frac{\delta^2 H_k^{\text{int}}}{\delta \zeta_{<} \delta \zeta_{<}} \cdot \partial_k C_{>} \right) e^{-H_k^{\text{int}}}.
\end{aligned} \tag{73}$$

Finally, the *exact* evolution equation for H_k^{int} , known as the Polchinski equation [166] (see also [167]), writes explicitly:

$$\begin{aligned}
\partial_k H_k^{\text{int}}[\zeta_{<}] &= \frac{1}{2} \int \frac{d^d \mathbf{q}}{(2\pi)^d} \partial_k C_{>}(\mathbf{q}) \cdot \\
&\cdot \left(\frac{\delta^2 H_k^{\text{int}}}{\delta \zeta_{<}(\mathbf{q}) \delta \zeta_{<}(-\mathbf{q})} - \frac{\delta H_k^{\text{int}}}{\delta \zeta_{<}(\mathbf{q})} \frac{\delta H_k^{\text{int}}}{\delta \zeta_{<}(-\mathbf{q})} \right)
\end{aligned} \tag{74}$$

or, in real space:

$$\begin{aligned}
\partial_k H_k^{\text{int}}[\zeta_{<}] &= \frac{1}{2} \int d^d \mathbf{x} d^d \mathbf{y} \partial_k C_{>}(\mathbf{x} - \mathbf{y}) \cdot \\
&\cdot \left(\frac{\delta^2 H_k^{\text{int}}}{\delta \zeta_{<}(\mathbf{x}) \delta \zeta_{<}(\mathbf{y})} - \frac{\delta H_k^{\text{int}}}{\delta \zeta_{<}(\mathbf{x})} \frac{\delta H_k^{\text{int}}}{\delta \zeta_{<}(\mathbf{y})} \right)
\end{aligned} \tag{75}$$

with $\partial_k C_{>}(\mathbf{x} - \mathbf{y}) = \int \frac{d^d \mathbf{q}}{(2\pi)^d} \partial_k C_{>}(\mathbf{q}) e^{i\mathbf{q}(\mathbf{x}-\mathbf{y})}$. Note that in the preceding equations we have improperly used the same notation for the field $\zeta_{<}$ and regulator $C_{>}$ and for their Fourier transforms. Note also that, in the following, we shall use the notation ζ for $\zeta_{<}$. A graphical representation of the Polchinski equation is given in Fig. 3.

$$\partial_k H_k^{\text{int}} = \frac{1}{2} \left(\text{circle with cross} \right) - \frac{1}{2} \left(\text{dot-cross-dot} \right)$$

FIG. 3: A graphical representation of the Polchinski equation. The crosses represent the cut-off factor $\partial_k C_{>}(\mathbf{q})$. The black circles with n -external legs correspond to the n -th functional derivative of H_k^{int} with respect to the field.

Let us first make some remarks about Eq. (74). A first feature we would like to emphasize is that this equation involves the quantity H_k^{int} which is the effective Hamiltonian for the degrees of freedom that have *not* yet been integrated out, namely $\zeta_{<}$. The drawback with H_k^{int} is that it is an abstract object that has no direct physical meaning since it is a function of a field $\zeta_{<}$ that eventually fully disappears in the physical limit $k \rightarrow 0$, *i.e.* when *all* fluctuations have been integrated out. In particular, one should realize that $\zeta_{<}$ is *not* a precursor of the order parameter, *i.e.* *not* a local magnetization at scale k . Indeed this magnetization should come from a *thermodynamical average* at scale k while $\zeta_{<}$ is just a stochastic variable that represents the low-momentum part of the original spin field and is thus, roughly speaking, a *spatial average*

of this field. Consequently, the effective Hamiltonians by themselves do not contain all the information on the integration of the high-momentum degrees of freedom $\zeta_{>}$. For instance, the computation of correlation functions for the high-energy field $\zeta_{>}$ would require to first couple the system to a source J — a magnetic field — by adding in \mathcal{Z} a term $\exp(J\zeta)$ and to follow the flow of this term in order to obtain the full J -dependence of \mathcal{Z} , a rather difficult task. Thus, Eq. (74) provides at best a flow of the running coupling constants that parametrize the effective Hamiltonian H_k^{int} at scale k .

As shown mainly by Wilson, equations like Eq. (74) are, in principle, sufficient to compute the critical exponents once a fixed point Hamiltonian $H_k^{\text{int}*}$ has been found. Actually, even for the evaluation of the RG flow, Eq. (74) suffers from an important difficulty: although this equation looks simple — its only nonlinearity is a term quadratic in H_k^{int} — it is nevertheless a functional-partial-integro-differential equation that has no known solution in general. Therefore, in order to render it manageable, one has to truncate the Hamiltonian H_k^{int} .

1. Derivative expansion

A natural truncation consists in an expansion of the effective Hamiltonian in powers of the derivatives of the field [41, 44, 168]. For instance, for a one-component scalar field theory one has:

$$H_k^{\text{int}}[\zeta] = \int d^d \mathbf{x} \left(U_k(\zeta) + \frac{1}{2} Z_k(\zeta) (\partial \zeta)^2 + O(\partial^4) \right) \tag{76}$$

where $U_k(\zeta)$ stands for the potential — *i.e.* the derivative-independent part — of the effective Hamiltonian and $Z_k(\zeta)$ is the quadratic — *field-dependent* — field renormalization. With such a truncation, one neglects higher-order derivative terms. This is justified *i)* when one is interested in the long-distance, low-energy physics, since these higher-order derivative terms should correspond to less important operators and *ii)* when there is no qualitative change of nature between the microscopic and macroscopic degrees of freedoms — such as the appearance of bound states at a finite scale k — that could induce non localities [169]. A practical guide to evaluate the validity of the derivative expansion is the value of the anomalous dimension η . If this quantity is small, one can expect that the inclusion of higher-order derivative terms provides small corrections to the results.

At first order in the derivative expansion one sets $Z_k(\zeta) = 0$ in Eq. (76) and derives an RG equation for $U_k(\zeta)$ from Eq. (74). This corresponds to the so-called *Local Potential Approximation* (LPA) which has been intensively explored in the past [33, 170, 171, 172]. In particular, this kind of approach has been used by Zumbach to analyze the physics of frustrated magnets in three dimensions [64, 65, 66]. The problem with the LPA is that, since by definition it neglects the field renormalization, it

leads to a trivial — vanishing — anomalous dimension. Consequently: *i*) this prohibits to compare the results obtained within this approach to that of a standard perturbative approach when this last one involves a nontrivial anomalous dimension (this is, for instance, the case of the NL σ model around $d = 2$ already at one-loop), *ii*) this prevents an accurate evaluation of critical exponents for systems for which the anomalous dimension is not expected to be small. In the context of frustrated magnets, these drawbacks are serious since we are precisely interested in relating the different perturbative approaches and, to some extent, by a satisfactory determination of the critical exponents. We thus need to compute the field renormalization.

This kind of computation however encounters several difficulties. First, whereas the RG equation for $U_k(\zeta)$ in the LPA of the Polchinski equation is universal — cut-off independent —, the RG equation derived for $U_k(\zeta)$ and $Z_k(\zeta)$ at second order in the derivative expansion explicitly depends on the regulator $C_>(\mathbf{q})$ chosen to separate the high- and low-energy degrees of freedom in Eq. (67) [168, 173]. Another related problem is that of reparametrization invariance. The partition function (63) and, thus, the physical quantities like critical exponents, are invariant under a general change of field of the kind $\zeta \rightarrow \zeta + G(\zeta)$ where G is an arbitrary function starting at order ζ^2 . As a consequence of this invariance, the normalization of the field $Z_k(\zeta = 0)$ in the Hamiltonian is *a priori* an arbitrary parameter. Unfortunately, the reparametrization invariance is broken as soon as one performs a truncation of the Hamiltonian. As a result the critical exponents and, in particular η , depend on the normalization $Z_k(\zeta = 0)$. It follows from these considerations that, in any practical computation, one encounters the problem that physical quantities depend on nonuniversal parameters such as cut-off functions and normalizations. Different techniques, such as the Principle of Minimum Sensitivity (PMS), have been used to decrease the dependence of the critical quantities on the cut-off function [173, 174]. Also, some criterions have been proposed to find the best normalization, *i.e.* to find a value $Z_k(\zeta = 0)$ such that the derivative expansion converges the most rapidly [174]. These considerations, having for aim to exploit the Polchinski equation at the next to leading order in derivative expansion, have led to the determination of rather satisfactory critical exponents.

At the same time, there has been a great activity devoted to the search of other formulations of the RG ideas that could avoid some of the troubles encountered in the use of the Polchinski equation. The effective average action method is the result of this search.

C. The effective average action method

The basic — and physically very appealing — idea of this new formulation is to consider as the funda-

mental object, not the abstract effective Hamiltonian $H_k^{\text{int}}[\zeta]$, functional of the stochastic low-energy field $\zeta_<$ but, rather, the Gibbs free energy Γ — called effective action in field theory — functional of the order parameter $\phi = \langle \zeta \rangle$. To implement this idea in the RG context, it is necessary to build a running Gibbs free energy Γ_k for the high-energy modes that have already been integrated out at this scale k . The argument of Γ_k is, therefore, the order parameter at this scale that eventually becomes, when $k \rightarrow 0$, the true order parameter.

These requirements imply several constraints on the definition of Γ_k . First, at the scale of the lattice spacing, $k = \Lambda = a^{-1}$, Γ_k should correspond to the microscopic Hamiltonian H since no fluctuations have been taken into account. Second, when the running scale k is lowered to 0, Γ_k , which then includes *all* fluctuations, must identify with the standard effective action Γ from which all thermodynamical quantities like magnetization, correlation length, etc, are computed. To summarize, Γ_k must respect the constraints:

$$\begin{cases} \Gamma_{k=\Lambda} = H \\ \Gamma_{k=0} = \Gamma \end{cases} \quad (77)$$

and has to interpolate smoothly between these two limits.

1. Construction

Let us again consider, for simplicity, the case of a system described by a scalar field $\zeta(\mathbf{x})$. The construction of the effective average action proceeds in two steps. First, one should decouple the low-energy modes — with momenta $\mathbf{q}^2 > k^2$ — in the partition function in order to get a theory involving only the high-energy ones that will be summed over. Second, in this modified theory, one builds the Gibbs free energy, as usual, by a Legendre transform. This gives Γ_k . Let us now study how this is implemented in practice.

The first step is conveniently implemented by changing the partition function \mathcal{Z} into \mathcal{Z}_k for which a k -dependent term, quadratic in the fields and thus analogous to a mass-term is added to the microscopic Hamiltonian [43, 44]. With this “mass-term”, the partition function in presence of a source J writes:

$$\mathcal{Z}_k[J] = \int \mathcal{D}\zeta \exp\left(-H[\zeta] - \Delta H_k[\zeta] + J\zeta\right) \quad (78)$$

with $J\zeta = \int d^d\mathbf{q} J(\mathbf{q})\zeta(-\mathbf{q})$ and

$$\Delta H_k[\zeta] = \frac{1}{2} \int \frac{d^d\mathbf{q}d^d\mathbf{q}'}{(2\pi)^{2d}} \mathcal{R}_k(\mathbf{q}, \mathbf{q}')\zeta(\mathbf{q})\zeta(\mathbf{q}') \quad (79)$$

$$= \frac{1}{2} \int \frac{d^d\mathbf{q}}{(2\pi)^d} R_k(\mathbf{q}^2)\zeta(\mathbf{q})\zeta(-\mathbf{q}) \quad (80)$$

with $\mathcal{R}_k(\mathbf{q}, \mathbf{q}') = (2\pi)^d \delta(\mathbf{q} + \mathbf{q}')R_k(\mathbf{q}^2)$. In Eq. (80), $R_k(\mathbf{q}^2)$ is the cut-off function that controls the separation

between the low- and high-energy modes. To decouple the low-energy modes, it must act as a large-mass term for small \mathbf{q} whereas it must vanish for large \mathbf{q} to keep unchanged the high-energy sector of the theory. Thus:

$$R_k(\mathbf{q}^2) \sim k^2 \quad \text{for} \quad \mathbf{q}^2 \ll k^2 \quad (81)$$

and

$$R_k(\mathbf{q}^2) \rightarrow 0 \quad \text{when} \quad \mathbf{q}^2 \gg k^2. \quad (82)$$

The first constraint means that, for momenta lower than k , $R_k(\mathbf{q}^2)$ essentially acts as a mass — *i.e.* an IR cut-off — which prevents the propagation of the low-energy modes. The second ensures that the high-energy modes are fully taken into account in $\mathcal{Z}_k[J]$ and thus in the effective average action. Moreover, since we want to recover the original theory when $k \rightarrow 0$, *i.e.* when all fluctuations have been integrated out, $R_k(\mathbf{q}^2)$ must vanish in this limit. Thus we require:

$$R_k(\mathbf{q}^2) \rightarrow 0 \quad \text{identically when} \quad k \rightarrow 0 \quad (83)$$

which ensures that $\mathcal{Z}_{k=0}[J] = \mathcal{Z}[J]$. On the other hand, when $k \rightarrow \Lambda$, *i.e.* when no fluctuation has been integrated out, Γ_k should coincide with the microscopic Hamiltonian. This is achieved by requiring (see below for the proof):

$$R_k(\mathbf{q}^2) \rightarrow \infty \quad \text{identically when} \quad k \rightarrow \Lambda. \quad (84)$$

Note that, since we shall not be interested in the precise relation between the microscopic characteristics — defined at scale Λ — of a given system and its critical or pseudo-critical properties, we set $\Lambda = \infty$ in the following.

A widely used cut-off function is provided by [45]:

$$R_k(\mathbf{q}^2) = \frac{Z\mathbf{q}^2}{e^{\mathbf{q}^2/k^2} - 1} \quad (85)$$

where Z is the field renormalization. Including it in R_k allows to suppress the explicit Z dependence in the final RG equations — see below. The cut-off function $R_k(\mathbf{q}^2)$ corresponding to Eq. (85) is plotted on Fig. 4. Another

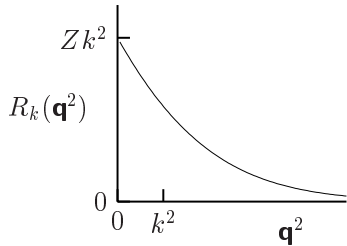


FIG. 4: A typical realization of the separation of high- and low-momentum modes provided by the cut-off function $R_k(\mathbf{q}^2)$. At low momentum, $R_k(\mathbf{q}^2)$ acts as an effective mass of order Zk^2 while the high-momentum behavior is not modified.

useful cut-off function, called theta cut-off, has been proposed by Litim [175]. It writes:

$$R_k(\mathbf{q}^2) = Z(k^2 - \mathbf{q}^2) \Theta(k^2 - \mathbf{q}^2) \quad (86)$$

where Θ is the usual step function.

The second step consists in defining the effective average action. The free energy at scale k is given — up to a factor $-k_B T$ — by:

$$W_k[J] = \ln \mathcal{Z}_k[J]. \quad (87)$$

From Eq. (87), one defines the order parameter $\phi_k(\mathbf{q})$ at scale k as the average value of the microscopic field $\zeta(\mathbf{q})$ in the modified theory:

$$\phi_k(\mathbf{q}) = \langle \zeta(\mathbf{q}) \rangle = \frac{\delta W_k[J]}{\delta J(-\mathbf{q})}. \quad (88)$$

Thanks to the properties of $R_k(\mathbf{q}^2)$, the contribution to the average value in Eq. (88) coming from modes with momenta $\mathbf{q}^2 \ll k^2$ is strongly suppressed. Also $\phi_k(\mathbf{q})$ identifies with the true order parameter in the limit $k \rightarrow 0$. Note that, for simplicity, we omit, in the following, the index k to ϕ_k .

The effective average action is defined by [43]:

$$\Gamma_k[\phi] = -W_k[J] + J\phi - \Delta H_k[\phi] \quad (89)$$

where $J = J[\phi]$, see Eq. (88). Thus $\Gamma_k[\phi]$ essentially corresponds to a Legendre transform of $W_k[J]$ for the macroscopic field ϕ — up to the mass-like term ΔH_k . The relation (89) implies several unconventional relations. First, taking its derivative with respect to $\phi(\mathbf{q})$ provides the relation between the source and $\Gamma_k[\phi]$:

$$J(-\mathbf{q}) = \frac{\delta \Gamma_k}{\delta \phi(\mathbf{q})} + \int \frac{d^d \mathbf{q}'}{(2\pi)^{2d}} \mathcal{R}_k(\mathbf{q}, \mathbf{q}') \phi(\mathbf{q}'). \quad (90)$$

Taking the derivative of this relation with respect to $\phi(\mathbf{q}')$ implies a second important relation [211]:

$$\Gamma_k^{(2)}(\mathbf{q}, \mathbf{q}') + \frac{\mathcal{R}_k(\mathbf{q}, \mathbf{q}')}{(2\pi)^{2d}} = \frac{\delta J(-\mathbf{q})}{\delta \phi(\mathbf{q}')} \quad (91)$$

$$= (2\pi)^{-2d} \left(\frac{\delta^2 W_k}{\delta J(\mathbf{q}) \delta J(\mathbf{q}')} \right)^{-1} \quad (92)$$

where $\Gamma_k^{(2)}(\mathbf{q}, \mathbf{q}') = \delta^2 \Gamma_k / \delta \phi(\mathbf{q}) \delta \phi(\mathbf{q}')$.

Let us now show that the definition of Γ_k , Eq. (89), ensures that it satisfies the requirements given in Eq. (77), *i.e.* that it interpolates between the microscopic Hamiltonian H for $k = \infty$ and the (true) effective action Γ for $k \rightarrow 0$. This last property follows directly from Eq. (89) and the fact that for $k = 0$ the IR cut-off $R_k(\mathbf{q}^2)$ identically vanishes. The fact that Γ_k identifies with H when $k \rightarrow \infty$ can be shown in the following way. One deduces from Eqs. (78), (87), (89) and (90) the functional identity:

$$e^{-\Gamma_k[\phi]} = \int \mathcal{D}\zeta \exp \left(-H[\zeta] + \frac{\delta \Gamma_k[\phi]}{\delta \phi} \cdot (\zeta - \phi) - \Delta H_k[\zeta - \phi] \right). \quad (93)$$

In the limit $k \rightarrow \infty$, $R_k(\mathbf{q}^2)$ goes to infinity. In this limit, the mass-term $\exp(-\Delta H_k[\zeta - \phi])$ acts as a hard constraint on the functional integration — $\exp(-\Delta H_k[\zeta - \phi]) \simeq \delta[\zeta - \phi]$ — so that $\Gamma_{k=\infty}[\phi] = H[\phi]$. With these properties, $\Gamma_k[\phi]$ has the meaning of a coarse-grained Gibbs free energy at scale k^{-1} : lowering k corresponds to including more and more fluctuations.

2. The equation

Let us now derive the exact RG equation for Γ_k . We start from the expression:

$$e^{W_k[J]} = \int \mathcal{D}\zeta \exp\left(-H[\zeta] - \Delta H_k[\zeta] + J\zeta\right) \quad (94)$$

which results from Eqs. (78) and (87). One first writes the variation of $\exp(W_k[J])$ with respect to the scale k

$$\begin{aligned} \partial_k e^{W_k[J]} &= \\ &= - \int \mathcal{D}\zeta \left(\partial_k \Delta H_k[\zeta] \right) \exp\left(-H[\zeta] - \Delta H_k[\zeta] + J\zeta\right) \\ &= - \left(\partial_k \Delta H_k \left[\frac{\delta}{\delta J} \right] \right) e^{W_k[J]} \\ &= - \frac{1}{2} \int \frac{d^d \mathbf{q}}{(2\pi)^d} \left(\frac{\delta}{\delta J(\mathbf{q})} \cdot \partial_k R_k(\mathbf{q}^2) \cdot \frac{\delta}{\delta J(-\mathbf{q})} \right) e^{W_k[J]} \end{aligned} \quad (95)$$

from which follows:

$$\begin{aligned} \partial_k W_k[J] &= - \frac{1}{2} \int \frac{d^d \mathbf{q}}{(2\pi)^d} \partial_k R_k(\mathbf{q}^2) \cdot \\ &\cdot \left(\frac{\delta W_k[J]}{\delta J(\mathbf{q})} \frac{\delta W_k[J]}{\delta J(-\mathbf{q})} + \frac{\delta^2 W_k[J]}{\delta J(\mathbf{q}) \delta J(-\mathbf{q})} \right) \end{aligned} \quad (96)$$

which looks like the Polchinski equation (74).

Let us now differentiate the expression (89) with respect to k , at fixed ϕ :

$$\begin{aligned} \partial_k \Gamma_k[\phi] &= -\partial_k W_k[J] \Big|_J - \frac{\delta W_k[J]}{\delta J} \cdot \partial_k J + \\ &+ (\partial_k J) \cdot \phi - \partial_k \Delta H_k[\phi] \quad (97) \\ &= -\partial_k W_k[J] - \partial_k \Delta H_k[\phi] \end{aligned}$$

since $\phi = \frac{\delta W_k}{\delta J}$. Together with Eq. (96) this gives:

$$\partial_k \Gamma_k[\phi] = \frac{1}{2} \int \frac{d^d \mathbf{q}}{(2\pi)^d} \partial_k R_k(\mathbf{q}^2) \frac{\delta^2 W_k[J]}{\delta J(\mathbf{q}) \delta J(-\mathbf{q})} \quad (98)$$

Using Eq. (92) one obtains an equation involving only Γ_k and its second functional derivative $\Gamma_k^{(2)}$ [36, 40, 43, 44]:

$$\begin{aligned} \partial_t \Gamma_k[\phi] &= \frac{1}{2} \int \frac{d^d \mathbf{q}}{(2\pi)^d} \dot{R}_k(\mathbf{q}^2) \cdot \\ &\cdot \text{Tr} \left((2\pi)^{2d} \Gamma_k^{(2)}[\phi] + \mathcal{R}_k \right)^{-1}(\mathbf{q}, -\mathbf{q}) \end{aligned} \quad (99)$$

with $t = \ln k$ and $\dot{R}_k = \partial_t R_k$. In Eq. (99), Tr must be understood as a trace on internal indices — vectorial or tensorial — if ζ spans a nontrivial representation of a group.

Let us finally give a form of Eq. (99) more convenient for practical use [212] :

$$\partial_t \Gamma_k[\phi] = \frac{1}{2(2\pi)^d} \tilde{\partial}_t \text{Tr} \left(\ln \left((2\pi)^{2d} \Gamma_k^{(2)}[\phi] + \mathcal{R}_k \right) \right) \quad (100)$$

where the “time derivative” $\tilde{\partial}_t$ only acts on R_k , *i.e.* $\tilde{\partial}_t \hat{=} \dot{R}_k \partial / \partial R_k$ and where the trace Tr now also means a momentum-integral $\int d^d \mathbf{q} d^d \mathbf{q}' (2\pi)^{-d} \delta(\mathbf{q} + \mathbf{q}')$. Eq. (99) (or Eq. (100)) controls the evolution of Γ_k with the running scale k . According to the preceding discussion, it describes, when k is lowered, how the running effective average action is modified when more and more (low-energy) fluctuations are integrated out.

3. Properties

We now give some important properties of Eq. (99). The reader interested in more details can consult Ref. [45].

1) Eq. (99) is *exact*. It thus contains all perturbative [176, 177] and nonperturbative features of the underlying theory: weak- or strong-coupling behaviors, tunneling between different minima [178], bound states [169, 179], topological excitations [55], etc.

2) While it has been derived here in the case of a one-component scalar field theory, Eq. (99) obviously holds for any number of components and, more generally, for any kind of order parameter. The extension to fermions is also trivial (see [45] for instance).

3) With a cut-off function $R_k(\mathbf{q}^2)$ which meets the condition (81) or, more generally, with a finite limit when $\mathbf{q}^2 \rightarrow 0$, the integral in Eq. (99) is infrared (IR) *finite* for any $k > 0$. This IR finiteness is ensured by the presence of the mass-term R_k which makes the quantity $\Gamma_k^{(2)}[\phi] + R_k$ positive for $k > 0$ even *at* the critical temperature. This allows to explore the low-temperature phase even in presence of massless — Goldstone — modes. From the UV side, the finiteness of the integral in Eq. (99) is ensured by a requirement of fast decaying behavior of $\dot{R}_k(\mathbf{q}^2)$.

4) One can give a graphical representation of Eq. (99), see Fig. 5. It displays a *one-loop* structure. Obviously, this one-loop structure must not be mistaken for that of a weak-coupling expansion. Actually, the loop involves here the *full* — *i.e.* field-dependent — inverse propagator $\Gamma_k^{(2)}[\phi]$ so that the graphical representation of Fig. 5 implicitly contains *all* powers of the coupling constants entering in the model. Note also that this one-loop structure automatically ensures that all integrals over internal momenta involved in this formalism have a one-loop structure and are thus one-dimensional. Thus they can

be easily evaluated numerically and, when some particular cut-off are used, analytically. This radically differs from a weak-coupling expansion which leads to multiple loop diagrams and thus, multiple integrals. Another important feature of Eq. (99) is that very simple *ansätze* on Γ_k allow to recover in a unique framework the one-loop perturbative results obtained by standard perturbative calculations around two and four dimensions as well as in a large- N expansion.

$$\partial_t \Gamma_k = \frac{1}{2} \text{ (Diagram: a circle with a cross inside) }$$

FIG. 5: A graphical representation of Eq. (99). The cross represents the function R_k and the line the propagator $(\Gamma_k^{(2)}(\phi) + R_k)^{-1}$.

Let us make a final remark. The one-loop structure of Eq. (99) contrasts with the Polchinski equation (74) which, in addition to the loop term, involves a tree part (see Fig. 3). An interesting consequence of the structure of this “Legendre version” of the NPRG equation is that reparametrization invariance is preserved by the derivative expansion when a power-law cut-off is used. This means that with such a cut-off function, the anomalous dimension is no longer ambiguously defined [180]. This would apparently select the power-law cut-off as the best one. The situation is, in fact, more involved since the power-law cut-off is afflicted with bad convergence properties when used within the derivative expansion. It has appeared that for instance, the exponential cut-off — Eq. (85) — or the theta cut-off — Eq. (86) — that do not respect the reparametrization invariance of the RG equation, lead to better results when optimization criteria are used. We do not enter into more details in these problems of reparametrization invariance [41, 47, 174, 180] and optimization of the results [49, 50, 175, 181, 182, 183, 184, 185] and refer to the literature. The main reason for this is that, as we shall see in the following, we shall only deal with pseudo-critical exponents that, being given their lack of universality, *i.e.* their strong dependence with respect to the microscopic parameters, makes superfluous an optimization of the computations.

4. Truncations

As it is the case for the Polchinski equation, Eq. (99) is too complicated to be solved exactly. Its nonlinearities are even worse than in the Polchinski case since it involves all powers of $\Gamma_k^{(2)}$. As a consequence, the functional Γ_k has to be truncated. Different kinds of expansions have been considered [44]:

1) Field expansion where Γ_k is expanded in powers of the order parameter ϕ . For a scalar field theory, one has:

$$\Gamma_k[\phi] = \sum_{n=0}^{\infty} \frac{1}{n!} \int \prod_{i=0}^n d^d \mathbf{x}_i \phi(\mathbf{x}_1) \dots \phi(\mathbf{x}_n) \Gamma_k^{(n)}(\mathbf{x}_1, \dots, \mathbf{x}_n) \quad (101)$$

where $\Gamma_k^{(n)}(\mathbf{x}_1, \dots, \mathbf{x}_n)$ denotes the n -th functional derivative of Γ_k .

2) Derivative expansion where Γ_k is expanded in powers of the derivatives of the order parameter. For a scalar field theory, one has:

$$\Gamma_k[\phi] = \int d^d \mathbf{x} \left(U_k(\phi) + \frac{1}{2} Z_k(\phi) (\partial\phi)^2 + O(\partial^4) \right) \quad (102)$$

$U_k(\phi)$ being the potential — *i.e.* derivative-independent — part of Γ_k while $Z_k(\phi)$ corresponds to the kinetic term.

3) Combined derivative and field expansions where one further expands in Eq. (102) the functions $U_k(\phi)$ and $Z_k(\phi)$ in powers of ϕ around a given field configuration ϕ_0 . Technically, this kind of approximation allows to transform the functional equation (99) into a set of ordinary coupled differential equations for the coefficients of the expansion. In practice, it is interesting to consider an expansion around (one of) the field configuration ϕ_0 that minimizes the potential U_k . For the simplest — Ising — model, this expansion writes:

$$\Gamma_k[\phi] = \int d^d \mathbf{x} \left(\frac{1}{2} U_k''(\tilde{\rho}_0) (\rho - \tilde{\rho}_0)^2 + \frac{1}{3!} U_k'''(\tilde{\rho}_0) (\rho - \tilde{\rho}_0)^3 + \dots \right. \\ \left. + \frac{1}{2} Z_k(\tilde{\rho}_0) (\partial\phi)^2 + \frac{1}{2} Z_k'(\tilde{\rho}_0) (\rho - \tilde{\rho}_0) (\partial\phi)^2 + \dots \right) \quad (103)$$

where $\tilde{\rho} = \frac{1}{2} \phi^2$ and $\tilde{\rho}_0 = \frac{1}{2} \phi_0^2$, ϕ_0 being the magnetization at scale k . The rationale behind this choice is that the minimum of U_k is physically the location that we want to describe the best since thermodynamical quantities at vanishing external field are determined from the minimum of Γ_k at $k = 0$. The relevance of such a parametrization is confirmed by many works showing that the convergence of the critical quantities, when more and more powers of the field ϕ are added in the truncation, is improved when compared with the same calculation performed with an expansion of $U_k(\phi)$ and $Z_k(\phi)$ around the $\phi = 0$ configuration [186, 187].

The choice of a good truncation is a complex problem. One has to choose a manageable truncation that however encodes the relevant physics. In practice, it appears that, surprisingly, even at low-orders in powers of derivatives and fields, Eq. (99) provides correct qualitative features of the RG flow. However, the precise determination of the critical quantities requires to push the expansion to rather large orders in the field and involves a heavy algebra [49, 50].

To illustrate how the technique works we now consider the simplest case, *i.e.* the vectorial $O(N)$ model. The $O(N) \times O(2)$ model relevant to frustrated magnets is

technically more involved but the procedure to derive the RG equations follows the same steps. Details of the technicalities in this latter case will be given in Section VII.

D. The $O(N)$ model

We present here the effective average action approach of the $O(N)$ model [44, 188]. We essentially follow the presentation given, for instance, in [44] with some differences, ensuring a self-contained presentation. We use a truncation similar to the one we use to deal with frustrated magnets, *i.e.* where Γ_k is expanded both in derivatives and fields. Let us first consider the derivative expansion of the effective average action for the $O(N)$ model at order ∂^2 :

$$\Gamma_k[\vec{\phi}] = \int d^d \mathbf{x} \left(U_k(\rho) + \frac{1}{2} Z_k(\rho) (\partial \vec{\phi})^2 + \frac{1}{4} Y_k(\rho) (\partial \rho)^2 + O(\partial^4) \right) \quad (104)$$

where $\vec{\phi}$ is a N -component vector field and $\rho = \vec{\phi}^2/2$. In Eq. (104), $U_k(\rho)$ is the potential — *i.e.* derivative-independent — part of Γ_k while $Z_k(\rho)$ and $Y_k(\rho)$ correspond to kinetic terms. These two last terms embody the renormalization for the Goldstone and massive fields, respectively. Note that the term proportional to $(\partial \rho)^2$ is always absent from the GLW action used for a *perturbative* analysis in coupling constant. The reason for this is that, in this context, it is power-counting irrelevant. On the contrary, in the context of the effective average action method, there is no perturbative expansion and, thus, no power-counting argument works. One, however, expects that the terms of lowest degrees in the field (for $d > 2$) and in the derivative are the most important for the long distance physics.

The case $Z_k(\rho) = 1$ and $Y_k(\rho) = 0$ in Eq. (104) corresponds to the LPA. A nontrivial anomalous dimension is obtained by going beyond this simplest truncation. As said above, we use here a truncation that mixes the derivative and field expansions. We thus consider:

$$\Gamma_k[\vec{\phi}] = \int d^d \mathbf{x} \left(\frac{1}{2} U_k''(\tilde{\rho}_0) (\rho - \tilde{\rho}_0)^2 + \frac{1}{3!} U_k'''(\tilde{\rho}_0) (\rho - \tilde{\rho}_0)^3 + \dots + \frac{1}{2} Z_k(\tilde{\rho}_0) (\partial \vec{\phi})^2 + \frac{1}{2} Z_k'(\tilde{\rho}_0) (\rho - \tilde{\rho}_0) (\partial \vec{\phi})^2 + \dots + \frac{1}{4} Y_k(\tilde{\rho}_0) (\partial \rho)^2 + \frac{1}{4} Y_k'(\tilde{\rho}_0) (\rho - \tilde{\rho}_0) (\partial \rho)^2 + \dots \right) \quad (105)$$

where $\tilde{\rho}_0 = \frac{1}{2} \vec{\phi}_0^2$ parametrizes the k -dependent field configuration that minimizes U_k . Since our aim here is only pedagogical and not devoted to the calculation of precise critical quantities, we consider the following *ansatz*

which is limited to the smallest expression providing a nonvanishing anomalous dimension:

$$\Gamma_k[\vec{\phi}] = \int d^d \mathbf{x} \left(\frac{1}{2} Z(\partial \vec{\phi})^2 + \frac{1}{2} \tilde{u}_2 (\rho - \tilde{\rho}_0)^2 \right) \quad (106)$$

where $Z \doteq Z_k(\rho_0)$ and $\tilde{u}_2 \doteq U_k''(\tilde{\rho}_0)$. This approximation looks very much like the GLW Hamiltonian used to study perturbatively the $O(N)$ model, up to a trivial reparametrization. There is, however, a major difference. Here the *ansatz* (106) is *not studied perturbatively* in the $\vec{\phi}^4$ coupling constant \tilde{u}_2 . It is to be inserted in the *exact* RG equation (99).

Let us now establish the RG equations for the coupling constants entering in Eq. (106). The calculation proceeds in four steps:

i) We first define the running coupling constants $\tilde{\rho}_0$, \tilde{u}_2 and Z from functional derivatives of the *ansatz* of Γ_k , Eq. (106). This is analogous to imposing renormalization prescriptions for the renormalized coupling constants in usual perturbative calculations. As in this case, the coupling constants are defined as (combinations of) functional derivatives of Γ_k — the “vertex functions” — taken in a specific field-configuration of the model. However, contrarily to the perturbative approach which is generally performed in the high-temperature phase and thus, around a zero field configuration, we perform this expansion around a nontrivial running field configuration $\vec{\phi}_0$.

ii) We then apply the operator ∂_t on these definitions. This is implemented by the use of the evolution equation (99) or (100). The flow equations for the coupling constants are then expressed as traces of products of vertex functions that are evaluated from the *ansatz* Eq. (106).

iii) The flow equations involve integrals over the internal momentum. It is convenient to express these integrals in terms of dimensionless functions, known as threshold functions [44]. The properties of these functions are such that they make explicit the phenomenon of decoupling of massive modes, see below.

iv) Also, as usual, one introduces dimensionless renormalized quantities to study the scale invariant solutions of the RG equations.

1. Definition of the coupling constants

Let us first choose one of the uniform field configurations that minimize the effective average action Γ_k :

$$\vec{\phi}^{\text{Min}}(\mathbf{x}) = \begin{pmatrix} \phi_0 \\ 0 \\ \vdots \\ 0 \end{pmatrix}, \quad (107)$$

or equivalently:

$$\phi_i^{\text{Min}}(\mathbf{q}) = (2\pi)^d \phi_0 \delta_{i1} \delta(\mathbf{q}) \quad (108)$$

where $\phi_0 = (2\tilde{\rho}_0)^{1/2}$ is a k -dependent quantity. Due to the $O(N)$ symmetry of Γ_k , which is preserved at any t by the RG flow Eq. (99), the choice of a particular direction for $\vec{\phi}^{\text{Min}}$ is irrelevant and thus does not affect the RG equations.

Let us now define the coupling constants. To do this we introduce the notation:

$$\Gamma_{k \{ \alpha_1, \mathbf{p}_1 \}, \dots, \{ \alpha_n, \mathbf{p}_n \}}^{(n)} = \frac{\delta^n \Gamma_k[\phi]}{\delta \phi_{\alpha_1}(\mathbf{p}_1) \dots \delta \phi_{\alpha_n}(\mathbf{p}_n)}. \quad (109)$$

As said above, $\tilde{\rho}_0$ specifies the position of the — running — minimum of Γ_k . It is implicitly defined by:

$$\Gamma_{k \{ \alpha, \mathbf{0} \}}^{(1)} \Big|_{\text{Min}} = 0 \quad (110)$$

where the notation “Min” refers to the configuration given in Eq. (107). Because of our particular choice of $\vec{\phi}^{\text{Min}}$ the previous equality is trivially satisfied for $\alpha = 2, \dots, N$ and we shall consider only the case $\alpha = 1$ in the following.

The coupling constant \tilde{u}_2 is defined along the same line as:

$$\tilde{u}_2 = \frac{(2\pi)^d}{2\tilde{\rho}_0 \delta(\mathbf{0})} \Gamma_{k \{ 1, \mathbf{0} \}, \{ 1, \mathbf{0} \}}^{(2)} \Big|_{\text{Min}}. \quad (111)$$

Finally, the k -dependent field renormalization Z is obtained by considering the term quadratic in momentum of a momentum dependent configuration:

$$Z = \frac{(2\pi)^d}{\delta(\mathbf{0})} \lim_{\mathbf{p}^2 \rightarrow 0} \frac{d}{d\mathbf{p}^2} \left(\Gamma_{k \{ 2, \mathbf{p} \}, \{ 2, -\mathbf{p} \}}^{(2)} \Big|_{\text{Min}} \right). \quad (112)$$

In this last equation, the index 2 specifies a direction orthogonal to that defined by the minimum (see Eq. (107)). Note that one could have considered any of the $N - 1$ directions orthogonal to that defined by the minimum. Note finally that the $\delta(\mathbf{0})$ term appearing in Eqs. (111) and (112) is the volume of the system and is present here since Γ_k is an extensive quantity while the coupling constants are not.

2. The t -derivation

The flow equations for the coupling constants $\tilde{\rho}_0$, \tilde{u}_2 and Z are obtained by derivating, with respect to t , the previous definitions Eqs. (110), (111) and (112).

Let us start by $\tilde{\rho}_0$. One has to take care of the t -dependence of both $\Gamma_{k \{ \alpha, \mathbf{0} \}}^{(1)}$ and its argument, the configuration $\vec{\phi}^{\text{Min}}$ — Eq. (107) — which has a nontrivial t -dependence through that of ϕ_0 :

$$\begin{aligned} & \partial_t \left(\Gamma_{k \{ \alpha, \mathbf{0} \}}^{(1)} \Big|_{\text{Min}} \right) = \\ & = \partial_t \Gamma_{k \{ \alpha, \mathbf{0} \}}^{(1)} \Big|_{\text{Min}} + \Gamma_{k \{ \alpha, \mathbf{0} \}, \{ 1, \mathbf{0} \}}^{(2)} \Big|_{\text{Min}} \frac{(2\pi)^d \partial_t \tilde{\rho}_0}{\sqrt{2\tilde{\rho}_0}} \\ & = 0. \end{aligned} \quad (113)$$

The RG flow for $\tilde{\rho}_0$ follows from this equation, taken for $\alpha = 1$:

$$\partial_t \tilde{\rho}_0 = - \frac{\sqrt{2\tilde{\rho}_0}}{(2\pi)^d \Gamma_{k \{ 1, \mathbf{0} \}, \{ 1, \mathbf{0} \}}^{(2)} \Big|_{\text{Min}}} \partial_t \Gamma_{k \{ 1, \mathbf{0} \}}^{(1)} \Big|_{\text{Min}}. \quad (114)$$

In the same way, one obtains:

$$\begin{aligned} \partial_t \tilde{u}_2 & = \frac{(2\pi)^d}{2\tilde{\rho}_0 \delta(\mathbf{0})} \partial_t \Gamma_{k \{ 1, \mathbf{0} \}, \{ 1, \mathbf{0} \}}^{(2)} \Big|_{\text{Min}} + \\ & + \frac{(2\pi)^d \partial_t \tilde{\rho}_0}{2\tilde{\rho}_0 \delta(\mathbf{0})} \left(- \frac{1}{\tilde{\rho}_0} \Gamma_{k \{ 1, \mathbf{0} \}, \{ 1, \mathbf{0} \}}^{(2)} \Big|_{\text{Min}} + \right. \\ & \left. + \frac{(2\pi)^d}{\sqrt{2\tilde{\rho}_0}} \Gamma_{k \{ 1, \mathbf{0} \}, \{ 1, \mathbf{0} \}, \{ 1, \mathbf{0} \}}^{(3)} \Big|_{\text{Min}} \right) \end{aligned} \quad (115)$$

and:

$$\begin{aligned} \partial_t Z & = \frac{(2\pi)^d}{\delta(\mathbf{0})} \lim_{\mathbf{p}^2 \rightarrow 0} \frac{d}{d\mathbf{p}^2} \left(\partial_t \Gamma_{k \{ 2, \mathbf{p} \}, \{ 2, -\mathbf{p} \}}^{(2)} \Big|_{\text{Min}} + \right. \\ & \left. + \frac{(2\pi)^d \partial_t \tilde{\rho}_0}{\sqrt{2\tilde{\rho}_0}} \Gamma_{k \{ 2, \mathbf{p} \}, \{ 2, -\mathbf{p} \}, \{ 1, \mathbf{0} \}}^{(3)} \Big|_{\text{Min}} \right). \end{aligned} \quad (116)$$

The RG flows for the coupling constants $\tilde{\rho}_0$, \tilde{u}_2 and Z involve successive functional derivatives of $\partial_t \Gamma_k$ with respect to different $\phi_i(\mathbf{q}_i)$. These quantities are easily obtained from Eq. (100). Let us take its derivative with respect to $\phi_{i_1}(\mathbf{q}_1)$. Using:

$$\begin{aligned} \frac{\delta}{\delta \phi_{i_1}(\mathbf{q}_1)} \ln \left((2\pi)^{2d} \Gamma_k^{(2)} + \mathcal{R}_k \right) & = \\ & = (2\pi)^{2d} \Gamma_{k \{ i_1, \mathbf{q}_1 \}}^{(3)} \cdot \mathcal{P}_r, \end{aligned} \quad (117)$$

where we have introduced the notation:

$$\mathcal{P}_r = \left((2\pi)^{2d} \Gamma_k^{(2)} + \mathcal{R}_k \right)^{-1} \quad (118)$$

one obtains:

$$\partial_t \Gamma_{k \{ i_1, \mathbf{q}_1 \}}^{(1)} = \frac{(2\pi)^d}{2} \tilde{\partial}_t \text{Tr} \left\{ \Gamma_{k \{ i_1, \mathbf{q}_1 \}}^{(3)} \cdot \mathcal{P}_r \right\} \quad (119)$$

for the one-point vertex function. Note that, in the right hand side of the preceding expression, we have only specified the external indices $\{ i_1, \mathbf{q}_1 \}$ and omitted the integrated (or summed over) variables. The dot is here to remind that these integrations and summations have to be performed. The equation (119) admits a graphical representation:

$$\partial_t \Gamma_{k \{ i_1, \mathbf{q}_1 \}}^{(1)} = \frac{(2\pi)^d}{2} \tilde{\partial}_t \text{---} \bigcirc \text{---}. \quad (120)$$

In this representation, the external leg implicitly carries an index of internal symmetry i_1 and a momentum \mathbf{q}_1 . Now taking the derivative of Eq. (119) with respect to $\phi_{i_2}(\mathbf{q}_2)$ and using:

$$\frac{\delta}{\delta \phi_i(\mathbf{q})} \mathcal{P}_r = - \mathcal{P}_r \cdot \Gamma_{k \{ i, \mathbf{q} \}}^{(3)} \cdot \mathcal{P}_r, \quad (121)$$

one obtains:

$$\begin{aligned} \partial_t \Gamma_k^{(2)} \{i_1, \mathbf{q}_1\}, \{i_2, \mathbf{q}_2\} &= \frac{(2\pi)^d}{2} \tilde{\partial}_t \text{Tr} \left\{ \Gamma_k^{(4)} \{i_1, \mathbf{q}_1\}, \{i_1, \mathbf{q}_2\} \cdot \mathcal{P}_r - \right. \\ &\quad \left. - \Gamma_k^{(3)} \{i_1, \mathbf{q}_1\} \cdot \mathcal{P}_r \cdot \Gamma_k^{(3)} \{i_2, \mathbf{q}_2\} \cdot \mathcal{P}_r \right\} \end{aligned} \quad (122)$$

which can be graphically represented by:

$$\partial_t \Gamma_k^{(2)} \{i_1, \mathbf{q}_1\}, \{i_2, \mathbf{q}_2\} = \frac{(2\pi)^d}{2} \tilde{\partial}_t \left(\text{---} \bigcirc \text{---} - \text{---} \bigcirc \text{---} \right) \quad (123)$$

3. The renormalization group flow

We now explicitly write the flow equations for the coupling constants. This requires to know the vertex functions taken at the minimum $\Gamma_k^{(n)} \{ \alpha_1, \mathbf{p}_1 \}, \{ \alpha_2, \mathbf{p}_2 \}, \dots, \{ \alpha_n, \mathbf{p}_n \} \Big|_{\text{Min}}$ appearing in Eqs. (114), (115) and (116). To evaluate them, one uses the truncation Eq. (106). One obtains:

$$\begin{cases} \Gamma_k^{(1)} \{i_1, \mathbf{q}_1\} \Big|_{\text{Min}} = 0 \\ \Gamma_k^{(2)} \{i_1, \mathbf{q}_1\}, \{i_2, \mathbf{q}_2\} \Big|_{\text{Min}} = (Z \mathbf{q}_1^2 \delta_{i_1 i_2} + 2\tilde{\rho}_0 \tilde{u}_2 \delta_{i_1 1} \delta_{i_2 1}) \frac{\delta(\mathbf{q}_1 + \mathbf{q}_2)}{(2\pi)^d} \\ \Gamma_k^{(3)} \{i_1, \mathbf{q}_1\}, \{i_2, \mathbf{q}_2\}, \{i_3, \mathbf{q}_3\} \Big|_{\text{Min}} = \sqrt{2\tilde{\rho}_0} \tilde{u}_2 (\delta_{i_1 i_2} \delta_{i_3 1} + \delta_{i_2 i_3} \delta_{i_1 1} + \delta_{i_3 i_1} \delta_{i_2 1}) \frac{\delta(\mathbf{q}_1 + \mathbf{q}_2 + \mathbf{q}_3)}{(2\pi)^{2d}} \\ \Gamma_k^{(4)} \{i_1, \mathbf{q}_1\}, \{i_2, \mathbf{q}_2\}, \{i_3, \mathbf{q}_3\}, \{i_4, \mathbf{q}_4\} \Big|_{\text{Min}} = \tilde{u}_2 (\delta_{i_1 i_2} \delta_{i_3 i_4} + \delta_{i_1 i_3} \delta_{i_2 i_4} + \delta_{i_1 i_4} \delta_{i_2 i_3}) \frac{\delta(\mathbf{q}_1 + \mathbf{q}_2 + \mathbf{q}_3 + \mathbf{q}_4)}{(2\pi)^{3d}} \end{cases} \quad (124)$$

In this last set of equations, $\Gamma_k^{(2)} \{i_1, \mathbf{q}_1\}, \{i_2, \mathbf{q}_2\} \Big|_{\text{Min}}$ is of particular interest since its inverse provides the propagator \mathcal{P}_r at scale k and, thus, the spectrum of excitations of the theory, at *this scale*. We easily get from Eq. (124):

$$\begin{aligned} \mathcal{P}_r \{i_1, \mathbf{q}_1\}, \{i_2, \mathbf{q}_2\} \Big|_{\text{Min}} &= (2\pi)^d \delta(\mathbf{q}_1 + \mathbf{q}_2) \cdot \\ &\begin{cases} \frac{1}{Z \mathbf{q}_1^2 + R_k(\mathbf{q}_1^2)} & \text{if } i_1 = i_2 = 1 \\ \frac{1}{Z \mathbf{q}_1^2 + R_k(\mathbf{q}_1^2) + 2\tilde{\rho}_0 \tilde{u}_2} & \text{if } i_1 = i_2 \neq 1 \\ 0 & \text{if } i_1 \neq i_2 \end{cases} \end{aligned} \quad (125)$$

where $R_k(\mathbf{q}_1^2)$ is the contribution of the regulating term (80).

It is clear on the expression (125) that the $N \times N$ matrix $\mathcal{P}_r \{i_1, \mathbf{q}_1\}, \{i_2, \mathbf{q}_2\} \Big|_{\text{Min}}$ is diagonal. This holds independently of the kind of truncation used. The spectrum of excitations around the minimum, at scale k , is thus directly read on Eq. (125). We find — up to the R_k term — one massive mode of squared mass $2\tilde{\rho}_0 \tilde{u}_2$ in the longitudinal direction and $N - 1$ massless modes in the directions orthogonal to the magnetization $\vec{\phi}_0$. The deformations of the vector $\vec{\phi}$ associated to these modes are represented in Fig. 6.

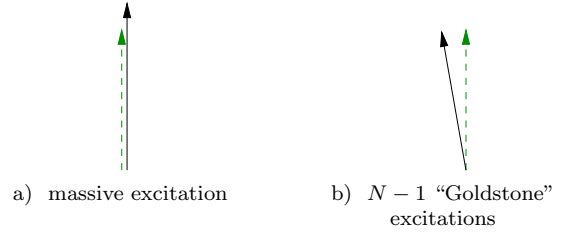


FIG. 6: Schematic description of the deformations of the vector $\vec{\phi}$ associated with the proper excitations of the $O(N)$ model: dotted arrows display the configuration chosen at the minimum of Γ_k and plain arrows display the relevant deformations: a) massive singlet, b) “Goldstone” $N - 1$ -uplet.

It is important to keep in mind that this spectrum corresponds to effective masses — at scale k — for which only high-momentum fluctuations — higher than k — have been considered. It is only in the limit $k \rightarrow 0$ that one retrieves the physical spectrum. In particular, we stress that a qualitative change in the spectrum can occur when k is varied. For instance, the following situation can happen: for large k , the minimum of U_k is nonvanishing so that, at this scale, the system behaves as if it was in its broken phase. However, when k is decreased, the minimum moves toward zero and eventually vanishes for some $k > 0$. Thus, while the system, for $k = \Lambda$, looks as if it was in its broken phase, it is actually, *i.e.* for

$k = 0$, in the high-temperature phase. This is what happens when the temperature lies between the true critical and the mean-field critical temperature. Another subtlety is that, in order to analyze the critical behavior, we have to consider the dimensionless renormalized quantities. Again, one has to be careful about the conclusions deduced from the behavior of these quantities. For instance, the dimensionless renormalized position of the minimum at $k = 0$ can be nonvanishing even at the critical temperature whereas the “true” magnetization is, of course, vanishing at T_c . This is possible since the dimensionful quantities are the products of their dimensionless counterparts and of positive powers of k .

Using Eqs. (114), (115), (116), (119), (122) and (124), one obtains the flow for $\tilde{\rho}_0$:

$$\partial_t \tilde{\rho}_0 = -\frac{1}{2} \tilde{\partial}_t \int \frac{d^d \mathbf{q}}{(2\pi)^d} \left(\frac{N-1}{Z\mathbf{q}^2 + R_k(\mathbf{q}^2)} + \frac{3}{Z\mathbf{q}^2 + R_k(\mathbf{q}^2) + 2\tilde{\rho}_0 \tilde{u}_2} \right), \quad (126)$$

for \tilde{u}_2 :

$$\partial_t \tilde{u}_2 = -\frac{\tilde{u}_2^2}{2} \tilde{\partial}_t \int \frac{d^d \mathbf{q}}{(2\pi)^d} \left(\frac{N-1}{(Z(\mathbf{q}^2 + R_k(\mathbf{q}^2))^2)} + \frac{9}{(Z\mathbf{q}^2 + R_k(\mathbf{q}^2) + 2\tilde{\rho}_0 \tilde{u}_2)^2} \right), \quad (127)$$

and for the field renormalization Z :

$$\partial_t Z = -2\tilde{\rho}_0 \tilde{u}_2^2 \lim_{\mathbf{p}^2 \rightarrow 0} \frac{d}{d\mathbf{p}^2} \left(\tilde{\partial}_t \int \frac{d^d \mathbf{q}}{(2\pi)^d} \frac{1}{Z\mathbf{q}^2 + R_k(\mathbf{q}^2)} \cdot \frac{1}{Z(\mathbf{p} + \mathbf{q})^2 + R_k((\mathbf{p} + \mathbf{q})^2) + 2\tilde{\rho}_0 \tilde{u}_2} \right). \quad (128)$$

The search for fixed point requires to introduce dimensionless renormalized coupling constants. We define:

$$\begin{cases} \rho_0 = Zk^{2-d} \tilde{\rho}_0 \\ u_2 = Z^{-2} k^{d-4} \tilde{u}_2. \end{cases} \quad (129)$$

These changes of variables are devised so that k and Z disappear from the flow equations of the renormalized dimensionless quantities.

The corresponding flow equations thus write:

$$\begin{cases} \partial_t \rho_0 = -(d-2+\eta)\rho_0 + 2v_d(N-1)l_1^d(0) + 6v_d l_1^d(2u_2\rho_0) \\ \partial_t u_2 = (d-4+2\eta)u_2 + 2v_d(N-1)u_2^2 l_2^d(0) + 18v_d u_2^2 l_2^d(2u_2\rho_0) \end{cases} \quad (130)$$

that depend on Z only through η , the running “anomalous dimension”:

$$\eta = -\partial_t \log Z. \quad (131)$$

In our truncation, it is given by:

$$\eta = \frac{16v_d}{d} u_2^2 \rho_0 m_{2,2}^d(2u_2\rho_0). \quad (132)$$

The usual anomalous dimension is given by the fixed point value of Eq. (132). In Eqs. (130) and (132), we have introduced the — dimensionless — threshold functions l_n^d and $m_{2,2}^d$:

$$\begin{cases} l_n^d(w) = -\frac{Z^n k^{-d+2n}}{4v_d} \tilde{\partial}_t \int \frac{d^d \mathbf{q}}{(2\pi)^d} \frac{1}{(Z\mathbf{q}^2 + R_k(\mathbf{q}^2) + Zk^2 w)^n} \\ m_{2,2}^d(w) = -\frac{dZ^2 k^{6-d}}{8v_d} \lim_{\mathbf{p}^2 \rightarrow 0} \frac{d}{d\mathbf{p}^2} \left(\tilde{\partial}_t \int \frac{d^d \mathbf{q}}{(2\pi)^d} \cdot \frac{1}{Z\mathbf{q}^2 + R_k(\mathbf{q}^2)} \cdot \frac{1}{Z(\mathbf{p} + \mathbf{q})^2 + R_k((\mathbf{p} + \mathbf{q})^2) + Zk^2 w} \right) \end{cases} \quad (133)$$

with $v_d^{-1} = 2^{d+1} \pi^{d/2} \Gamma(d/2)$. Some properties of these threshold functions are provided in the Appendix C. We concentrate here on the main physical aspects of the threshold functions:

1) Note first that the arguments of the threshold functions entering in Eqs. (130) and (132) are either 0 or $2u_2\rho_0$ that are — up to $R_k(\mathbf{q}^2)$ — the dimensionless renormalized square masses associated with the excitations around the minimum.

2) The threshold functions $l_n^d(w)$ and $m_{2,2}^d(w)$ decrease as power-laws when their arguments increase:

$$\begin{cases} l_n^d(w) \propto w^{-n-1} \\ m_{2,2}^d(w) \propto w^{-2} \end{cases} \quad (134)$$

for $w \gg 1$. The RG equation (99) makes thus explicit the phenomenon of decoupling of massive modes: if the renormalized square mass M_k^2 — here $2u_2\rho_0$ — of a massive mode increases when the scale k is lowered, the contribution of this mode to the flow becomes negligible below a scale k_c defined by $M_{k_c} \sim 1$.

3) The threshold functions are nonpolynomial functions of their arguments. Thus the flow equations (130) and (132) are nonperturbative with respect to the coupling constant u_2 as well as to $1/\rho_0$ which, as we shall see, is proportional to the coupling constant — the temperature T — that parametrizes the perturbative expansion of NL σ model.

As we now show, the effective average action approach allows to recover the perturbative results obtained at low-temperature around $d = 2$, at weak-coupling around $d = 4$ and in a $1/N$ expansion.

4. The weak-coupling expansion around $d = 4$

Just below four dimensions, the nontrivial fixed point governing the phase transition of the $O(N)$ model is very close to the Gaussian fixed point. This justifies to expand the RG flow equations (130) and (132) both in the coupling constant u_2 and in $\epsilon = 4 - d$. At lowest order, the function η is vanishing. Since ρ_0 remains finite, the quantity $2u_2\rho_0$ is of order ϵ and one can perform a small mass expansion. The flows of the coupling u_2 and of ρ_0 are obtained using $l_n^d(\omega) \simeq l_n^d(0) - n\omega l_{n+1}^d(0)$ for $\omega \ll 1$ and $l_2^4(0) = 1$. This leads to:

$$\begin{cases} \partial_t \rho_0 = -(2 - \epsilon)\rho_0 + \frac{(N + 2)}{16\pi^2} l_1^4(0) - \frac{3}{8\pi^2} u_2 \rho_0 \\ \partial_t u_2 = -\epsilon u_2 + \frac{N + 8}{16\pi^2} u_2^2. \end{cases} \quad (135)$$

At leading order, the roots of these equations are the gaussian fixed point — $u_2^* = 0$ and $\rho_0^* = (N + 2)l_1^4(0)/32\pi^2$ — and a nontrivial fixed point obtained for $u_2^* = 16\pi^2\epsilon/(N + 8)$ and $\rho_0^* = (N + 2)l_1^4(0)/32\pi^2$. One easily deduces the critical exponent ν from Eqs. (135), linearized around the nontrivial fixed point:

$$\nu = \frac{1}{2} + \frac{\epsilon}{4} \frac{N + 2}{N + 8}. \quad (136)$$

It coincides with the one-loop expression obtained within a perturbative weak-coupling approach of the corresponding GLW model in $d = 4 - \epsilon$.

5. The low-temperature expansion around $d = 2$

Let us now show that Eq. (99) also allows to recover the one-loop results obtained around two dimensions in a low-temperature expansion of the NL σ model. We first make contact between the parameters — essentially the temperature — of the $O(N)$ NL σ model and those of the effective average action (106).

The partition function of the $O(N)$ NL σ model is given by:

$$\mathcal{Z} = \int \mathcal{D}\vec{\phi} \delta(\vec{\phi}^2 - 1) \exp\left(-\frac{1}{2T} \int d^d\mathbf{x} (\partial\vec{\phi})^2\right). \quad (137)$$

Let us replace the delta-constraint by a soft constraint. Using the field redefinition $\vec{\phi} \rightarrow \vec{\phi}\sqrt{T}$ one obtains:

$$\mathcal{Z} = \int \mathcal{D}\vec{\phi} \exp\left[-\frac{1}{2} \int d^d\mathbf{x} \left((\partial\vec{\phi})^2 - \lambda(\vec{\phi}^2 T - 1)^2\right)\right] \quad (138)$$

where the delta-constraint is recovered when $\lambda \rightarrow \infty$. Comparing this expression with the *ansatz* (106) and using the relation (129) one obtains the relation:

$$T = \frac{1}{2\rho_0}. \quad (139)$$

As a consequence, the low-temperature one-loop perturbative results can be recovered from a $1/\rho_0$ expansion. In fact, since the dimensionless renormalized mass of the massive modes is given by $2u_2\rho_0$, one has to perform a large-mass expansion. Physically, this corresponds to the known fact that, around two dimensions, the longitudinal modes of the $O(N)$ linear model are frozen and only the — transverse — “Goldstone” fluctuations are activated. This phenomenon corresponds to the decoupling of massive modes. Technically, this is realized through the behavior of the threshold functions. As already stated, the threshold functions decrease as power-laws for large arguments, Eq. (134). As a consequence, in the flow equations (130), the contribution of the massive mode — which is proportional to $l_n^d(2\rho_0\lambda)$ — is subdominant compared with the contribution of the Goldstone modes — proportional to $l_n^d(0)$. Now, using the large-mass expansion $m_{2,2}^{d=2}(\omega) = \omega^{-2} + O(\omega^{-3})$, one gets from Eq. (132):

$$\eta \simeq \frac{1}{4\pi\rho_0}. \quad (140)$$

Using this expression of the anomalous dimension and the value $l_1^2(0) = 1$, one gets:

$$\begin{cases} \partial_t \rho_0 \simeq -\epsilon\rho_0 + \frac{N - 2}{4\pi} \\ \partial_t u_2 \simeq -2u_2 + \frac{N - 1}{4\pi} u_2^2 l_2^2(0). \end{cases} \quad (141)$$

The flow equation for ρ_0 coincides exactly with the result obtained in the one-loop low-temperature expansion of the NL σ model for the temperature — which is given by Eq. (139). The fixed point coordinates are given by: $\rho_0^* = (N - 2)/(4\pi\epsilon)$ and $u_2^* = 8\pi/((N - 1)l_2^2(0))$. This leads to the critical exponents:

$$\begin{cases} \eta = \frac{\epsilon}{N - 2} \\ \nu = \frac{1}{\epsilon} \end{cases} \quad (142)$$

which identify with those given by the low-temperature perturbative expansion of the NL σ model at one-loop [162].

Note that the perturbative β function for u_2 — Eq. (135) — and for ρ — Eq. (141) — are *universal*, *i.e.* independent of the cut-off function $R_k(\mathbf{q})$. Indeed, these β functions only depend on the values of the threshold functions $l_n^d(\omega)$ at $\omega = 0$ and on $m_{2,2}^{d=2}(\omega)$ at large ω that, as shown in Appendix C 3, do not depend on the cut-off function $R_k(\mathbf{q})$. The matching with the perturbative results obtained around $d = 2$ and $d = 4$ is a very important feature of the effective average action method. First, it allows to interpolate smoothly between two and four dimensions in a unified framework. Second, it suggests that it is possible to reliably explore the behavior of the system in any dimension d and, in particular in $d = 3$, see below.

6. The large- N analysis

The flow equations (130) and (132) can easily be expanded in the large- N limit. The leading contributions come from the Goldstone modes, which appear with a multiplicative factor N . The β functions then read:

$$\begin{cases} \partial_t \rho_0 = (2-d)\rho_0 + 2N v_d l_1^d(0) \\ \partial_t u_2 = (d-4)u_2 + 2N v_d u_2^2 l_2^d(0) \end{cases} \quad (143)$$

where we have anticipated that the anomalous dimension vanishes at leading order, see below. The fixed point solutions are easily found to be: $\rho_0^* = 2N v_d l_1^d(0)/(d-2)$ and $u_2^* = (d-4)/(2v_d N l_2^d(0))$. From these results, we check that the anomalous dimension behaves like $1/N$ and thus gives subdominant corrections to the β functions. We can, finally, compute the critical exponents by diagonalizing the stability matrix. We then find $\nu = 1/(d-2)$, in agreement with the standard leading order result of the $1/N$ expansion.

We now check that the effective average action method provides reliable results in three dimensions.

7. The critical exponents in three dimensions

One of the main interest of the effective average action method is its ability to tackle with the physics in a nonperturbative regime, precisely when there is no small parameter, as it is the case in three dimensions. We provide, in Table VIII, the critical exponents ν and η obtained with this method, as functions of the order of the derivative and field expansions of $U_k(\rho)$, $Z_k(\rho)$ and $Y_k(\rho)$ (see Eq. (105)). We have also included the results of high-order perturbative expansion for comparison. The exponent ν is rather poorly determined with our simple truncation (106). However, the precision improves rapidly when more terms are added to the *ansatz* for Γ_k . For the best truncation, ν is determined at less than one percent compared with the world best estimates. Although we shall not be concerned in the following in truncations using the *full* potential $U_k(\rho)$ and the *full* kinetic terms $Z_k(\rho)$ and $Y_k(\rho)$ entering in Eq. (104), we have indicated, in Table VIII, the critical exponents computed with such *ansätze*. One notes that ν is in very good agreement with seven-loop resummed series [189] while the anomalous dimension is less precisely determined until the order ∂^4 terms of the derivative expansion have been included in the *ansatz*, see [50].

8. The XY and multicritical Ising models in two dimensions

Let us close this section devoted to the analysis of the $O(N)$ model by a discussion of the results obtained in $d = 2$ for the XY and Ising models. These are, in fact, two of

N	ν		η	
1	0.520 ^{a)}	0.6290(25) ^{g)}	0.057 ^{a)}	0.036(5) ^{g)}
	0.688 ^{b)}	0.6304(13) ^{h)}	0.038 ^{b)}	0.0335(15) ^{h)}
	0.635 ^{c)}		0.056 ^{c)}	
	0.635 ^{d)}		0.058 ^{d)}	
	0.6307 ^{e)}		0.0467 ^{e)}	
	0.632 ^{f)}		0.033 ^{f)}	
2	0.613 ^{a)}	0.6680(35) ^{g)}	0.058 ^{a)}	0.038(5) ^{g)}
	0.722 ^{b)}	0.6703(15) ^{h)}	0.038 ^{b)}	0.0354(25) ^{h)}
	0.683 ^{c)}		0.054 ^{c)}	
	0.666 ^{d)}		0.055 ^{d)}	
	0.666 ^{e)}		0.049 ^{e)}	
3	0.699 ^{a)}	0.7045(55) ^{g)}	0.051 ^{a)}	0.0375(45) ^{g)}
	0.756 ^{b)}	0.7073(35) ^{h)}	0.035 ^{b)}	0.0355(25) ^{h)}
	0.726 ^{c)}		0.051 ^{c)}	
	0.712 ^{d)}		0.048 ^{d)}	
	0.704 ^{e)}		0.049 ^{e)}	

TABLE VIII: The critical exponents in three dimensions for the $O(N)$ model. *a)* corresponds to the truncation where only the flow of $\{Z, \rho_0, u_2\}$ is considered. In *b)* one adds u_3 . In *c)*, one adds $\{u_3, u_4, Y(\rho_0)\}$ and in *d)* $\{u_3, u_4, Y_0, Z'(\rho_0)\}$. *e)* takes into account the full dependence of U_k , Z_k and Y_k in the field [55]. In *f)*, the order ∂^4 terms of the derivative expansion have been included [50]. *g)* corresponds to the five-loop resummed perturbative results in $4 - \epsilon$ [189]. *h)* are seven-loop perturbative results in three dimensions [189].

its most spectacular successes because they correspond to truly nonperturbative systems.

As well known, the physics of the XY model at finite temperature is governed by topologically nontrivial configurations — vortices — which are not taken into account in a low-temperature treatment. According to Eq. (141), the flow for ρ_0 — or T — vanishes identically in $d = 2$ and $N = 2$ so that the theory is free. However, as well known, the model actually exhibits a phase transition at a finite temperature T_{BKT} — the Berezinskii-Kosterlitz-Thouless phase transition — induced by the deconfinement of the vortices, see [52, 53]. Remarkably, the simplest RG equations (130) and (132) already allow to obtain the correct qualitative behavior of the XY model at finite temperature: a very small β -function of T is found between $T = 0$ and a finite T_{BKT} [54]. Recently, treating the full field-dependence of U_k , Z_k and Y_k , von Gersdorff and Wetterich [55] have recovered the correct behavior for the correlation length of the XY model around T_{BKT} :

$$\xi \simeq \exp\left(\frac{\text{Cte}}{(T - T_{\text{BKT}})^\tau}\right). \quad (144)$$

The exact results are $\tau = 1/2$ and $\eta = 1/4$ for the anomalous dimension at T_{BKT} [53, 190] while von Gersdorff and Wetterich have found $\tau = 0.502$ and $\eta = 0.287$. This shows that the physics of topological excitations is captured by the lowest orders of the derivative expansion, without including explicitly these degrees of freedom *à la* Villain [191].

As for the Ising model, it is known that, in two dimensions, it can undergo infinitely many nontrivial kinds of phase transitions associated with infinitely many multicritical fixed points [192]. It is shown in Ref.[14] that they all correspond to strong coupling fixed points. They are therefore very difficult to study by perturbative means. By a systematic search of fixed points in the two-dimensional scalar field theory, using an order ∂^2 truncation of the derivative expansion, Morris [61] has been able to find explicitly the first ten fixed points of this series. He has also shown that no other fixed point exists but the multicritical fixed points.

9. A difficulty related to the field expansion

Let us finally mention a difficulty linked to the field expansion of the potential U_k showing up, for instance, when the stable fixed point of the $O(N)$ model is followed from $d = 4$ down to $d = 2$. When the simplest ϕ^4 truncation, Eq. (106), is used no problem occurs: one can smoothly follow the stable — critical — fixed point from $d = 4$, where it identifies with that found in a weak coupling expansion of the GLW model, down to $d = 2$, where it coincides with that obtained within a low-temperature expansion of the $NL\sigma$ model, Eq. (141). However, once the ϕ^6 term is added, a new nontrivial fixed point emerges from the Gaussian fixed point in $d = 3$. This is a tricritical fixed point, *i.e.* a fixed point with two directions of instabilities. As d is lowered, the critical and tricritical fixed points move closer together and eventually coalesce in a dimension $2 < d < 3$. Actually, they both become complex. Note that when d is further lowered, the two fixed points become again real. In $d = 2 + \epsilon$, the stable fixed point can be identified with that found within the low-temperature expansion of the $NL\sigma$ model with the ϕ^4 truncation. Thus, there exists a small region between $d = 2$ and $d = 3$ where one fails to correctly describe the fate of the stable fixed point of the model using the ϕ^6 truncation. However, this is just an artefact of the field expansion, not of the method. To show this, let us describe what happens when the order p of the truncation is increased. First, when including a new monomial ϕ^p in the effective potential, a new — multicritical — fixed point emerges from the Gaussian fixed point in the dimension $2p/(p-2)$. Again the stable fixed point coalesces with one of these multicritical points and reappears close to $d = 2$. Second, as p increases, the coalescence of the stable fixed point occurs at smaller and smaller dimensions. Thus, one recovers a better and better description when increasing the order of the truncation. Also, it has been checked that when the full field-dependence of the potential is kept, the problem fully disappears and the stable fixed point can be followed smoothly between $d = 4$ and $d = 2$ [193]. Finally, it is important to indicate that, in the whole range of dimensions where the stable fixed point exists within a field expansion, the critical exponents found within this approach at sufficiently large order p ($p \geq 10$) and those found within a full poten-

tial computation are very close. The artefact of the field expansion described here can be bypassed using either a full potential computation or using a field expansion at sufficiently high order. Actually, it is not surprising that difficulties occur with the field expansion at low dimensions since the engineering dimension of the field vanishes as $d \rightarrow 2$. This strongly suggests that no power of the field can be safely discarded in U_k when $d \rightarrow 2$. This is confirmed by the fact that the effective potential, which is exactly known at $N = \infty$ for $d = 3$ and $d = 2$, is respectively a polynomial of order six and an infinite series.

E. Conclusion

We have described, in this section, the main features of the effective average action method. We now summarize them:

1) The effective average action method allows trivially to recover the perturbative results around the upper — $d = 4$ — and lower — $d = 2$ — critical dimensions and thus to make contact with these approaches.

2) The results obtained via this method are nonperturbative in the different parameters: coupling constant and temperature. In this sense, it provides an alternative approach to the usual perturbative methods. This is of great interest, especially when one suspects that the perturbative series could be not reliable as it is the case for frustrated magnets.

3) Even with a very simple truncation of the effective average action, it is possible to capture some genuine nonperturbative features — like nontrivial topological configurations — that are unreachable from a conventional low-temperature expansion. This aspect is particularly important in the context of frustrated magnets since one knows that the low-temperature expansion performed in $d = 2 + \epsilon$ does not provide the correct physics in $d = 3$, a possible explanation being the presence of vortex-like configurations in these systems.

VII. THE $O(N) \times O(2)$ MODEL

We now come back to the study of frustrated magnets. We derive the flow equations relevant to the study of frustrated magnets. The derivation follows the same lines as in the $O(N)$ case (see Section VI D above).

A. Truncation procedure

As emphasized previously, since the NPRG equation (100) cannot be solved exactly, a truncation for Γ_k is needed. We consider here a truncation involving only terms having at most two derivatives. At this order, the most general form of the $O(N) \times O(2)$ effective average action writes:

$$\Gamma_k[\vec{\phi}_1, \vec{\phi}_2] = \int d^d \mathbf{x} \left(U_k(\rho, \tau) + \frac{1}{2} Z_k(\rho, \tau) \left((\partial \vec{\phi}_1)^2 + (\partial \vec{\phi}_2)^2 \right) + \frac{1}{4} Y_k^{(1)}(\rho, \tau) \left(\vec{\phi}_1 \cdot \partial \vec{\phi}_2 - \vec{\phi}_2 \cdot \partial \vec{\phi}_1 \right)^2 + \right. \\ \left. + \frac{1}{4} Y_k^{(2)}(\rho, \tau) \left(\vec{\phi}_1 \cdot \partial \vec{\phi}_1 + \vec{\phi}_2 \cdot \partial \vec{\phi}_2 \right)^2 + \frac{1}{4} Y_k^{(3)}(\rho, \tau) \left(\left(\vec{\phi}_1 \cdot \partial \vec{\phi}_1 - \vec{\phi}_2 \cdot \partial \vec{\phi}_2 \right)^2 + \left(\vec{\phi}_1 \cdot \partial \vec{\phi}_2 + \vec{\phi}_2 \cdot \partial \vec{\phi}_1 \right)^2 \right) \right). \quad (145)$$

We recall that $\vec{\phi}_1$ and $\vec{\phi}_2$ are the two N -component vectors that constitute the order parameter, Eq. (8) while $\rho = \text{Tr}(^t \Phi \cdot \Phi)$ and $\tau = \frac{1}{2} \text{Tr}(^t \Phi \cdot \Phi - \mathbb{1} \rho/2)^2$ — with $\Phi = (\vec{\phi}_1, \vec{\phi}_2)$ — are the two independent $O(N) \times O(2)$ invariants (see Appendix B for a more detailed discussion). The truncation (145) is the analogue of Eq. (104), in the case of matrix fields. Here $U_k(\rho, \tau)$ is the potential part of the effective average action while $Z_k(\rho, \tau)$ and $Y_k^{(i)}(\rho, \tau)$, $i = 1, 2, 3$, are kinetic functions.

At this level of approximation, the RG analysis requires to specify the five functions U_k , Z_k and $Y_k^{(i)}$, $i = 1, 2, 3$. This is to say an infinite number of coupling constants. As in the case of the vectorial $O(N)$ model, we further simplify the *ansatz* by expanding these functions in powers of the fields. Again, we choose to expand around a nonvanishing field configuration which minimizes Γ_k . This constraint is satisfied when $\vec{\phi}_1$ and $\vec{\phi}_2$ are orthogonal, with the same norm. We choose:

$$\Phi^{\text{Min}}(\mathbf{x}) = \sqrt{\tilde{\kappa}} \begin{pmatrix} 1 & 0 \\ 0 & 1 \\ 0 & 0 \\ \vdots & \vdots \\ 0 & 0 \end{pmatrix} \quad (146)$$

the physical results being independent of this particular choice. The quantity $\sqrt{\tilde{\kappa}}$ entering in Eq. (146) is analogous to the quantity ϕ_0 in the $O(N)$ case, see Eq. (107) and we refer to it in the following as the magnetization.

While studying the critical properties of the system, we have considered various truncations differing by the number of monomials in ρ and τ included in the field expansion. Our largest truncations consist either in keeping all terms in U_k up to the eighth power of the fields and all terms in Z_k and in the $Y_k^{(i)}$'s including four powers of the fields or all terms in U_k up to the tenth power of the fields and the first term of the expansions of Z_k and of $Y_k^{(1)}$. With these truncations, we have verified that our results are stable with respect to addition of higher powers of the fields. However, in order to keep our presentation concise, we have chosen here to consider a reduced truncation that already enables to recover the different perturbative results — in $4 - \epsilon$, $2 + \epsilon$ and $1/N$ — in their respective domains of validity. Within this truncation, we expand U_k up to terms containing four powers of the fields and keep only the leading terms of Z_k and $Y_k^{(1)}$. We also completely discard the two other functions $Y_k^{(2)}$ and $Y_k^{(3)}$. This choice is motivated by the fact that, as we

will see in the next section, only the function $Y_k^{(1)}$ contributes directly to the physics of the Goldstone modes and is thus important around two dimensions. Since one of our aims is to recover the results obtained around two dimensions, we keep this term in our *ansatz*. We are then led to the simple truncation:

$$\Gamma_k[\vec{\phi}_1, \vec{\phi}_2] = \int d^d \mathbf{x} \left(\frac{Z}{2} \left((\partial \vec{\phi}_1)^2 + (\partial \vec{\phi}_2)^2 \right) + \frac{\tilde{\omega}}{4} \left(\vec{\phi}_1 \cdot \partial \vec{\phi}_2 - \vec{\phi}_2 \cdot \partial \vec{\phi}_1 \right)^2 + \frac{\tilde{\lambda}}{4} \left(\frac{\rho}{2} - \tilde{\kappa} \right)^2 + \frac{\tilde{\mu}}{4} \tau \right). \quad (147)$$

Let us now discuss the different terms appearing in this expression. The coupling constants $\tilde{\lambda}$ and $\tilde{\mu}$ have been already introduced in the GLW approach (see Eq. (51)). The coupling constant $\tilde{\kappa}$ describes the position of the minimum of the potential and appears in the truncation because we expand Γ_k around the nonvanishing field configuration Φ^{Min} . As in the $O(N)$ case, Z corresponds to the field renormalization. Finally, the unusual kinetic term with coupling $\tilde{\omega}$ corresponds to the current-term of Eq. (42) introduced in the discussion of the $NL\sigma$ model approach. This term is irrelevant by power counting around four dimensions since it is quartic in the fields and quadratic in derivatives. However its presence is *necessary* around two dimensions to recover the results of the low-temperature approach of the $NL\sigma$ model since it contributes to the field renormalization of the Goldstone modes. Being not constrained by the usual power counting one includes this term in the *ansatz*.

The above effective action has all the ingredients to describe accurately the physics at low-temperature around two dimensions as well as at weak-coupling regime around four dimensions. We can therefore anticipate that this simple truncation is actually rich enough to recover the perturbative results around $d = 2$ and $d = 4$. Of course, since our main goal is to go beyond the usual perturbative expansion, we have studied larger truncations and have controlled the convergence of our results.

1. The spectrum

We now discuss the spectrum of excitations around the minimum (146). The spectrum is given by the eigenvalues and eigenvectors of the matrix $\delta^2 \Gamma_k / \delta \phi_i^j \delta \phi_k^l$ — where $i, k \in \{1, 2\}$ and $j, l \in \{1, \dots, N\}$ — evaluated in the configuration (146). We find that the $2N$ degrees of freedom

of the order parameter Φ divide in four types that are described in Fig. 7:

1) a family of $2N - 4$ massless — Goldstone — modes which correspond to rotating rigidly the dihedral $(\vec{\phi}_1, \vec{\phi}_2)$ by keeping either $\vec{\phi}_1$ or $\vec{\phi}_2$ unchanged, see Fig. 7a.

The four remaining modes correspond to the situations where the two vectors $(\vec{\phi}_1, \vec{\phi}_2)$ remain in the same plane:

2) a massless — Goldstone — singlet mode corresponding to rotating the dihedral within its plane, see Fig. 7b. Together with the $2N - 4$ other ones, this gives the $2N - 3$ Goldstone mode of the model.

3) a massive singlet of square mass $\tilde{\lambda}\tilde{\kappa}$ corresponding to a dilation of the two vectors, see Fig. 7c.

4) a massive doublet of square mass $\tilde{\mu}\tilde{\kappa}$ corresponding to fluctuations of each vector of the dihedral, with the constraint that the sum of the lengths of the vectors $|\vec{\phi}_1| + |\vec{\phi}_2|$ remains unchanged, see Fig. 7d.

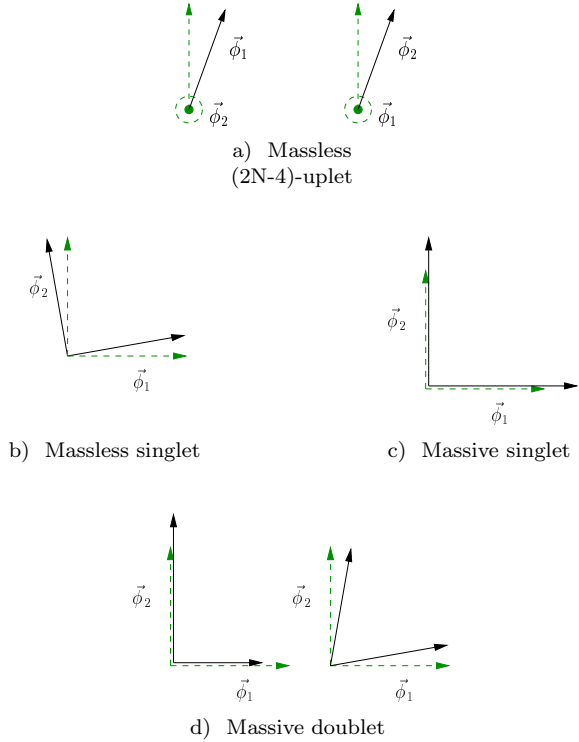


FIG. 7: Schematic description of the deformations of $(\vec{\phi}_1, \vec{\phi}_2)$ associated with the four types of proper excitations of the model. The dotted arrows display the ground state configuration and the plain arrows display the relevant deformations: a) massless $(2N - 4)$ -uplet, b) massless singlet, c) massive singlet, d) massive doublet.

In practice, it is very useful to work in the basis of the proper excitations of the model since then, the propagator being diagonal, the calculations are greatly simplified. We therefore introduce $2N$ directions in the internal space, corresponding to the $2N$ proper excitations of the

model. They are given by:

$$\begin{aligned}
 \delta_{1,\mathbf{p}} &= \frac{1}{\sqrt{2}} \left(\frac{\delta}{\delta\phi_1^1(\mathbf{p})} + \frac{\delta}{\delta\phi_2^2(\mathbf{p})} \right) \\
 \delta_{2,\mathbf{p}} &= \frac{1}{\sqrt{2}} \left(\frac{\delta}{\delta\phi_1^1(\mathbf{p})} - \frac{\delta}{\delta\phi_2^2(\mathbf{p})} \right) \\
 \delta_{3,\mathbf{p}} &= \frac{1}{\sqrt{2}} \left(\frac{\delta}{\delta\phi_2^1(\mathbf{p})} + \frac{\delta}{\delta\phi_1^2(\mathbf{p})} \right) \\
 \delta_{4,\mathbf{p}} &= \frac{1}{\sqrt{2}} \left(\frac{\delta}{\delta\phi_1^2(\mathbf{p})} - \frac{\delta}{\delta\phi_2^1(\mathbf{p})} \right) \\
 \delta_{5,\mathbf{p}} &= \frac{\delta}{\delta\phi_1^3(\mathbf{p})} \\
 \delta_{6,\mathbf{p}} &= \frac{\delta}{\delta\phi_2^3(\mathbf{p})} \\
 &\vdots \\
 \delta_{2N-1,\mathbf{p}} &= \frac{\delta}{\delta\phi_1^N(\mathbf{p})} \\
 \delta_{2N,\mathbf{p}} &= \frac{\delta}{\delta\phi_2^N(\mathbf{p})}.
 \end{aligned} \tag{148}$$

In this basis, the two-point vertex function, *i.e.* the inverse propagator — up to the R_k term — has the form:

$$\Gamma_{\{i,\mathbf{q}_1\},\{j,\mathbf{q}_2\}}^{(2)} \Big|_{\text{Min}} = \frac{\delta(\mathbf{q}_1 + \mathbf{q}_2)}{(2\pi)^d} \cdot \begin{pmatrix} Z\mathbf{q}_1^2 + \tilde{\lambda}\tilde{\kappa} & & & & & & \\ & Z\mathbf{q}_1^2 + \tilde{\mu}\tilde{\kappa} & & & & & 0 \\ & & Z\mathbf{q}_1^2 + \tilde{\mu}\tilde{\kappa} & & & & \\ & & & (Z + \tilde{\omega}\tilde{\kappa})\mathbf{q}_1^2 & & & \\ & & & & Z\mathbf{q}_1^2 & & \\ 0 & & & & & \ddots & \\ & & & & & & Z\mathbf{q}_1^2 \end{pmatrix} \tag{149}$$

In the matrix (149), the first three lines correspond to the massive modes and the last $2N - 3$ to the massless modes. Note that a nonstandard kinetic term appears on the fourth line through an additional field renormalization $\tilde{\omega}\tilde{\kappa}$ for the Goldstone singlet. Let us add that if one keeps, in the truncation (147), contributions from the functions $Y^{(2)}$ and $Y^{(3)}$ (see Eq. (145)), the field renormalizations in the first three lines get extra contributions similar to what is obtained in the fourth line. Note that $Y^{(2)}$ and $Y^{(3)}$ affect only the field renormalization of massive modes. It is therefore not necessary to take them into account in order to retrieve the leading order behavior in a low-temperature expansion around $d = 2$ which is entirely governed by Goldstone modes. This is why we do not keep them in our simplest truncation (147).

B. The flow equations

We now display the flow equations for the coupling constants entering in the truncation Eq. (147). We recall the four major steps of this procedure (see Section VI D):

i) The running coupling constants are defined as functional derivatives of the *ansatz* of Γ_k , Eq. (147).

ii) The operator ∂_t is then applied on these definitions. By making use of the NPRG equation (100), flow equations for the coupling constants are obtained as traces of vertex functions. These expressions are evaluated by using the truncated form of Γ_k Eq. (147).

iii) The flow equations are expressed in terms of threshold functions.

iv) Dimensionless renormalized quantities are introduced.

1. Definition of the coupling constants

As in the vectorial model, the coupling constants are defined as values of the vertex functions in the specific configuration Φ^{Min} around which is made the field expansion, Eq. (146).

Let us start with the definition of $\tilde{\kappa}$. This coupling constant parametrizes the ground state configuration Φ^{Min} . One has, as in the $O(N)$ case, an implicit definition of $\tilde{\kappa}$:

$$\delta_{\alpha, \mathbf{p}=\mathbf{0}} \Gamma_k \Big|_{\text{Min.}} = 0 \quad (150)$$

with $\delta_{\alpha, \mathbf{p}}$ given by Eq. (148). In the following, as in the $O(N)$ case, we shall consider only the case $\alpha = 1$.

The other coupling constants are defined using the two-point vertex function in different directions:

$$\begin{cases} \tilde{\lambda} = \frac{(2\pi)^d}{\tilde{\kappa} \delta(\mathbf{0})} \delta_{1, \mathbf{0}} \delta_{1, \mathbf{0}} \Gamma_k \Big|_{\text{Min}} \\ \tilde{\mu} = \frac{(2\pi)^d}{\tilde{\kappa} \delta(\mathbf{0})} \delta_{2, \mathbf{0}} \delta_{2, \mathbf{0}} \Gamma_k \Big|_{\text{Min}} \end{cases} \quad (151)$$

These two definitions come directly from the study of the

spectrum discussed previously (see Eq. (149)).

We finally define the coupling constants associated with the momentum-dependent part of our truncation (147), *i.e.* the field renormalization factor Z and the current-term coupling constant $\tilde{\omega}$:

$$\begin{cases} Z = \frac{(2\pi)^d}{\delta(\mathbf{0})} \lim_{\mathbf{p}^2 \rightarrow 0} \frac{d}{d\mathbf{p}^2} \left(\delta_{5, \mathbf{p}} \delta_{5, -\mathbf{p}} \Gamma_k \Big|_{\text{Min}} \right) \\ \tilde{\omega} = \frac{(2\pi)^d}{\tilde{\kappa} \delta(\mathbf{0})} \lim_{\mathbf{p}^2 \rightarrow 0} \frac{d}{d\mathbf{p}^2} \left(\delta_{4, \mathbf{p}} \delta_{4, -\mathbf{p}} \Gamma_k \Big|_{\text{Min}} \right) - \frac{Z}{\tilde{\kappa}} \end{cases} \quad (152)$$

2. The t -derivation and the flow equations

We now apply the operator ∂_t to the definitions (150–152). In order to derive the flow equations, we have to compute the functional derivatives of $\partial_t \Gamma_k$ with respect to the fields. This is similar to what has been done previously in the context of the $O(N)$ model (see Section VI D 2 above), except that the tensorial structure in the internal space is more involved so that the computation of the traces is more cumbersome. We do not give the details here. We now introduce the dimensionless renormalized quantities defined as:

$$\begin{cases} \kappa = Z k^{2-d} \tilde{\kappa} \\ \lambda = Z^{-2} k^{d-4} \tilde{\lambda} \\ \mu = Z^{-2} k^{d-4} \tilde{\mu} \\ \omega = Z^{-2} k^{d-2} \tilde{\omega} \end{cases} \quad (153)$$

as well as the threshold functions which are defined and discussed in Appendix C. We then get the following flow equations [118]:

$$\begin{aligned} \frac{d\kappa}{dt} = & -(d-2+\eta)\kappa + 4v_d \left[\frac{1}{2} l_{01}^d(0, 0, \kappa\omega) + (N-2) l_{10}^d(0, 0, 0) + \frac{3}{2} l_{10}^d(\kappa\lambda, 0, 0) + \left(1 + 2\frac{\mu}{\lambda}\right) l_{10}^d(\kappa\mu, 0, 0) + \right. \\ & \left. + \frac{\omega}{\lambda} l_{01}^{2+d}(0, 0, \kappa\omega) \right] \end{aligned} \quad (154a)$$

$$\begin{aligned} \frac{d\lambda}{dt} = & (d-4+2\eta)\lambda + v_d \left[2\lambda^2 (N-2) l_{20}^d(0, 0, 0) + \lambda^2 l_{02}^d(0, 0, \kappa\omega) + 9\lambda^2 l_{20}^d(\kappa\lambda, 0, 0) + \right. \\ & \left. + 2(\lambda+2\mu)^2 l_{20}^d(\kappa\mu, 0, 0) + 4\lambda\omega l_{02}^{2+d}(0, 0, \kappa\omega) + 4\omega^2 l_{02}^{4+d}(0, 0, \kappa\omega) \right] \end{aligned} \quad (154b)$$

$$\begin{aligned} \frac{d\mu}{dt} = & (d-4+2\eta)\mu - 2v_d\mu \left[-\frac{2}{\kappa} l_{01}^d(0,0,\kappa\omega) + \frac{3(2\lambda+\mu)}{\kappa(\mu-\lambda)} l_{10}^d(\kappa\lambda,0,0) + \frac{8\lambda+\mu}{\kappa(\lambda-\mu)} l_{10}^d(\kappa\mu,0,0) + \right. \\ & \left. + \mu l_{11}^d(\kappa\mu,0,\kappa\omega) + \mu(N-2)l_{20}^d(0,0,0) \right] \end{aligned} \quad (154c)$$

$$\begin{aligned} \eta = & -\frac{d \ln Z}{dt} = 2\frac{v_d}{d\kappa} \left[(4-d)\kappa\omega l_{01}^d(0,0,\kappa\omega) + 2\kappa^2\omega^2 l_{02}^{2+d}(0,0,\kappa\omega) + 2m_{02}^d(0,0,\kappa\omega) - 4m_{11}^d(0,0,\kappa\omega) + \right. \\ & + 2(-2+d)\kappa\omega l_{10}^d(0,0,0) + 2m_{20}^d(0,0,\kappa\omega) + 2\kappa^2\lambda^2 m_{2,2}^d(\kappa\lambda,0,0) + 4\kappa^2\mu^2 m_{2,2}^d(\kappa\mu,0,0) + \\ & \left. + 4\kappa\omega n_{02}^d(0,0,\kappa\omega) - 8\kappa\omega n_{11}^d(0,0,\kappa\omega) + 4\kappa\omega n_{20}^d(0,0,\kappa\omega) \right] \end{aligned} \quad (154d)$$

$$\begin{aligned} \frac{d\omega}{dt} = & (d-2+2\eta)\omega + \frac{4v_d}{d\kappa^2} \left[\kappa\omega \left\{ \frac{(4-d)}{2} l_{01}^d(0,0,\kappa\omega) + \frac{(d-16)}{2} l_{01}^d(\kappa\lambda,0,\kappa\omega) + \kappa\omega l_{02}^{2+d}(0,0,\kappa\omega) - \right. \right. \\ & - 3\kappa\omega l_{02}^{2+d}(\kappa\lambda,0,\kappa\omega) + (d-2)l_{10}^d(0,0,0) - (d-8)l_{10}^d(\kappa\lambda,0,0) + 8\kappa\lambda l_{11}^d(\kappa\lambda,0,\kappa\omega) + 2\kappa\omega l_{20}^{2+d}(\kappa\mu,0,0) \\ & \left. + 2\kappa\omega(N-2)l_{20}^{2+d}(0,0,0) \right\} + m_{02}^d(0,0,\kappa\omega) - m_{02}^d(\kappa\lambda,0,\kappa\omega) - 2m_{11}^d(0,0,\kappa\omega) + 2m_{11}^d(\kappa\lambda,0,\kappa\omega) + \\ & + m_{20}^d(0,0,\kappa\omega) - m_{20}^d(\kappa\lambda,0,\kappa\omega) + \kappa^2\lambda^2 m_{22}^d(\kappa\lambda,0,0) + 2\kappa^2\mu^2 m_{22}^d(\kappa\mu,0,0) + 2\kappa\omega n_{02}^d(0,0,\kappa\omega) - \\ & \left. - 4\kappa\omega n_{02}^d(\kappa\lambda,0,\kappa\omega) - 4\kappa\omega n_{11}^d(0,0,\kappa\omega) + 8\kappa\omega n_{11}^d(\kappa\lambda,0,\kappa\omega) + 2\kappa\omega n_{20}^d(0,0,\kappa\omega) - 4\kappa\omega n_{20}^d(\kappa\lambda,0,\kappa\omega) \right] \end{aligned} \quad (154e)$$

VIII. TESTS OF THE METHOD AND FIRST RESULTS

This section is devoted to all possible tests of our method in the $O(N) \times O(2)$ case. We show, in particular, how the various perturbative results are recovered as it was already the case in the $O(N)$ model. We also give our determination of $N_c(d)$ which is compared with the three-loop improved perturbative computation. Finally, we give our determination of the exponents in the $N=6$ case and we compare them with those of the Monte Carlo simulation.

A. The weak-coupling expansion around $d=4$

Around $d=4$, we expect a nontrivial fixed point close to the gaussian. One can expand the flow equations at leading order in the quartic coupling constants and in ϵ , as we did in the $O(N)$ case (see Section VID 4). As expected from power counting, we find that the fixed point value of the coupling constant ω associated with the current-term is vanishing at leading order. This is also the case of η . As in the $O(N)$ case, the square masses $\lambda\kappa$ and $\mu\kappa$ are of order ϵ so that the threshold functions can be expanded in powers of their arguments. Once this expansion is performed one recovers the standard one-loop β -functions for the coupling constants λ and μ given in Eq. (53) that we recall here:

$$\begin{cases} \beta_\lambda = -\epsilon\lambda + \frac{1}{16\pi^2} (4\lambda\mu + 4\mu^2 + \lambda^2(N+4)) \\ \beta_\mu = -\epsilon\mu + \frac{1}{16\pi^2} (6\lambda\mu + N\mu^2) \end{cases} \quad (155)$$

One can also expand the β function for κ , Eq. (154a):

$$\begin{aligned} \beta_\kappa = & -(2-\epsilon)\kappa + \frac{l_1^4(0)}{8\pi^2} \left(N+1 + \frac{2\mu}{\lambda} \right) - \\ & - \frac{3\kappa\lambda}{16\pi^2} - \frac{\kappa\mu}{8\pi^2} \left(1 + \frac{2\mu}{\lambda} \right) \end{aligned} \quad (156)$$

from which we can deduce the expression of ν at order ϵ , which coincide with the one-loop result of Eq. (54).

B. The low-temperature expansion around $d=2$

As explained in the context of the $O(N)$ model (see Section VID 5), in order to recover the NL σ model results, we need to expand the flow equations at large masses. Using the behavior of the threshold functions for large arguments (see Appendix C), we get [63]:

$$\begin{cases} \frac{d\kappa}{dt} = -(d-2+\eta)\kappa + \frac{N-2}{2\pi} + \frac{1}{4\pi(1+\kappa\omega)} \\ \frac{d\omega}{dt} = (-2+d+2\eta)\omega + \\ \quad + \frac{1+\kappa\omega + (N-1)\kappa^2\omega^2 + (N-2)\kappa^3\omega^3}{2\pi\kappa^2(1+\kappa\omega)} \\ \eta = \frac{3+4\kappa\omega + 2\kappa^2\omega^2}{4\pi\kappa(1+\kappa\omega)} \end{cases} \quad (157)$$

By making the change of variables:

$$\begin{cases} \eta_1 = 2\pi\kappa \\ \eta_2 = 4\pi\kappa(1+\kappa\omega) \end{cases} \quad (158)$$

we recover the β -functions found in the framework of the NL σ model at one-loop order (see Eq. (49)).

C. The large- N expansion in $d = 3$

As in the $O(N)$ case (see Section VID 6), our equations allow to recover the critical exponents at leading order in $1/N$. We have computed η and ν for a large range of

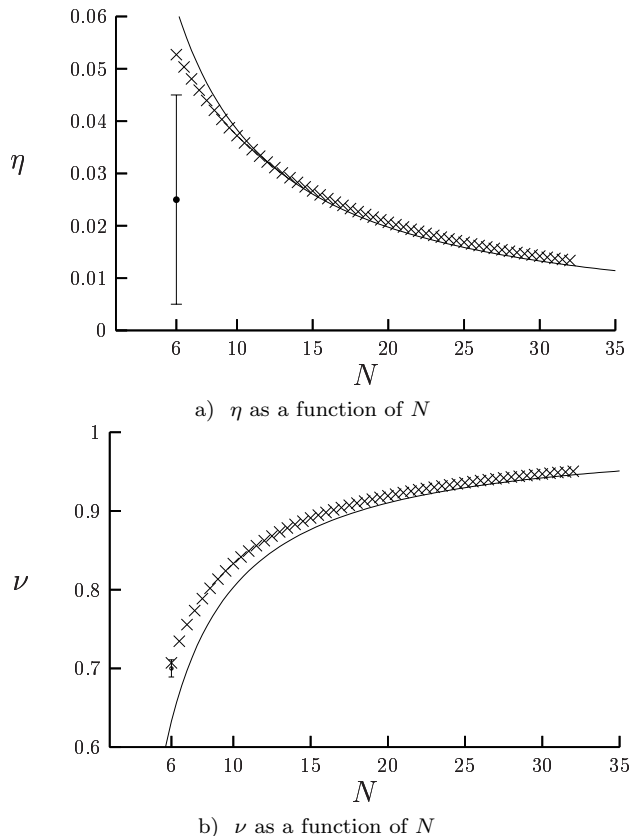


FIG. 8: The exponents η and ν as functions of N in $d = 3$. The crosses represent our results and the full line the values obtained from the $1/N$ expansion, Eqs. (58). The circles and error bars are the Monte Carlo results obtained for $N = 6$ [22].

values of N and have compared our results with those calculated perturbatively at order $1/N^2$, Eq. (58). We find an excellent agreement — better than 1% — for ν , for all $N > 10$, see Fig. 8, a domain of values of N where one expects the $1/N^2$ results to be very close to the exact values. We also quote in Table IX our results and those obtained by the six-loop calculation for $N = 16$ and $N = 32$.

D. The determination of $N_c(d)$

Let us now interpolate between the results we have obtained around $d = 2$ and $d = 4$ and discuss, in par-

N	Method	ν	η
16	1/N[156]	0.885	0.0245
	NPRG	0.898	0.0252
	six-loop	0.858(4)[155], 0.863(4)[132]	0.0246(2)[132]
32	1/N[156]	0.946	0.0125
	NPRG	0.950	0.0134
	six-loop	0.936(2)[155], 0.936(1)[132]	0.01357(1) [132]

TABLE IX: Exponents ν and η computed from the $1/N$ expansion [156], by our method (NPRG) and from the six-loop calculation [132, 155].

ticular, the curve $N_c(d)$ that separate the regions of first and second order.

We have computed $N_c(d)$ with our best truncation and with the cut-off function (86). In Fig. 9, we give our re-

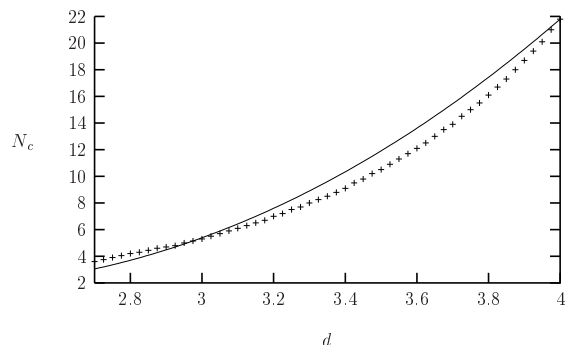


FIG. 9: The full line represents the curve $N_c(d)$ obtained by the three-loop results improved by the constraint $N_c(d = 2) = 2$, Eq. (56). The crosses represent our calculation.

sult (crosses) from $d = 4$ down to $d = 2.7$. We also indicate the improved three-loop results given by Eq. (56) for comparison. The two curves agree very well. Note that it is probably a coincidence that the curves cross very close to $d = 3$. In this dimension, the NPRG method leads to $N_c(d = 3) \simeq 5.1$ and the improved three loop result: $N_c(d = 3) \simeq 5.3(2)$. Let us emphasize that, within the NPRG method, the quantity $N_c(d)$ is very sensitive to the order of the truncation [60], much more than the critical exponents. This means that one probably should not consider the previous results as very reliable. In this respect, we recall the results obtained by means of the six-loop calculation in $d = 3$ *et al.* [132]: $N_c(d = 3) = 6.4(4)$ and by means of the $4 - \epsilon$ expansion at five-loops [159]: $N_c(d = 3) \simeq 6.1(6)$.

Let us finally mention that, for the reason already explained in Section VID 9, the field expansion we have performed at order ϕ^{10} forbids us to follow the chiral fixed point C_+ in dimensions typically between $d = 2.5$ and $d = 2.1$ and thus to determine reliably the curve $N_c(d)$ in these dimensions. As in the $O(N)$ case, this artefact could be overcome by keeping the full field dependence of the effective potential $U_k(\rho, \tau)$.

E. The critical exponents for $N = 6$

As already said, for $N = 6$, the transition is either of second order or extremely weakly of first order. In both cases scaling should exist on a large domain of temperature. The critical exponents obtained with our best truncation are given in Table X. Note that ν and η are computed directly while γ , β and α are computed using the scaling relations. Our results agree very well with

Method	α	β	γ	ν	η
NPRG	-0.121	0.372	1.377	0.707	0.053
MC[22]	-0.100(33)	0.359(14)	1.383(36)	0.700(11)	0.025(20)

TABLE X: The exponents for $N = 6$ obtained from the NPRG — first line — and from the Monte Carlo (MC) simulation — second line.

the numerical ones [22]. In particular, the error on ν , which is as usual the best determined exponent, is only 1%. This constitutes a success of the NPRG approach from the methodological point of view.

F. Conclusion

Our method has successfully passed *all* possible tests. This gives us a great confidence in the reliability and the convergence of our results. We are now in a position to explore the physics of frustrated magnets in three dimensions.

IX. THE PHYSICS IN $d = 3$

We now tackle with the physics in three dimensions. Before embarking in this discussion, two points need to be clarified. The first concerns the existence of a fixed point for $N < N_c(d = 3)$. The second one concerns the situation just below $N_c(d = 3)$.

A. The search of fixed points for $N < N_c(d)$

Let us first discuss the search, within the NPRG method, of fixed points in $d = 3$ and for $N < N_c(d = 3) \simeq 5.1$. We recall that, for this critical value of N , the two fixed points C_+ and C_- — see Fig. 2 — coalesce. This means that these fixed points — that can be followed smoothly in the (d, N) plane from the gaussian in $d = 4$ — cease to be real below this value. However, this does not imply the absence of other real fixed points. One has to test the existence of fixed points non trivially connected with C_+ and C_- , as advocated by Pelissetto *et al.* [155]. We have thus searched such fixed points both by directly looking for zeroes of the β -functions and by integrating numerically the RG flow — see below. After an intensive search, we have found *no* such fixed point.

This result and its relation with that of Pelissetto *et al.* will be discussed in the following.

B. The physics in $d = 3$ just below $N_c(d)$: scaling with a pseudo-fixed point and minimum of the flow

In a fixed dimension d , the disappearance of the non-trivial fixed points C_+ and C_- , when N crosses $N_c(d)$, could seem to be an abrupt process: the two fixed points collapse and disappear. Actually, when extended to the space of complex coupling constants, this process is continuous since the only change is that, when going from $N > N_c(d)$ to $N < N_c(d)$, the fixed points acquire a small complex part. This continuous character manifests itself as smooth changes of the RG flow that can be explained thanks to continuity arguments.

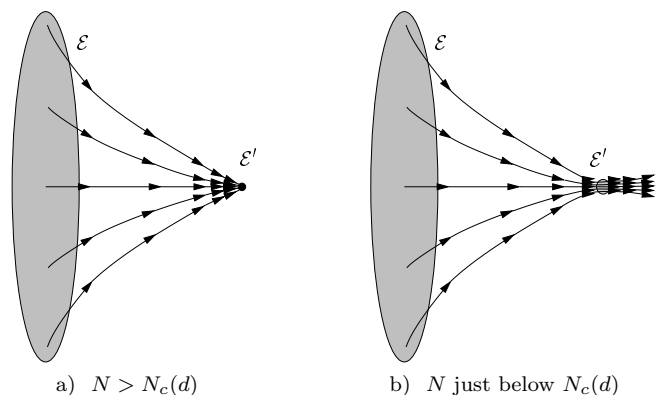


FIG. 10: Schematic representation of the flow a) for N above $N_c(d)$ and b) for N just below $N_c(d)$. For the sake of clarity, we have represented \mathcal{E}' outside \mathcal{E} while it can be included in it.

To understand the evolution of the RG flow as N is decreased, we need to consider the space of *all* coupling constants, *i.e.* the space such that to each point corresponds a microscopic Hamiltonian of a system. In this space, we focus on the subspace \mathcal{E} containing the representative points, at $T = T_c$, of STA, STAR, $V_{N,2}$, BCT and of all real materials studied experimentally and, more generally, of all systems of physical interest. Let us now describe qualitatively the change of the RG trajectories as N crosses $N_c(d)$.

i) When N is larger than $N_c(d)$, there exists a true stable fixed point of the RG flow so that all trajectories emerging from \mathcal{E} eventually end on this fixed point, see Fig. 10a. All systems exhibit scaling around the transition and universality holds.

ii) As already stated, when N is decreased slightly below $N_c(d)$, the fixed point C_+ gets complex coordinates and loses its direct physical meaning. In particular, the flow no longer stops at a point, see Fig. 10b. Consequently, the correlation lengths of systems in \mathcal{E} do not diverge at T_c . Strictly speaking, all systems undergo first order phase transitions. However two facts must

be noted. Firstly, all the trajectories emerging from \mathcal{E} are attracted toward a small region in coupling constant space, denoted by \mathcal{E}' in Fig. 10b. Secondly, the flow in \mathcal{E}' is very slow.

From the second observation, we deduce that for all systems in \mathcal{E} the correlation lengths at the transition are very large — although finite — since they typically behave as the exponential of the RG time spent around \mathcal{E}' , which is large. Therefore, the transitions are all extremely weakly of first order for systems in \mathcal{E} . We thus expect scaling behaviors with pseudo-critical exponents for all physical quantities, with the subtlety that this scaling aborts very close to T_c where the true first order nature of the transitions shows up.

As for the first observation — *i.e.* all trajectories are attracted toward a small region \mathcal{E}' —, it allows to conclude that all phase transitions are governed by a small region in coupling constant space and that, therefore, universality almost holds. In particular, the pseudo-critical exponents should be roughly the same for all systems whose microscopic Hamiltonian corresponds to a point in \mathcal{E} .

Let us study in greater detail the case where N is just below $N_c(d = 3)$. For such values of N , it is reasonable to approximate \mathcal{E}' by a point. The best approximation is clearly to choose the point in \mathcal{E}' that mimics best a fixed point, *i.e.* the point where the flow is the slowest: the minimum of the flow [65]. To determine this so-called “pseudo-fixed point”, Zumbach [65] has proposed to introduce a norm for the flow and to determine the point where the norm is minimum. He has performed this approach in the context of a NPRG equation (LPA of the Polchinski equation) where he has built the needed mathematical structures. He has shown that, when a minimum exists, pseudo-critical exponents characterizing pseudo-scaling can be associated with the pseudo-fixed point, in the same way that true exponents are associated with a true fixed point (see Appendix D for more details).

A natural assumption to explain the pseudo-scaling behaviors observed in real systems is that the minimum of the RG flow mimics a true fixed point even for values of N not very close to $N_c(d = 3)$. For the Heisenberg systems, this position has been advocated by Zumbach [65] and by the present authors [63].

Within our present approach we have confirmed the existence of a minimum of the flow, for values of N just below $N_c(d = 3)$, leading to pseudo-scaling and pseudo-universality [63]. By following this minimum we have confirmed that it persists down to $N = 3$ and have computed the associated pseudo-critical exponents, see Table XI. We also give in this table the exponents found by Zumbach within the LPA of the Polchinski equation for the same model [65] and recall those found within the six-loop approach of Pelissetto *et al.* [155].

The values that we have obtained within our calculation for the critical exponents are not too far from — some of — those found experimentally for group 2 of ma-

Method	Ref.	α	β	γ	ν	η
NPRG	[63]	0.38	0.29	1.04	0.54	0.072
LPA	[65]	0.11	0.31	1.26	0.63	0.0
6-loop	[155]	0.35(9)	0.30(2)	1.06(5)	0.55(3)	0.08

TABLE XI: The critical and pseudo-critical exponents for $N = 3$. α, β and γ have been computed assuming that the scaling relations hold. The first line corresponds to our non-perturbative approach, the second to Zumbach’s work. In the third line, we have recalled the six-loop results of Pelissetto *et al.* for comparison.

terials, see Eq. (37), as well as those found numerically for the STA, Table V. As usual, our truncation overestimates η and thus, at fixed β , underestimates ν . It is remarkable that the values of the pseudo-critical exponents we have found at the minimum are in good agreement with those obtained within the six-loop approach. This strongly suggests that there is a common origin to these two sets of critical exponents. We shall come back on this point later.

C. Scaling with or without pseudo-fixed point: the Heisenberg and XY cases

Let us now argue that the preceding analysis, based solely on the notion of minimum, is too naive to give an explanation of the pseudo-critical behaviors in the physically interesting cases. Let us also give a qualitative picture that supplements the concept of minimum.

We have found that, when N is lowered below $N = 3$, the minimum of the flow is less and less pronounced and that, for some value of N between 2 and 3, it completely disappears. Since several XY systems exhibit pseudo-scaling in experiments or in numerical simulations, this means that the concept of minimum of the flow does not constitute the definitive explanation of scaling in absence of a fixed point. One encounters here the limit of the concept of minimum of the flow. First, it darkens the important fact that the notion relevant to scaling is not the existence of a minimum but that of a whole region in coupling constant space in which the flow is slow, *i.e.* the β functions are small. Put it differently, the existence of a minimum does not guarantee that the flow is sufficiently slow to produce large correlation lengths. Reciprocally, one can encounter situations where the RG flow is slow, the correlation length being large so that scaling occurs even in absence of a minimum. The existence of a minimum is thus neither necessary nor sufficient to explain pseudo-scaling. Second, even when the minimum exists, reducing the region \mathcal{E}' to a point rules out the possibility of testing the violation of universality. For instance, one knows that for $N = 3$ universality is, in fact, violated, see Table V, while a minimum of the RG flow is found. This feature cannot be reproduced by the unique set of exponents computed at the minimum. The opposite assumption, done first by Zumbach [65] and by the present

authors [63], was thus unjustified.

Thus, even for very weak first order transitions, the beautiful simplicity of second order transitions is lost and the finite extend of the attractive region \mathcal{E}' has to be taken into account. To be precise, one needs to define two subsets of \mathcal{E} and \mathcal{E}' : \mathcal{D} which is the region in \mathcal{E} leading to pseudo-scaling and \mathcal{R} , the subset of \mathcal{E}' which is the image of \mathcal{D} in the RG flow, see Figs. 11a and 11b. Let us now consider the characteristics of the flow when N is varied.

Since for $N > N_c(d=3)$ all the systems in \mathcal{E} undergo a second order phase transition, one expects — thanks to continuity arguments — that for N slightly below $N_c(d=3)$, all systems in \mathcal{E} exhibit pseudo-scaling and thus that $\mathcal{D} = \mathcal{E}$. At the same time, \mathcal{E}' , the image of \mathcal{E} is almost point-like — see Fig.10b — and universality holds.

As N is decreased below $N_c(d)$, two phenomena occur.

i) While \mathcal{D} remains equal to \mathcal{E} , the domain \mathcal{E}' , which is initially point-like, grows, see Fig. 11a. This means that while pseudo-scaling should be generically observed, universality starts to be significantly violated: a whole spectrum of exponents should be observed, the size of \mathcal{E}' providing a measure of this violation of universality.

ii) For low values of N , the region \mathcal{D} leading to pseudo-scaling become smaller than \mathcal{E} , see Fig. 11b. For systems defined by initial conditions in \mathcal{D} , the correlation lengths are still relatively large but the pseudo-critical exponents can vary from system to system according to the size of \mathcal{R} . For systems defined by initial conditions in \mathcal{E} but not in \mathcal{D} , the RG flow is always fast, producing small correlation lengths at T_c . The corresponding systems undergo strong first order phase transitions. Moreover, as N decreases, the flow in \mathcal{E}' should become more and more rapid so that, for systems in \mathcal{E} , the correlation lengths at the phase transitions should decrease. The transitions are thus expected to become more strongly of first order for lower N .

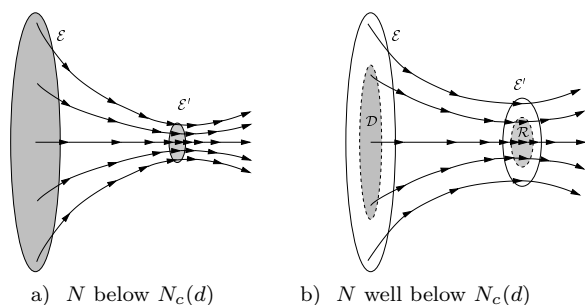


FIG. 11: Schematic representation of the flow a) for N below $N_c(d)$ — $N \simeq 3$ — and b) for N well below $N_c(d)$ — $N \simeq 2$. For the sake of clarity, we have represented \mathcal{E}' outside \mathcal{E} while it can be included in it. \mathcal{D} and \mathcal{R} are represented in grey. In a), $\mathcal{D} = \mathcal{E}$ and $\mathcal{R} = \mathcal{E}'$.

The precise values of N for which these changes of behaviors occur as well as the shapes and extents of \mathcal{D} , \mathcal{R} and \mathcal{E}' can only be obtained from a detailed analysis of both the microscopic Hamiltonian and of the RG

flow. However, independently of the details of the model under study, of the precise value of $N_c(d)$, etc, one expects the following behavior: as N is decreased, a system that undergoes at large N a second order transition undergoes, for N just smaller than $N_c(d)$, a very weak first order transition governed by the minimum. Then, it should undergo a weak first order transition where the notion of minimum is no longer relevant and for which universality does not hold anymore. Finally, it should undergo a strong first order phase transition. In the spectrum of models studied numerically, it is easy to see that the STAR, $V_{N,2}$ and BCT models with XY and Heisenberg spins nicely obey this prediction. For $N = 3$, they all show scaling and the phase transitions should be very weakly of first order. However, their exponents are clearly incompatible with those of STA and with those associated with the minimum, see Tables V and XI. The RG trajectories associated with these systems are thus expected to pass through \mathcal{R} , but far from the minimum. One thus naturally expects that, when N is decreased down to $N = 2$, no scaling behavior is observed for these systems. This is indeed what is found in numerical simulations, see Table III. This strongly suggests that \mathcal{D} has shrunk between $N = 3$ and $N = 2$ and that $N = 3$ corresponds to Fig. 11a and $N = 2$ to Fig. 11b.

D. The integration of the RG flow for Heisenberg and XY systems

In the previous section we have shown that the notion of minimum — or pseudo-fixed point — in the RG flow is neither sufficient nor necessary to explain the existence of scaling without a fixed point. For this reason, one has to resort to another method to study the physics of XY and Heisenberg frustrated magnets. In practice, we integrate numerically the RG flow around the transition temperature T_c and determine the behavior of the physical quantities such as the correlation length, the susceptibility and the “magnetization” — defined as $\sqrt{\chi}$, see Eq. (146) — as functions of the reduced temperature $t_r = (T - T_c)/T_c$.

1. Three difficulties

Let us mention three difficulties encountered during the integration of the flow.

First, in principle, in the absence of universality, we should study each system independently of the others. Thus, to correctly specify the initial conditions of the RG flow, we should also keep all the microscopic information relevant to the description of a given material. This program remains, in the most general case, a difficult challenge since this would consist in keeping track of the lattice structure as well as of the infinite number of coupling constants involved in the microscopic Hamiltonian. However this is, in principle, possible. Actually,

this has been done with much success for certain classes of magnetic systems and fluids described by $O(N)$ models [48] mostly within the LPA [194, 195]. Our truncations — even the best one — are too restricted approximations to reach this goal since this would at least require to keep the *full* field dependence of the potential $U_k(\rho, \tau)$. We have thus used our flow equations to explain the generic occurrence of pseudo-scaling in frustrated systems without trying to describe the behavior of a specific system. In practice, we have computed the correlation length, magnetization and susceptibility using a simplified version of our truncation keeping only the potential part expanded up to order eight in the fields, a field-independent field renormalization and discarding all the current-terms involving four fields and two derivatives. We have checked that this *ansatz* leads to stable results with respect to the addition of higher powers of the fields and inclusion of current terms.

Second, the truncations we have considered do not allow to determine accurately the critical temperature. Indeed, in our approach we perform a local description of the potential around the nontrivial minimum Eq. (146). For a second order phase transition this does not matter since the nontrivial minimum, when it exists, is always the true one. However, for a first order transition, the zero-field configuration, *i.e.* with $\vec{\phi}_1 = \vec{\phi}_2 = \vec{0}$, plays a crucial role. In effect, in this case, the transition temperature precisely coincides with the temperature at which the energy at the nontrivial minimum and at the zero-field configuration are equal. Since we cannot expect that our truncation describes accurately the potential around the zero-field configuration, we are not able to compare the energy of this configuration with the energy of the nontrivial minimum and to determine the transition temperature accurately. We discuss in more details this point in Appendix E and show that, for a *weak* first order transition, this fact should not bias significantly our analysis.

The third difficulty encountered in the integration of the flow is that, in the absence of universality, the temperature dependence of the physical quantities relies on the precise temperature dependence of the microscopic coupling constants. We have used several *ansätze* for the temperature dependence of the coupling constants and have observed that, although it could be important for the details of the results, it does not affect much the general conclusions. Thus, we illustrate our results with the simplest *ansatz* consisting in fixing all the couplings to temperature-independent values and by taking a linear temperature dependence for κ at the lattice scale:

$$\kappa_{k=\Lambda} = a + bT. \quad (159)$$

For each temperature, we have integrated the flow equations and have deduced the t_r -dependence of the physical quantities, such as the “magnetization”, the correlation length, etc, around T_c . The different coupling constants parametrizing the initial condition of the flow have been varied to test the robustness of our conclusions. This has allowed us to establish the following facts.

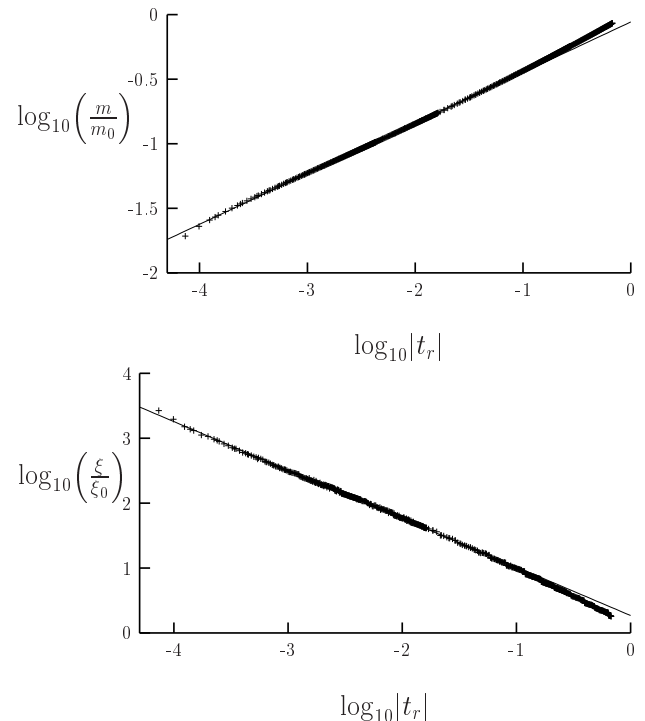


FIG. 12: Log-log plot of the magnetization m and of the correlation length ξ for $N = 3$ as functions of the reduced temperature t_r . The straight lines correspond to the best power law fit of the data.

2. The Heisenberg case

- For $N = 3$, we can find initial conditions of the flow such that for a wide range of reduced temperatures — up to four decades — the physical quantities behave as power laws. From an experimental viewpoint, this is all what is needed since scaling has been found on temperature ranges that are even smaller. The kind of pseudo-critical behaviors we find is illustrated on Fig. 12.

- Varying the initial conditions of the flow, we observe that this phenomenon happens in a wide domain of the coupling constant space. This corresponds to the domain \mathcal{D} previously defined, see Fig. 11a.

- Within \mathcal{D} , the pseudo-critical exponents vary smoothly: β varies typically between 0.27 and 0.42 and ν between 0.56 and 0.71. These are only typical values since it has been impossible to explore the whole space of coupling constants. Since for $\beta \simeq 0.27$ one can find $\nu \simeq 0.56$, the exponents of group 2 are satisfactorily reproduced, see Tables IV and V. This shows in particular that there exists, in \mathcal{D} , a set of “microscopic” coupling constants that lead to the behavior observed in group 2.

- It is easy to find initial conditions leading to pseudo-critical exponents in good agreement with those obtained in the six-loop calculation, see Table VII. Actually, a whole set of initial conditions lead to exactly the same (pseudo-) critical exponents as those found at six-loop $\beta = 0.30(2)$, $\nu = 0.55(3)$. This corresponds to the region

of the minimum of the flow, see Table XI.

- In contrast, we have not found initial conditions of the RG flow reproducing correctly the critical exponents of group 1, of STAR, $V_{3,2}$ and BCT as well as negative values for η . This can originate *i*) in the overestimation of η produced by our truncation of Γ_k in powers of the derivatives at order ∂^2 , Eq. (145), *ii*) in the impossibility to sample the whole coupling constant space, *iii*) in the too simple temperature dependence of κ_Λ that we have considered, see Eq. (159).

- For a given value of one exponent, it is possible to find several values for the other exponents. Thus we expect to find systems sharing for instance almost the same β but having quite different values for ν and γ .

- At the border of \mathcal{D} , the temperature ranges over which power laws hold become smaller and smaller. In a log-log plot, the t_r -dependence becomes less and less linear and the pseudo-critical exponents more and more sensitive to the choice of T_c made for the fit. Finally, outside \mathcal{D} , no more power-law behavior is observed.

- When we go from $N = 3$ to $N = 4$, we have observed, as expected, that \mathcal{D} becomes far wider and that the power laws hold generically on larger temperature ranges. This is consistent with our discussion of Section IX C. Reciprocally, and as also expected, when going from $N = 3$ to $N = 2$, \mathcal{D} becomes much smaller and the power laws hold generically on smaller temperature ranges. Let us discuss this point in greater detail now.

3. The XY case

- For $N = 2$, one observes qualitatively the same type of behaviors as for $N = 3$. However, as predicted above, \mathcal{D} is smaller and the power laws hold at best only on two decades of reduced temperature, which is consistent with what is observed experimentally. This is illustrated in Fig. 13 where we have represented log-log plots of the magnetization and correlation length as functions of the reduced temperature. Note also the surprising behavior of the correlation length that increases at small reduced temperature (see Appendix E for an explanation of this phenomenon.).

- Within \mathcal{D} the exponents vary on the intervals: $0.25 < \beta < 0.38$ and $0.47 < \nu < 0.58$.

- We find initial conditions leading to exponents close to those of group 2 (for Ho and Dy, see Table II): $\beta = 0.38$, $\nu = 0.58$, $\gamma = 1.13$. These results are quite stable with respect to changes of microscopic parameters. This is in agreement with the stability of β in group 2. Interestingly, these initial conditions correspond to small $\tilde{\mu}$ in our truncation Eq. (147), *i.e.* to initial conditions close the $O(4)$ -invariant line: $\tilde{\mu} = 0$, see Fig. 2 where the $O(4)$ fixed point is denoted by V [213]. Thus, during a large part of the flow, the trajectory remains close to the $O(4)$ fixed point before bifurcating away from this point. This is perhaps the reason why the value of β for materials of group 2 is close to that associated with

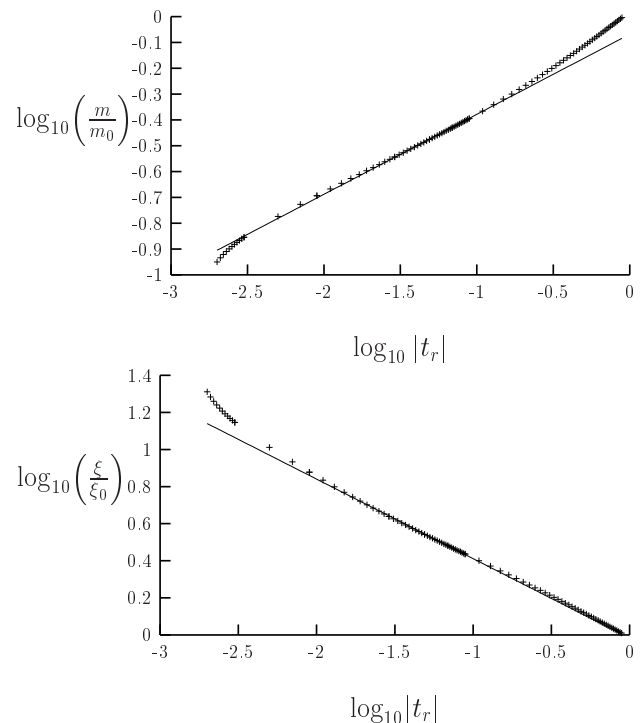


FIG. 13: Log-log plot of the of the magnetization m and of the correlation length ξ for $N = 2$ as functions of the reduced temperature t_r . The straight lines correspond to the best power law fit of the data. The power-law behavior observed far from the critical temperature breaks down for small t_r . The behavior of the correlation length at small t_r is an artefact of our truncation, see Appendix E

an $O(4)$ behavior — $\beta_{O(4)} = 0.382$ — a fact that has been repeatedly noticed by experimentalists. Note however that the other exponents are not close to the $O(4)$ values: $\nu_{O(4)} = 0.738$, $\gamma_{O(4)} = 1.449$.

- We also easily find initial conditions leading to $\beta = 0.25$, corresponding to group 1, essentially composed of STA systems. The power laws then hold on smaller ranges of temperatures and the critical exponent β is more sensitive to the determination of T_c and to the initial conditions. For such values of β , we find that ν varies between 0.47 and 0.49, which is somewhat below the value found for CsMnBr_3 , see Table I.

- The two previous points suggest that both helimagnets — such as Ho or Dy — and STA — such as CsMnBr_3 — can be described by the same field theory but with exponents at the two ends of the spectrum. It is actually also possible that helimagnets display a different kind of physics because of the presence of long range interactions or because of the presence of surface effects [196].

- As in the $N = 3$ case, we can easily find initial conditions leading to pseudo-critical exponents close to those found in the six-loop calculation, Table VII. For instance, for initial conditions leading to $\beta = 0.33$, we find typically: $\nu = 0.56$ and $\gamma = 1.07$.

- As in the Heisenberg case, we have not been able to

find initial conditions of the RG flow leading to negative values of η .

Let us now comment our results.

4. Comments

The main feature of the physics of Heisenberg and XY frustrated magnets — scaling behaviors *without* universality — is reproduced, at least qualitatively and, to some extent, quantitatively. This behavior finds a *natural* explanation: there exists a whole domain \mathcal{D} in the space of coupling constants such that the RG trajectories starting in \mathcal{D} are “attracted” toward a region \mathcal{R} where the RG flow is slow so that there is pseudo-scaling. Since \mathcal{R} is *not* reduced to a point, there exists a whole spectrum of exponents and not a *unique* set. The occurrence of strong first order phase transitions, that are observed in some materials and simulated systems, is explained by the RG trajectories starting out of \mathcal{D} .

Let us now stress that since universality is lost, the determination of the precise pseudo-critical exponents associated with a given material or system is obviously more difficult than the determination of the usual — universal — critical exponents characterizing a second order phase transition. As already said, computing them would indeed require to know precisely the microscopic structure of the materials or systems studied — providing the initial conditions of the RG flow — and to take into account the full field-dependence of the potential $U_k(\rho, \tau)$.

X. POSSIBLE TESTS OF OUR SCENARIO

There are several tests that can be performed both experimentally and numerically to confirm our proposals. Let us start by the Heisenberg case.

- It is not clear, up to now, whether the materials of group 1 — VCl_2 and VBr_2 — are really three-dimensional Heisenberg STA, at least for a temperature range wide enough to measure exponents. It would be very interesting to re-study these materials and to measure all exponents for each of them. This could allow to confirm experimentally the absence of universality.

- Since we predict that they can be violated, there is clearly a need to check the scaling relations as well as the negativity of η . The experimental determination of the exponents γ and ν for the two groups of Heisenberg materials is still much too poor. It is also necessary to have an estimation of both the systematic and statistical errors to strengthen our conclusion on the negativity of η . Let us however recall that the first order nature of the transitions in Heisenberg systems is likely to be much weaker than in XY systems. Thus the violations of both the scaling relations and the positivity of η should be much more difficult to prove experimentally in this case.

- It remains mysterious why, in $CsMn(Br_{0.19}I_{0.81})_3$, such strange values of the exponents γ and ν have been

found, see Table IV. As we have already discussed in point *i*) of Section III C 1, we find unconvincing the arguments proposed in [141] to explain them. Remeasuring these exponents could provide accurate results for γ and ν from which universality and the negativity of η could be tested.

- Most probably STAR and the $V_{3,2}$ model undergo both first order transitions since η is found negative for these models. It would be extremely interesting to study a sequence of models that interpolate between STA and STAR to see how the effective exponents change with the deformation of the model.

- We have already noticed that the exponents found in the six-loop calculation are very close to the pseudo-critical exponents found at the minimum of the RG flow in our approach. It is important to know if this is just an accidental coincidence or if they correspond to the same fixed point, real in one approach complex in the other.

Let us now discuss the XY case. Most of the points discussed in the Heisenberg case can be transposed here: necessity to check the scaling relations and the positivity of η , possibility to interpolate between the STA and STAR. Here, however, we are in a better position to obtain conclusive results since the transition is expected to be more strongly of first order.

- A better determination of ν in $CsMnBr_3$ would help to confirm that η is indeed negative. We also expect to have a weaker universality and thus a faster change of the exponents as the microscopic details of the model are varied. In particular, a precise determination of α in the different materials of group 1 could lead to incompatible exponents — they are up to now only marginally compatible — and would give a direct proof of the lack of universality.

- On the numerical side, the sequence of models interpolating between STA and STAR should lead to rapidly varying exponents. Thus the lack of universality in this case should be much simpler to prove numerically than in the Heisenberg case. For STA, it would also be extremely interesting to determine η independently by the two scaling relations $\eta = 2\beta/\nu - 1$ and $\eta = 2 - \gamma/\nu$. As far as we know η has mainly been determined using γ/ν . According to our scenario the two determinations should not coincide. However, they are probably both negative.

XI. CONSEQUENCES FOR PERTURBATION THEORIES

Frustrated magnets represent a unique controversial example of systems for which almost all the possible perturbative and nonperturbative approaches have been used, sometimes with a very high precision. This allows to draw several conclusions about the relative predictive power of these different methods. Firstly, it appears that the *low-order* results obtained within the $NL\sigma$ or GLW models fail to correctly describe the physics in three dimensions. Indeed, we recall that the one-loop result of

the $NL\sigma$ model predicts a second order phase transition with a $O(4)$ behavior while the GLW approach leads to first order phase transitions for all values of N smaller than 21.8. Secondly, frustrated magnets probably provides the first example where high-order perturbative results is questionable. We shall now discuss the status of the various perturbative approaches at the light of our results.

A. The $NL\sigma$ model approach

Let us first consider the $NL\sigma$ model approach, focusing on the Heisenberg case since it is notorious that this approach does not work for XY spins. The very likely existence of a line $N_c(d)$ going from $d = 2$ to $d = 4$ confirms what has been already anticipated in Section V: the predictions based on this approach are incorrect as for the physics in $d = 3$. Indeed, the shape of this line implies that the $O(4)$ fixed point predicted in the Heisenberg case — that likely exists at all orders of perturbation theory — very probably disappears between two and three dimensions. Actually, following this fixed point, that we call C_+ for an obvious reason, from $d = 2$ with the simplest ϕ^4 -like truncation, we have found several interesting features. First, infinitesimally close to $d = 2$, we find that C_+ is characterized by an exponent ν of the $O(4)$ universality class. Second, as d is increased, the exponent ν associated with C_+ becomes more and more different from that characterizing an $O(4)$ transition. Third, we find that an unstable fixed point, C_- , shows up in a dimension $d > 2$. As the dimension is further increased, the fixed points C_+ and C_- get closer together and eventually coalesce in a dimension less than three. This phenomenon is illustrated in Fig (14) in the case of the $O(3) \times O(3)$ model at the lowest order in the field expansion [62].

The collapse of the fixed points for different values of N generates the curve $N_c(d)$. This curves is well known from the perturbative expansion performed around four dimensions. Within our approach, this curve can be followed when the dimension is lowered down to $d = 2$. There, for a given — low — value of N , the curve $N_c(d)$ provides the value of $d_c(N)$ for which the stable fixed point obtained within the $NL\sigma$ model approach collapses with another — unstable — fixed point. Since this unstable fixed point is *not* found in the low-temperature perturbative expansion we therefore obtain here a non-perturbative solution to the breakdown of the $NL\sigma$ model approach. For $N = 3$, one gets $d_c \simeq 2.8$. Note that obtaining an accurate determination of the dimension d_c where the fixed points collapse would require to consider better truncations in fields of Γ_k than those we have considered. However, as already explained in the $O(N)$ case, see Section VID9, the stable fixed point coalesces in this case with one of the multicritical points. Thus it is impossible, within our truncation, to follow it smoothly for $2.1 \lesssim d \lesssim 2.5$. With our best truncation, we are anyway

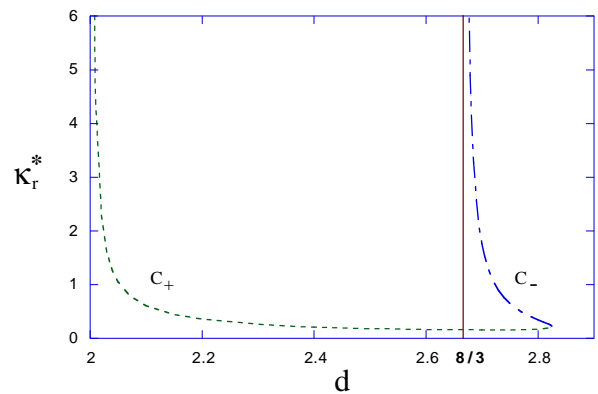


FIG. 14: The stable — C_+ — and unstable — C_- — fixed points as functions of the dimension d . The fixed points are parametrized by the quantity κ_r^* which is proportionnal to the inverse temperature of the $NL\sigma$ model. The fixed point C_- appears in a dimension $8/3$ and collapses with the stable fixed point C_+ in $d \simeq 2.83$.

able to give an estimate of this dimension: $d_c \simeq 2.6 - 2.7$ which fits well with the results of Pelissetto *et al.* [156], see Fig. 9.

Frustrated magnets thus provide a situation where there is a manifest breakdown of the low-temperature expansion of the $NL\sigma$ model. This is not the first occurrence of such a breakdown. The case of the two-component nonfrustrated $O(2)$ system has already exemplified the inadequacy of the low-temperature expansion to explain the existence of a phase transition for these systems in two dimensions, the Berezinskii-Kosterlitz-Thouless phase transition [52, 53]. There is however an important difference between the case of XY nonfrustrated spins and that of Heisenberg frustrated spins. Indeed, in the former case, the low-temperature expansion performed on the corresponding $O(2)$ $NL\sigma$ model leads to a free theory to all orders in the temperature T in $d \geq 2$. This result is however known to be incorrect for XY spins themselves or for the systems that belong to the same universality class — like ^4He — that both undergo a phase transition in $d \geq 2$. In this case, the inability of the low-temperature expansion to correctly describe the physics makes no doubt and one is invited to turn to other methods: Coulomb-gas [191] or spin-vortices [52, 53] formulations in two dimensions or GLW model approach in three dimensions. On the contrary, in the case of Heisenberg frustrated spins, the low-temperature expansion leads to a nontrivial behavior — due to the nonabelian character of the $SO(3)$ group — so that the inadequacy of the low-temperature perturbation theory is not so obvious.

It remains to understand the very origin of this failure of the low-temperature perturbation theory. In the case of XY nonfrustrated spins, it clearly lies in the existence of nontrivial topological configurations, called vortices, that are not taken into account in a low-temperature ex-

pansion. In the case of Heisenberg frustrated magnets, the influence of nontrivial topological configurations on the phase transition in three dimensions has also been invoked (see Section V-A). It remains however to confirm that these configurations indeed play a fundamental role and to know, for instance, if they are responsible for the first order character of the transitions in three dimensions.

This is a delicate question. Indeed, whereas the perturbative approach to the $NL\sigma$ model misses topologically nontrivial configurations, the GLW and effective average action approaches are very likely sensitive to such vortices. In effect, both approaches correctly reproduce the physics of three-dimensional XY nonfrustrated spin systems at the transition which is very likely driven by vortices [197, 198]. However, within these approaches, it is still not clear how the vortices are taken into account. Therefore, disentangling vortices and spin-waves and understanding the respective role of each kind of excitation within the phase transition remains a theoretical challenge.

B. The GLW model approach vs the NPRG approach

We now discuss the relationship between the weak-coupling results obtained within the GLW model approach — in particular, the six-loop computation — and our results. A natural question arises: how is it possible to reconcile these results together and what does this imply for the different approaches?

We have noted an important fact: the critical exponents found for $N = 3$ in the six-loop calculation and in our approach — at the minimum of the flow — are very close (see Sections IX B and IX D). We have also found very close exponents for $N = 2$ (see Section IX D) with the only difference that there is no minimum in the flow in this case. This is a rather strong indication that the two sets of exponents have a common origin. This leads us to formulate some proposals to reconcile the two approaches.

The first one is that the fixed point that appears as real in the six-loop calculation and complex in our approach is, actually, a complex one. This would mean that the computations of Pelissetto *et al.* and Calabrese *et al.* is, actually, not converged as for the nature — real or complex — of this fixed point whereas it is almost converged as for the exponents. We shall not speculate too much about the origin of this — hypothetical — failure of the weak-coupling approach. Let us mention again however that the perturbative series obtained in the case of frustrated magnets appear to be rather particular since the critical properties deduced from them strongly depend on the order of the series. We recall that there is no nontrivial fixed point for $N = 2$ and $N = 3$ up to three loops; they only appear at five loops. Also, the six-loop results has been obtained in a region where the pertur-

bative expansions are *not* Borel summable [155]. It is clear that this question deserves further investigations. Frustrated magnets could appear as the first example of a breakdown of a weak-coupling perturbative analysis.

The second proposal is that, reciprocally, within the NPRG method, the lack of fixed point in the XY and Heisenberg cases is due to artefacts of the truncation in fields and/or derivatives. Only the recourse to other kinds of expansions of the effective action Γ_k — involving either the *full* function $U_k(\rho, \tau)$ or the *full* momentum dependence — could lead to unambiguous statements. In this respect, we however recall that the LPA approach of Zumbach, that involves the full field-dependence of the potential, has led to no fixed point for $N = 2$ and $N = 3$.

XII. CONCLUSION AND PROSPECTS

On the basis of their specific symmetry breaking scheme, it has been proposed [67, 68, 70, 122, 123, 130] that the critical physics of XY and Heisenberg frustrated systems in three dimensions could be characterized by critical exponents associated with a *new* universality class. From this point of view, the study of frustrated magnets has been rather disappointing, the experimental and numerical contexts excluding such an hypothesis. At the same time, the phenomenology of frustrated magnets has displayed a novel kind of critical behavior — *generic* scaling *without* universality [118] — requiring the use of new theoretical approaches.

High-order perturbative calculations in $d = 3$ [131, 132, 155] provide an explanation to the lack of universality in frustrated magnets: the focus character of the fixed point induces spiral-like RG trajectories from which, according to Calabrese *et al.* [132], follows varying effective critical exponents [131, 132]. We have, however, underlined several drawbacks of this explanation. The major one lies in its lack of naturalness: a fine-tuning of initial conditions seems to be necessary to match with the phenomenology. Another drawback of the perturbative approach is that, being restricted to investigate the physics in three dimensions, it cannot provide a general picture of what happens between two and four dimensions. In particular it provides no explanation to the failure of the $NL\sigma$ model approach.

Within the framework of a NPRG approach, the generic and nonuniversal scaling finds a natural explanation in terms of the slowness and “geometry” of the flow. This method also explains the mismatch between the different perturbative approaches by means of a mechanism of annihilation of fixed points in a dimension between two and three that invalidates the low-temperature perturbative approach performed from the $NL\sigma$ model. As said along this article, more work, in particular the recourse to ansatz involving the full field-dependence or full momentum dependence of the effective action, is probably necessary to completely understand the situation. This includes the clarification of the relation between our ap-

proach and the six-loop results. However, the main features of frustrated magnets appear now to be well described.

The main result of this article is the explanation of the *generic* character of weak first order phase transitions in frustrated magnets. Being given the closeness between these systems and others systems — see the Introduction — it is natural to speculate about the degree of generality of this phenomenon.

Within our approach, the generic character of the weak first order phase transition appear to be strongly related to the proximity of the number of components N of the system under study with $N_c(d = 3)$. For frustrated systems, it appears that this value is of the same order than the physically relevant values of N , $N = 2$ and $N = 3$. This could be a very specific property of the frustrated systems. We now argue that, on the contrary, this property is likely to be common to many other systems.

Let us recall that the line $N_c(d)$ corresponds to the collapse of two fixed points, one of them governing the phase transition. This phenomenon cannot happen in theories with only one ϕ^4 coupling constant (*i.e.* in $O(N)$ models) since, in this case, there is only one fixed point apart from the gaussian. However, for theories with c coupling constants, we expect 2^c perturbative — real or complex — fixed points in $d = 4 - \epsilon$ since, at one-loop, the β -functions are quadratic in the coupling constants. When the number of components of the field is varied, these fixed points move in the coupling constant space and it is generically observed that they meet and collapse for some critical value $N_c(d)$. Many examples are now known in the literature. Let us review some of them.

Let us first consider the generalization of the model studied in this article consisting in P orthonormal N -component vectors. It has a P -dependent critical value of N given at one-loop by [65]: $N_c \sim 10P$. For $P = 3$, one finds at two loop order [156]:

$$N_c(4 - \epsilon) = 32.49 - 33.72\epsilon. \quad (160)$$

In the Abelian Higgs model coupled to a N -component scalar field, relevant to superconductors, $N_c(d)$ is found at two-loop order to be [5, 199, 200]:

$$N_c(d = 4 - \epsilon) = 182.9 - 242.7\epsilon. \quad (161)$$

In a $SU(2)$ gauge model coupled to bosons, it is given at two loop order by [200]:

$$N_c(d = 4 - \epsilon) = 718 - 990.8\epsilon. \quad (162)$$

In a $O(p)$ gauge theory coupled to N scalar fields (in the vector representation) it is given at one-loop by [201]: $N_c \sim 40p$.

In all these examples, we observe that $N_c(d)$ decreases very steeply when d decreases. This is in line with our expectation that large N and small d favour continuous phase transitions. In particular, as far as we know, in all $NL\sigma$ models relevant to systems whose order parameter is

continuous, a stable fixed point is found in $d = 2 + \epsilon$ for all $N > 2$. This is in particular the case for the $NL\sigma$ model supposed to describe the physics of the abelian Higgs model in $d = 2$ [11, 202]. This suggests that $N_c(d = 2)$ is always smaller or equal to 2. It is interesting to notice that this bound is probably reached in frustrated systems [156], see Section VB3. It is thus extremely probable that in many systems the curve $N_c(d)$ has a similar shape as the one found in frustrated systems, see Fig. 9. This suggests that many systems could exhibit weakly first order transitions in $d = 3$ *without any fine-tuning of parameters* [214]. The effective average action method should be ideally suited to study these situations.

Acknowledgments

We thank D. Loison for useful remarks and J. Vidal for a careful reading of manuscript and helpful remarks.

APPENDIX A: THE POSITIVITY OF THE ANOMALOUS DIMENSION

In this appendix, we sketch the proof showing that the anomalous dimension η must be positive in a second order phase transition if the underlying theory is given by a usual ϕ^4 -like GLW theory. This excludes, for instance, theories involving gauge fields or replica field theories of disordered systems using the formal $N \rightarrow 0$ limit. The argument goes as follows. On one hand, using the Källén-Lhemann decomposition, it is possible to prove that the field renormalization Z is positive and less or equal to one: $0 \leq Z \leq 1$ [119]. On the other hand, using the RG equations, it is possible to show that, around the fixed point describing the second order phase transition, Z behaves with the RG scale μ as:

$$Z(\mu) \sim \mu^\eta \quad (A1)$$

when $\mu \rightarrow 0$, which corresponds to the long distance — *i.e.* critical — physics. By combining these two results we find $\eta \geq 0$.

APPENDIX B: THE INVARIANTS OF THE SYMMETRY GROUP

We show, in this appendix, that all field combinations invariant under $O(N) \times O(2)$ can be rewritten in terms of the two invariants ρ and τ introduced in Eq.(52) and given by $\rho = \text{Tr}({}^t\Phi\Phi)$ and $\tau = \frac{1}{2}\text{Tr}({}^t\Phi\Phi - \mathbb{1}\rho/2)^2$. This property is *a priori* nontrivial since we can easily build an infinite number of invariants by considering, for instance, $\text{Tr}({}^t\Phi\Phi)^n$ for any value of n or $\det({}^t\Phi\Phi)$. The result is easily obtained by using the properties of the characteristic polynomial of the square matrix X :

$$P_X(\lambda) = \det(X - \lambda\mathbb{1}). \quad (B1)$$

In the case of a two by two matrix, the characteristic polynomial reads:

$$P_X(\lambda) = \lambda^2 - \lambda \text{Tr}X + \det X . \quad (\text{B2})$$

The Cayley-Hamilton theorem states that any matrix is a root of its characteristic polynomial:

$$P_X(X) = 0 . \quad (\text{B3})$$

Applying this last result to the two by two matrix ${}^t\Phi \cdot \Phi$ we get:

$$({}^t\Phi \cdot \Phi)^2 - {}^t\Phi \cdot \Phi \text{Tr}({}^t\Phi \cdot \Phi) + \det({}^t\Phi \cdot \Phi) = 0 . \quad (\text{B4})$$

By taking the trace of this equation, we see that $\det({}^t\Phi \cdot \Phi) = \rho^2/4 - \tau$. Moreover, if we multiply Eq. (B4) by ${}^t\Phi \cdot \Phi$ and take the trace of this equation, we observe that $\text{Tr}({}^t\Phi \cdot \Phi)^3$ can be expressed in terms of $\text{Tr}({}^t\Phi \cdot \Phi)^2$, $\text{Tr}({}^t\Phi \cdot \Phi)$ and $\det({}^t\Phi \cdot \Phi)$ which, themselves, can be expressed in terms of ρ and τ . By iteration, we can show that all $O(N) \times O(2)$ invariants can be expressed in terms of ρ and τ . This property can be generalized to the $O(N) \times O(P)$ model (with $N \geq P$), which admits P independent invariants.

APPENDIX C: THE THRESHOLD FUNCTIONS

We discuss in this appendix the different threshold functions l , m and n appearing in the flow equations, which encode the nonperturbative properties of the theory. We consider here a general case, where the threshold functions depend on three arguments. For particular truncations — for instance that discussed in the $O(N)$ vectorial model — it may happen that some of these arguments are vanishing. In such case, we do not write the associated argument so that, for instance, $l_{n,0}^d(w, 0, 0)$ is denoted by $l_n^d(w)$

1. Definitions

The threshold functions are defined as:

$$l_{n_1, n_2}^d(w_1, w_2, a) = -\frac{1}{2} \int_0^\infty dy y^{d/2-1} \tilde{\partial}_t \left\{ \frac{1}{(P_1 + w_1)^{n_1} (P_2 + w_2)^{n_2}} \right\}, \quad (\text{C1a})$$

$$m_{n_1, n_2}^d(w_1, w_2, a) =$$

$$-\frac{1}{2} \int_0^\infty dy y^{d/2-1} \tilde{\partial}_t \left\{ \frac{y(\partial_y P_1)^2}{(P_1 + w_1)^{n_1} (P_2 + w_2)^{n_2}} \right\}, \quad (\text{C1b})$$

$$n_{n_1, n_2}^d(w_1, w_2, a) =$$

$$-\frac{1}{2} \int_0^\infty dy y^{d/2-1} \tilde{\partial}_t \left\{ \frac{y \partial_y P_1}{(P_1 + w_1)^{n_1} (P_2 + w_2)^{n_2}} \right\}, \quad (\text{C1c})$$

where we have introduced:

$$\begin{cases} P_1 = P_1(y, a) = y(1 + r(y) + a) \\ P_2 = P_2(y) = y(1 + r(y)) \end{cases} \quad (\text{C2})$$

with $r(y)$ being the dimensionless cut-off:

$$r(y) = \frac{R_k(yk^2)}{Zyk^2}. \quad (\text{C3})$$

We recall that the tilde in $\tilde{\partial}_t$ means that only the t dependence of the function R_k is to be considered. As a consequence, we should not consider the t -dependence of the coupling constants to perform this derivative. Therefore, in the preceding equations:

$$\tilde{\partial}_t P_i = \frac{\partial R_k}{\partial t} \frac{\partial}{\partial R_k} P_i \quad (\text{C4})$$

$$= -y(\eta r(y) + 2yr'(y)). \quad (\text{C5})$$

Now, threshold functions can be expressed as explicit integrals if we compute the action of $\tilde{\partial}_t$. To this end, it is interesting to notice the equality: $\partial_y \tilde{\partial}_t P_i = \tilde{\partial}_t \partial_y P_i$, so that:

$$\tilde{\partial}_t \partial_y r(y) = -\eta(r(y) + yr'(y)) - 2y(2r'(y) + yr''(y)) \quad (\text{C6})$$

We then get:

$$l_{n_1, n_2}^d(w_1, w_2, a) = -\frac{1}{2} \int_0^\infty dy y^{d/2} \frac{\eta r(y) + 2yr'(y)}{(P_1 + w_1)^{n_1} (P_2 + w_2)^{n_2}} \left(\frac{n_1}{P_1 + w_1} + \frac{n_2}{P_2 + w_2} \right) \quad (\text{C7})$$

$$n_{n_1, n_2}^d(w_1, w_2, a) = -\frac{1}{2} \int_0^\infty dy y^{d/2} \frac{1}{(P_1 + w_1)^{n_1} (P_2 + w_2)^{n_2}} \left\{ y(1 + a + r(y) + yr'(y))(\eta r(y) + 2yr'(y)) \cdot \right. \\ \left. \cdot \left(\frac{n_1}{P_1 + w_1} + \frac{n_2}{P_2 + w_2} \right) - \eta(r(y) + yr'(y)) - 2y(2r'(y) + yr''(y)) \right\}, \quad (\text{C8})$$

$$m_{n_1, n_2}^d(w_1, w_2, a) = -\frac{1}{2} \int_0^\infty dy y^{d/2} \frac{1 + a + r(y) + yr'(y)}{(P_1 + w_1)^{n_1} (P_2 + w_2)^{n_2}} \left\{ y(1 + a + r(y) + yr'(y))(\eta r(y) + 2yr'(y)) \cdot \right. \\ \left. \cdot \left(\frac{n_1}{P_1 + w_1} + \frac{n_2}{P_2 + w_2} \right) - 2\eta(r(y) + yr'(y)) - 4y(2r'(y) + yr''(y)) \right\}. \quad (\text{C9})$$

Once a regulator $r(y)$ has been chosen, the threshold functions can be computed numerically and, in some cases, analytically.

2. Substitution rules

We give here the rules which relate the different integrals appearing in the calculation to the threshold func-

tions. When calculating the flow equation for the coupling constants related to the potential part, a single function l appears:

$$\tilde{\partial}_t \int \frac{d^d \mathbf{q}}{(2\pi)^d} (R_k(\mathbf{q}^2) + (Z + A)\mathbf{q}^2 + W_1)^{-n_1} (R_k(\mathbf{q}^2) + Z\mathbf{q}^2 + W_2)^{-n_2} = \\ = -4v_d Z^{-n_1 - n_2} k^{d-2(n_1+n_2)} l_{n_1, n_2}^d \left(\frac{W_1}{Zk^2}, \frac{W_2}{Zk^2}, \frac{A}{Z} \right). \quad (\text{C10})$$

For the coupling constants associated with the derivative terms, two more functions appear:

$$\frac{d}{d\mathbf{p}^2} \tilde{\partial}_t \int \frac{d^d \mathbf{q}}{(2\pi)^d} \mathbf{q}^\alpha (R_k((\mathbf{p} + \mathbf{q})^2) + (Z + A)(\mathbf{p} + \mathbf{q})^2 + W_1)^{-n_1} (R_k(\mathbf{q}^2) + Z\mathbf{q}^2 + W_2)^{-n_2} = \\ = \frac{4v_d n_1}{d} Z^{-n_1 - n_2} k^{d+\alpha-2(n_1+n_2+1)} \left\{ -\alpha n_{n_1+1, n_2}^{d+\alpha-2} \left(\frac{W_1}{Zk^2}, \frac{W_2}{Zk^2}, \frac{A}{Z} \right) + \right. \\ \left. + 2n_2 \left(m_{n_1+1, n_2+1}^{d+\alpha} \left(\frac{W_1}{Zk^2}, \frac{W_2}{Zk^2}, \frac{A}{Z} \right) - \frac{A}{Z} n_{n_1+1, n_2+1}^{d+\alpha} \left(\frac{W_1}{Zk^2}, \frac{W_2}{Zk^2}, \frac{A}{Z} \right) \right) \right\} \quad (\text{C11})$$

$$\begin{aligned} \frac{d}{d\mathbf{p}^2} \tilde{\partial}_t \int \frac{d^d \mathbf{q}}{(2\pi)^d} \mathbf{p} \cdot \mathbf{q} \mathbf{q}^\alpha (R_k((\mathbf{p} + \mathbf{q})^2) + (Z + A)(\mathbf{p} + \mathbf{q})^2 + W_1)^{-n_1} (R_k(\mathbf{q}^2) + Z\mathbf{q}^2 + W_2)^{-n_2} = \\ = \frac{8v_d}{d} n_1 Z^{-n_1 - n_2} k^{d + \alpha - 2(n_1 + n_2)} n_{n_1 + 1, n_2}^{d + \alpha} \left(\frac{W_1}{Zk^2}, \frac{W_2}{Zk^2}, \frac{A}{Z} \right). \end{aligned} \quad (\text{C12})$$

Notice that the powers of k and Z appearing in the preceding expressions are chosen so that when the flow equations are reexpressed in terms of dimensionless renormalized quantities, there is no explicit dependence on these parameters.

3. Universal values of the threshold functions

For particular arguments, the threshold functions take values independent of the choice of the regulating function $r(y)$. This is particularly important when we extract the first coefficients of the perturbative β functions out of the nonperturbative ones, since the former are universal. From Eq. (C7) we can compute the value of $l_{n,0}^{2n}(0, 0, a)$ which enters in the β function for the coupling constant of the GLW model around four dimensions:

$$\begin{aligned} l_{n,0}^{2n}(0, 0, a) &= -n \int_0^\infty dy \frac{r'(y)}{(1 + a + r(y))^{n+1}} \\ &= \left[(1 + a + r(y))^{-n} \right]_0^\infty \\ &= \frac{1}{(1 + a)^n}. \end{aligned} \quad (\text{C13})$$

The last equality follows from the asymptotic behaviors of $r(y)$ that are given by Eqs. (81) and (82):

$$\begin{cases} \lim_{y \rightarrow \infty} r(y) = 0 \\ \lim_{y \rightarrow 0} y r(y) = 1 \end{cases} \quad (\text{C14})$$

and are independent of the actual form chosen for $r(y)$.

Similarly, one finds:

$$l_{0,n}^{2n}(0, 0, a) = 1. \quad (\text{C15})$$

Also, the threshold function $m_{2,2}^d(w, 0, 0)$ takes a universal form for large argument ω , which enters in the β function of the temperature in the NL σ model around two dimensions. Using Eq. (C7), one gets:

$$\begin{aligned} \lim_{w \rightarrow \infty} w^2 m_{2,2}^d(w, 0, 0) &= \int_0^\infty dy \partial_y \left(\frac{1 + r(y) + yr'(y)}{1 + r(y)} \right)^2 \\ &= 1 \end{aligned} \quad (\text{C16})$$

where, again, we have used the asymptotic behaviors of $r(y)$, Eq. (C14).

4. Threshold functions from the θ cut-off

For certain regulating functions $r(y)$, it is possible to compute analytically the threshold functions. Using such regulating functions is very helpful in practice and simplifies considerably the numerical procedures. In this section, we give the threshold functions associated with the θ cut-off, see Eq. (86). One has, for $a = 0$:

$$\begin{aligned} l_{n_1, n_2}^d(w_1, w_2, 0) &= \frac{2}{d} \left(1 - \frac{\eta}{d+2} \right) \\ &\quad \frac{1}{(1+w_1)^{n_1} (1+w_2)^{n_2}} \left(\frac{n_1}{1+w_1} + \frac{n_2}{1+w_2} \right) \end{aligned} \quad (\text{C17})$$

$$m_{2,2}^d(w_1, w_2, 0) = \frac{1}{(1+w_1)^{n_1} (1+w_2)^{n_2}}. \quad (\text{C18})$$

APPENDIX D: THE MINIMUM OF THE RG FLOW

In this appendix, we describe in more details the notions of pseudo-fixed point and of minimum of the flow. We then explain how these ideas have been implemented in practice to determine effective exponents for very weakly first order phase transitions.

As described previously, the RG flow equations for STA with a large number of spin components ($N > N_c(d)$) admit two fixed points. When N is decreased slightly below $N_c(d)$, the two fixed points acquire a small complex part and lose their direct physical relevance. Strictly speaking, there is no more attractor in the real coupling constant space but the flow remains sensitive to the presence of complex fixed points. Zumbach [64, 65, 66] proposed that a particular point, the minimum of the flow, should mimic to some extent the behavior of an attractor. This point is defined as the location, in coupling constant space, where the flow is the slowest and the quantity:

$$A(\{g_i\}) = \frac{1}{2} \sum_i \beta_i^2 \quad (\text{D1})$$

— where β_i are the β -functions for the different coupling constants g_i — is minimum. Let us stress on few properties of the minimum of the flow:

- when a true fixed point exists, $A(\{g_i^*\}) = 0$ and, in this case, the minimum *is* a fixed point.

- When two fixed points annihilate, we are left with a single minimum of the flow sitting right at the position where the fixed points have collapsed.
- For trajectories getting close to the minimum, the RG time spent in its vicinity is large and so is the correlation length.

We therefore see that a minimum shares some features with a true fixed point.

One easily obtains the equation characterizing a minimum:

$$\frac{\partial A}{\partial g_i} = \sum_j M_{i,j} \beta_j = 0 \quad (\text{D2})$$

with

$$M_{i,j} = \frac{\partial \beta_j}{\partial g_i}. \quad (\text{D3})$$

Under the assumption that the minimum of the flow mimics correctly the attractor of the trajectories, it is natural to compute the critical pseudo-critical exponents in the standard way. The anomalous dimension is obtained by evaluating $\eta(\{g_i\})$ at the minimum of the flow and ν by diagonalizing the matrix $M_{i,j}$ at this point. It is important to notice that the pseudo-critical exponents thus obtained are invariant under reparametrization of coupling constants, as it should be, since Eq. (D2) transforms as components of a vector.

APPENDIX E: THE DISCONTINUOUS CHARACTER OF THE PHASE TRANSITION

In this appendix, we discuss in more details the problems that we encounter in our description of the first order phase transition that occurs in frustrated magnets. We also explain the surprising increase of the correlation length observed at small reduced temperatures (see Fig. 13b).

To this end, let us discuss the following toy model of first order phase transition. We consider a scalar \mathbf{Z}_2 -invariant model characterized by one field ϕ and by a “ $\phi^4 - \phi^6$ ” potential:

$$U(\phi) = r \frac{\phi^2}{2} - \frac{\phi^4}{2} + \frac{\phi^6}{6}. \quad (\text{E1})$$

As usual, we assume that r varies linearly with the temperature.

For low reduced temperatures — small r — the potential has a local minimum for $\phi = 0$ and a global minimum for:

$$(\phi^{\text{Min}}(r))^2 = 1 + \sqrt{1-r} \quad (\text{E2})$$

so that the system exhibits a spontaneous magnetization, see Fig. 15. When the temperature — r — is increased, the energy difference between the configurations $\phi = 0$

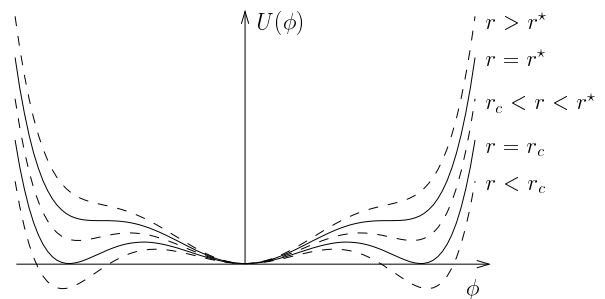


FIG. 15: Shape of the potential Eq. (E1) for different temperatures, *i.e.* different values of the parameter r . The plain lines correspond to $r = r_c$ and $r = r^*$, while the dotted lines correspond to different generic values of r .

and $\phi = \phi^{\text{Min}}(r)$ decreases and eventually vanishes for $r = r_c = 3/4$ which defines the critical temperature. For r larger than r_c , the ground state of the system is given by the configuration $\phi = 0$ so that the system has no more spontaneous magnetization. Therefore, when one crosses the critical temperature, one observes a jump of the magnetization from $\phi^{\text{Min}}(r_c)$ to 0, which is the consequence of the competition between two minima of the potential, see Fig. 15.

For $r > r_c$, the field configuration $\phi^{\text{Min}}(r)$ which is no longer the ground state becomes a metastable state. One sees from Eq. (E2) that, for $r > r^* = 1$, this metastable state disappears and we are left with $\phi = 0$ as the only physically relevant state, see Fig. 15. Finally, it must be noted that, for $r = r^*$, the curvature of the potential at the configuration $\phi^{\text{Min}}(r^*)$ vanishes: $U''(\phi^{\text{Min}}(r^*)) = 0$. This means that the susceptibility in the metastable state diverges at $r = r^*$. Similarly, one can show that the correlation length in the metastable state also diverges.

Let us now come back to the NPRG method. In the truncation of the effective average action that we use — an expansion in powers of the fields of the form Eq. (147) — we retain only *local* informations on the potential around its nontrivial minimum — which is equivalent to the configuration $\phi^{\text{Min}}(r)$ discussed above. In particular we do not accurately describe the physics around the zero-field configuration $\vec{\phi}_1 = \vec{\phi}_2 = \vec{0}$. We are thus unable to compare the energies of different local minima and to determine the temperature of transition at which the energies of the two minima are equal. Also, in a small domain of temperatures — equivalent here to $r_c < r < r^*$ — the configuration that we probe corresponds actually to the metastable state and not to the true equilibrium state. However, these phenomena should not induce a large bias in our analysis as long as the transition is *weakly* of first order since, in this case, the temperature range where metastable states exist is very small. This means that the error induced on the determination of the critical temperature is very small too.

Moreover in our study, as in the toy model above, we should observe when r reaches r^* — the temperature at

which the metastable state must disappear — the associated divergence of the correlation length discussed previously. This is precisely what we found in frustrated magnets for small reduced temperature — see Fig. 13b.

Note that this increase of the correlation length as well as the error associated with our determination of the crit-

ical temperature both rely on the truncation that we have considered. These problems can be cured by considering truncations of the form Eq. (145) which retains the full field-dependence of the potential (see for instance [45] for a treatment of a first order phase transition in a NPRG approach).

-
- [1] K. G. Wilson and J. Kogut, Phys. Rep. C **12**, 75 (1974).
 [2] D. J. Amit, J. Phys. A **9**, 1441 (1976).
 [3] R. G. Priest and T. C. Lubensky, Phys. Rev. B **13**, 4159 (1976).
 [4] Y. Holovatch, V. Blavats'ka, M. Dudka, C. V. Ferber, R. Folk, and T. Yavors'kii, Int. J. Mod. Phys. B **16**, 4027 (2002).
 [5] T. C. Lubensky, B. I. Halperin, and S. K. Ma, Phys. Rev. Lett. **32**, 292 (1974).
 [6] C. Dasgupta and B. I. Halperin, Phys. Rev. Lett. **47**, 1556 (1981).
 [7] S. Teitel and C. Jayaprakash, Phys. Rev. B **27**, 598 (1983).
 [8] D. R. T. Jones, A. Love, and M. A. Moore, J. Phys. C: Solid St. Phys. **9**, 743 (1976).
 [9] D. Bailin, A. Love, and M. A. Moore, J. Phys. C: Solid State Phys. **10**, 1159 (1977).
 [10] B. I. Halperin and T. C. Lubenski, Solid State Commun. **14**, 997 (1974).
 [11] I. D. Lawrie and C. Athorne, J. Phys. A **16**, L587 (1983).
 [12] J. March-Russel, Phys. Lett. B **296**, 364 (1992).
 [13] H. T. Diep, ed., *Magnetic systems with competing interactions* (World Scientific, 1994).
 [14] C. Itzykson and J. Drouffe, *Statistical Field Theory* (Cambridge University Press, Cambridge, England, 1989).
 [15] H. Kleinert, Phys. Lett. A **264**, 357 (2000).
 [16] A. J. Bray, T. McCarthy, M. A. Moore, J. D. Reger, and A. P. Young, Phys. Rev. B **36**, 2212 (1987).
 [17] A. J. McKane, Phys. Rev. B **49**, 12003 (1994).
 [18] B. N. Shalaev, S. A. Antonenko, and A. I. Sokolov, Phys. Lett. A **230**, 105 (1997).
 [19] R. Folk, Yu. Holovatch, and T. Yavors'kii, JETP Lett. **69**, 747 (1999).
 [20] G. Alvarez, V. Martin-Mayor, and J. J. Ruiz-Lorenzo, J. Phys. A **33**, 841 (2000).
 [21] J. M. Carmona, A. Pelissetto, and E. Vicari, Phys. Rev. B **61**, 15136 (2000).
 [22] D. Loison, A. I. Sokolov, B. Delamotte, S. A. Antonenko, K. D. Schotte, and H. T. Diep, JETP Lett. **72**, 337 (2000).
 [23] R. Folk, Yu. Holovatch, and T. Yavors'kii, Phys. Rev. B **61**, 15114 (2000).
 [24] A. D. Sokal, Europhys. Lett. **27**, 661 (1994).
 [25] A. D. Sokal, Europhys. Lett. **30**, 123 (1995).
 [26] C. Bagnuls and C. Bervillier, J. Phys. Stud. **1**, 366 (1997).
 [27] A. Pelissetto and E. Vicari, Nucl. Phys. B **519**, 626 (1998).
 [28] A. Pelissetto and E. Vicari, Phys. Rep. **368**, 549 (2002).
 [29] L. P. Kadanoff, Physics **2**, 263 (1966).
 [30] F. J. Wegner and A. Houghton, Phys. Rev. A **8**, 401 (1973).
 [31] J. F. Nicoll, T. S. Chang, and H. E. Stanley, Phys. Lett. A **57**, 7 (1976).
 [32] J. F. Nicoll and T. S. Chang, Phys. Lett. A **62**, 287 (1977).
 [33] A. Hasenfratz and P. Hasenfratz, Nucl. Phys. B [FS] **270**, 687 (1986).
 [34] C. Bagnuls and C. Bervillier, Phys. Rep. **348**, 91 (2001).
 [35] U. Ellwanger and L. Vergara, Nucl. Phys. B **398**, 52 (1993).
 [36] U. Ellwanger, Z. Phys. C **58**, 619 (1993).
 [37] U. Ellwanger, Phys. Lett. B **335**, 364 (1994).
 [38] U. Ellwanger and C. Wetterich, Nucl. Phys. B **423**, 137 (1994).
 [39] U. Ellwanger, Z. Phys. C **62**, 503 (1994).
 [40] T. R. Morris, Int. J. Mod. Phys. A **9**, 2411 (1994).
 [41] T. R. Morris, Phys. Lett. B **329**, 241 (1994).
 [42] C. Wetterich, Nucl. Phys. B **352**, 529 (1991).
 [43] C. Wetterich, Phys. Lett. B **301**, 90 (1993).
 [44] N. Tetradis and C. Wetterich, Nucl. Phys. B [FS] **422**, 541 (1994).
 [45] J. Berges, N. Tetradis, and C. Wetterich, Phys. Rep. **363**, 223 (2002).
 [46] K. I. Aoki, K. Morikawa, W. Souma, J. I. Sumi, and H. Terao, Prog. Theor. Phys. **99**, 451 (1998).
 [47] T. R. Morris, Int. J. Mod. Phys. B **12**, 1343 (1998).
 [48] S. Seide and C. Wetterich, Nucl. Phys. B **562**, 524 (1999).
 [49] L. Canet, B. Delamotte, D. Mouhanna, and J. Vidal, Phys. Rev. D **67**, 065004 (2003).
 [50] L. Canet, B. Delamotte, D. Mouhanna, and J. Vidal, Phys. Rev. B **68**, 064421 (2003).
 [51] C. Wetterich, Z. Phys. C **57**, 451 (1993).
 [52] V. L. Berezinskii, Sov. Phys. JETP **32**, 493 (1970).
 [53] J. M. Kosterlitz and D. J. Thouless, J. Phys. C **6**, 1181 (1973).
 [54] M. Gräter and C. Wetterich, Phys. Rev. Lett. **75**, 378 (1995).
 [55] G. v. Gersdorff and C. Wetterich, Phys. Rev. B **64**, 054513 (2001).
 [56] B. Bergerhoff, F. Freire, D. Litim, S. Lola, and C. Wetterich, Phys. Rev. B **53**, 5734 (1996).
 [57] L. Rosa, P. Vitale, and C. Wetterich, Phys. Rev. Lett. **86**, 958 (2001).
 [58] F. Höfling, C. Nowak, and C. Wetterich, Phys. Rev. B **66**, 205111 (2002).
 [59] M. Kindermann and C. Wetterich, Phys. Rev. Lett. **86**, 1034 (2001).
 [60] M. Tissier, D. Mouhanna, J. Vidal, and B. Delamotte, Phys. Rev. B **65**, 140402 (2002).
 [61] T. R. Morris, Phys. Lett. B **345**, 139 (1995).
 [62] M. Tissier, D. Mouhanna, and B. Delamotte, Phys. Rev. B **61**, 15327 (2000).

- [63] M. Tissier, B. Delamotte, and D. Mouhanna, *Phys. Rev. Lett.* **84**, 5208 (2000).
- [64] G. Zumbach, *Phys. Rev. Lett.* **71**, 2421 (1993).
- [65] G. Zumbach, *Nucl. Phys. B* **413**, 771 (1994).
- [66] G. Zumbach, *Phys. Lett. A* **190**, 225 (1994).
- [67] T. Garel and P. Pfeuty, *J. Phys. C: Solid St. Phys.* **9**, L245 (1976).
- [68] M. Yosefin and E. Domany, *Phys. Rev. B* **32**, 1778 (1985).
- [69] T. Dombre and N. Read, *Phys. Rev. B* **38**, 7181 (1988).
- [70] H. Kawamura, *Phys. Rev. B* **38**, 4916 (1988).
- [71] N. D. Mermin, *Rev. Mod. Phys.* **51**, 591 (1979).
- [72] H. Kawamura and S. Miyashita, *J. Phys. Soc. Japan* **53**, 4138 (1984).
- [73] W. Apel, M. Wintel, and H. Everts, *Z. Phys. B* **86**, 139 (1992).
- [74] B. W. Southern and A. P. Young, *Phys. Rev. B* **48**, 13170 (1993).
- [75] M. Wintel, H. U. Everts, and W. Apel, *Europhys. Lett.* **25**, 711 (1994).
- [76] B. W. Southern and H.-J. Xu, *Phys. Rev. B* **52**, 3836 (1995).
- [77] W. Stephan and B. W. Southern, *Phys. Rev. B* **61**, 11514 (2000).
- [78] M. Caffarel, P. Azaria, B. Delamotte, and D. Mouhanna, *Phys. Rev. B* **64**, 014412 (2001).
- [79] W. Maier and A. Saupe, *Z. Naturforsch. A* **14**, 882 (1959).
- [80] P. A. Lebwohl and G. Lasher, *Phys. Rev. A* **6**, 426 (1972).
- [81] P. E. Lammert, D. S. Rokhsar, and J. Toner, *Phys. Rev. Lett.* **70**, 1650 (1993).
- [82] P. E. Lammert, D. S. Rokhsar, and J. Toner, *Phys. Rev. E* **52**, 1778 (1995).
- [83] G. Kohring and R. E. Shrock, *Nucl. Phys. B* **285**, 504 (1987).
- [84] J. Villain, *J. Phys. C: Solid St. Phys.* **10**, 4793 (1977).
- [85] S. Miyashita and H. Shiba, *J. Phys. Soc. Japan* **53**, 1145 (1985).
- [86] V. P. Plakhty, J. Kulda, D. Visser, E. V. Moskvina, and J. Wosnitza, *Phys. Rev. Lett.* **85**, 3942 (2000).
- [87] G. C. DeFotis and S. A. Pugh, *Phys. Rev. B* **24**, 6497 (1981).
- [88] H. W. Blöte, E. Luijten, and J. R. Heringa, *J. Phys. A: Math. Gen.* **28**, 6289 (1995).
- [89] M. F. Collins and O. A. Petrenko, *Can. J. Phys.* **75**, 605 (1997).
- [90] H. B. Weber, T. Werner, J. Wosnitza, H. v. Löhneysen, and U. Schotte, *Phys. Rev. B* **54**, 15924 (1996).
- [91] B. D. Gaulin, T. E. Mason, M. F. Collins, and J. Z. Larese, *Phys. Rev. Lett.* **62**, 1380 (1989).
- [92] T. E. Mason, B. D. Gaulin, and M. F. Collins, *Phys. Rev. B* **39**, 586 (1989).
- [93] Y. Ajiro, T. Nakashima, Y. Unno, H. Kadowaki, M. Mekata, and N. Achiwa, *J. Phys. Soc. Japan* **57**, 2648 (1988).
- [94] T. E. Mason, M. F. Collins, and B. D. Gaulin, *J. Phys. C: Solid St. Phys.* **20**, L945 (1987).
- [95] J. Wang, D. P. Belanger, and B. D. Gaulin, *Phys. Rev. Lett.* **66**, 3195 (1991).
- [96] R. Deutschmann, H. von Löhneysen, J. Wosnitza, R. K. Kremer, and D. Visser, *Europhys. Lett.* **17**, 637 (1992).
- [97] H. Kadowaki, S. M. Shapiro, T. Inami, and Y. Ajiro, *J. Phys. Soc. Japan* **57**, 2640 (1988).
- [98] H. Weber, D. Beckmann, J. Wosnitza, H. von Löhneysen, and D. Visser, *Int. J. Mod. Phys. B* **9**, 1387 (1995).
- [99] M. Enderle, G. Fortuna, and M. Steiner, *J. Phys.: Condens. Matter* **6**, L385 (1994).
- [100] M. Enderle, R. Schneider, Y. Matsuoaka, and K. Kakurai, *Physica B* **234-236**, 554 (1997).
- [101] U. Schotte, N. Stusser, K. D. Schotte, H. Weinfurter, H. M. Mayer, and M. Winkelmann, *J. Phys.: Condens. Matter* **6**, 10105 (1994).
- [102] K. D. Jayasuriya, A. M. Stewart, S. J. Campbell, and E. S. R. Gopal, *J. Phys. F* **14**, 1725 (1984).
- [103] C. C. Tang, P. W. Haycock, W. G. Stirling, C. C. Wilson, D. Keen, and D. Fort, *Physica B* **205**, 105 (1995).
- [104] C. C. Tang, W. G. Stirling, D. L. Jones, C. C. Wilson, P. W. Haycock, A. J. Rollason, A. H. Thomas, and D. Fort, *J. Magn. Magn. Mater.* **103**, 86 (1992).
- [105] K. Hirota, Y. Nakazawa, and M. Ishikawa, *J. Phys.: Condens. Matter* **3**, 4721 (1991).
- [106] D. A. Tindall, M. O. Steinitz, and M. L. Plumer, *J. Phys. F* **7** (1977).
- [107] K. D. Jayasuriya, S. J. Campbell, and A. M. Stewart, *J. Phys. F: Met. Phys.* **15**, 225 (1985).
- [108] T. R. Thurston, G. Helgesen, J. P. Hill, D. Gibbs, B. D. Gaulin, and P. J. Simpson, *Phys. Rev. B* **49**, 15730 (1994).
- [109] G. H. F. Brits and P. de V. du Plessis, *J. Phys. F* **18**, 2659 (1988).
- [110] P. de V. Du Plessis, A. M. Venter, and G. H. F. Brits, *J. Phys.: Condens. Matter* **7**, 9863 (1995).
- [111] J. Eckert and G. Shirane, *Solid State Commun.* **19**, 911 (1976).
- [112] G. Helgesen, J. P. Hill, T. R. Thurston, D. Gibbs, J. Kwo, and M. Hong, *Phys. Rev. B* **50**, 2990 (1994).
- [113] B. D. Gaulin, M. Hagen, and H. R. Child, *J. Phys. (Paris) Colloq.* **49**, C8 (1988).
- [114] V. P. Plakhty, W. Schweika, T. Brückel, J. Kulda, S. V. Gavrilov, L.-P. Regnault, and D. Visser, *Phys. Rev. B* **64**, 100402 (2001).
- [115] E. Loh, C. L. Chien, and J. C. Walker, *Phys. Lett. A* **49**, 357 (1974).
- [116] P. de V. Du Plessis, C. F. van Doorn, and D. C. van Delden, *J. Magn. Magn. Mater.* **40**, 91 (1983).
- [117] K. D. Jayasuriya, S. J. Campbell, and A. M. Stewart, *Phys. Rev. B* **31**, 6032 (1985).
- [118] M. Tissier, B. Delamotte, and D. Mouhanna, *Phys. Rev. B* **67**, 134422 (2003).
- [119] J. Zinn-Justin, *Quantum Field Theory and Critical Phenomena* (Oxford University Press, New York, 1989), pp. 151, 578, 3rd ed.
- [120] H. Kawamura, *J. Phys. Soc. Japan* **61**, 1299 (1992).
- [121] H. Kawamura, *J. Phys. Soc. Japan* **58**, 584 (1989).
- [122] H. Kawamura, *J. Phys. Soc. Japan* **56**, 474 (1987).
- [123] H. Kawamura, *J. Phys. Soc. Japan* **55**, 2095 (1986).
- [124] M. L. Plumer and A. Mailhot, *Phys. Rev. B* **50**, 16113 (1994).
- [125] E. H. Boubcheur, D. Loison, and H. T. Diep, *Phys. Rev. B* **54**, 4165 (1996).
- [126] M. Itakura, *J. Phys. Soc. Jap.* **72**, 74 (2003).
- [127] D. Loison and K. D. Schotte, *Euro. Phys. J. B* **5**, 735 (1998).
- [128] H. Kunz and G. Zumbach, *J. Phys. A: Math. Gen.* **26**, 3121 (1993).
- [129] H. Diep, *Phys. Rev. B* **39**, 397 (1989).

- [130] H. Kawamura, J. Phys. Soc. Japan **54**, 3220 (1985).
- [131] P. Calabrese, P. Parruccini, and A. I. Sokolov, Phys. Rev. B **66**, 180403 (2002).
- [132] P. Calabrese, P. Parruccini, and A. I. Sokolov, cond-mat/0304154 .
- [133] H. Kadowaki, K. Ubukoshi, K. Hirakawa, J. L. Martinez, and G. Shirane, J. Phys. Soc. Japan **56**, 4027 (1987).
- [134] J. Wosnitzer, R. Deutschmann, H. von Löhneysen, and R. K. Kremer, J. Phys.: Condens. Matter **6**, 8045 (1994).
- [135] K. Koyama and M. Matsuura, J. Phys. Soc. Japan **54**, 4085 (1985).
- [136] G. C. DeFotis, S. A. Palacio, and R. L. Carlin, Physica B+C **95**, 380 (1978).
- [137] G. C. DeFotis and J. R. Laughlin, J. Magn. Magn. Mater. **54-57**, 713 (1986).
- [138] G. C. DeFotis, M. L. Laccheo, and H. A. Katori, Phys. Rev. B **65**, 94403 (2002).
- [139] D. Beckmann, J. Wosnitzer, H. v. Löhneysen, and D. Visser, Phys. Rev. Lett. **71**, 2829 (1993).
- [140] R. Bügel, J. Wosnitzer, H. v. Löhneysen, T. Ono, and H. Tanaka, Phys. Rev. B **64**, 094406 (2001).
- [141] T. Ono, H. Tanaka, T. Kato, K. Iio, K. Nakajima, and K. Kakurai, J. Magn. Magn. Mater. **177-181**, 735 (1998).
- [142] T. Ono, H. Tanaka, T. Kato, K. Nakajima, and K. Kakurai, J. Phys.: Condens. Matter **11**, 4427 (1999).
- [143] A. Mailhot, M. L. Plumer, and A. Caillé, Phys. Rev. B **50**, 6854 (1994).
- [144] T. Bhattacharya, A. Billoire, R. Lacaze, and T. Jolicœur, J. Phys. I (Paris) **4**, 181 (1994).
- [145] D. Loison and H. T. Diep, Phys. Rev. B **50**, 16453 (1994).
- [146] A. Peles and B. W. Southern, Phys. Rev. B **67**, 184407 (2003).
- [147] D. Loison and K. D. Schotte, Euro. Phys. J. B **14**, 125 (2000).
- [148] D. Loison, Physica A **275**, 207 (1999).
- [149] P. Bak, S. Krinsky, and D. Mukamel, Phys. Rev. Lett. **36**, 52 (1976).
- [150] Z. Barak and M. B. Walker, Phys. Rev. B **25**, 1969 (1982).
- [151] P. Azaria, B. Delamotte, and T. Jolicœur, Phys. Rev. Lett. **64**, 3175 (1990).
- [152] S. A. Antonenko and A. I. Sokolov, Phys. Rev. B **49**, 15901 (1994).
- [153] S. A. Antonenko, A. I. Sokolov, and V. B. Varnashev, Phys. Lett. A **208**, 161 (1995).
- [154] T. Jolicœur and F. David, Phys. Rev. Lett. **76**, 3148 (1996).
- [155] A. Pelissetto, P. Rossi, and E. Vicari, Phys. Rev. B **63**, 140414 (2001).
- [156] A. Pelissetto, P. Rossi, and E. Vicari, Nucl. Phys. B [FS] **607**, 605 (2001).
- [157] B. Delamotte, D. Mouhanna, and M. Tissier, cond-mat/ (2003).
- [158] P. Parruccini, cond-mat/0305287 .
- [159] P. Calabrese and P. Parruccini, cond-mat/0308037 .
- [160] D. H. Friedan, Ann. Phys. (N.Y.) **163**, 318 (1985).
- [161] P. Azaria, B. Delamotte, F. Delduc, and T. Jolicœur, Nucl. Phys. B [FS] **408**, 485 (1993).
- [162] J. Zinn-Justin, *Quantum Field Theory and Critical Phenomena* (Oxford University Press, New York, 1989), 3rd ed.
- [163] C. Wetterich, Z. Phys. C **60**, 461 (1993).
- [164] D.-U. Jungnickel and C. Wetterich, *Flow equations for phase transitions in statistical physics and QCD* (in: A. Krasnitz, R. Potting, P. Sa and Y.A. Kubishin (Eds.), The Exact Renormalization Group, World Scientific, Singapore, 1999), p. 41.
- [165] L. P. Kadanoff, W. Götze, D. Hamblen, R. Hecht, E. A. S. Lewis, V. V. Palciauskas, M. Rayl, J. Swift, D. Aspnes, and J. Kane, Rev. Mod. Phys. **39**, 395 (1967).
- [166] J. Polchinski, Nucl. Phys. B **231**, 269 (1984).
- [167] R. D. Ball and R. S. Thorne, Ann. Phys. (N.Y.) **236**, 117 (1994).
- [168] G. R. Golner, Phys. Rev. B **33**, 7863 (1986).
- [169] H. Gies and C. Wetterich, Phys. Rev. D **65**, 065001 (2002).
- [170] J. F. Nicoll, T. S. Chang, and H. E. Stanley, Phys. Rev. Lett. **33**, 540 (1974), err. ibid **33** 1525 (1974).
- [171] G. Felder, Commun. Math. Phys. **111**, 101 (1987).
- [172] G. Zumbach, Nucl. Phys. B **413**, 754 (1994).
- [173] R. D. Ball, P. E. Haagensen, J. I. Latorre, and E. Moreno, Phys. Lett. B **347**, 80 (1995).
- [174] J. Comellas, Nucl. Phys. B **509**, 662 (1998).
- [175] D. F. Litim, Nucl. Phys. B **631**, 128 (2002).
- [176] M. Bonini, M. D'Attanasio, and G. Marchesini, Nucl. Phys. B **409**, 441 (1993).
- [177] T. R. Morris and J. F. Tighe, JHEP **08**, 007 (1999).
- [178] K. I. Aoki, A. Horikoshi, M. Taniguchi, and H. Terao, Prog. Theor. Phys. **108**, 571 (2002).
- [179] U. Ellwanger, M. Hirsch, and A. Weber, Eur. Phys. J. p. 563 (1998).
- [180] T. R. Morris, Prog. Theor. Phys. Suppl. **131**, 395 (1998).
- [181] D. Litim, Phys. Lett. B **486**, 92 (2000).
- [182] D. Litim, Phys. Rev. D **64**, 105007 (2001).
- [183] D. Litim, Int. J. Mod. Phys. p. 2081 (2001).
- [184] D. Litim, JHEP **0111**, 059 (2001).
- [185] D. Litim, hep-th/0208117 .
- [186] T. R. Morris, Phys. Lett. B **334**, 355 (1994).
- [187] K. I. Aoki, K. Morikawa, W. Souma, J. I. Sumi, and H. Terao, Prog. Theor. Phys. **95**, 409 (1996).
- [188] T. R. Morris and M. D. Turner, Nucl. Phys. B **509**, 637 (1998).
- [189] R. Guida and J. Zinn-Justin, J. Phys. A **31**, 8103 (1998).
- [190] J. M. Kosterlitz, J. Phys. C **7**, 1046 (1974).
- [191] J. Villain, J. Physique (Paris) **36**, 581 (1975).
- [192] A. B. Zamolodchikov, Yad. Fiz. **44**, 821 (1986).
- [193] G. Pruessner and B. Delamotte, unpublished .
- [194] A. Parola and L. Reatto, Phys. Rev. A **31**, 3309 (1985).
- [195] A. Parola and L. Reatto, Adv. Phys. **44**, 211 (1995).
- [196] T. R. Thurston, G. Helgesen, D. Gibbs, J. P. Hill, B. D. Gaulin, and G. Shirane, Phys. Rev. Lett. **70**, 3151 (1993).
- [197] B. I. Halperin, *Physics of defects* (Les Houches XXXV NATO ASI, Eds. Balian, Kleman and Poirier, North Holland, 1981).
- [198] N. D. Antunes, L. M. A. Bettencourt, and A. Yates, Phys. Rev. D **64**, 065020 (2001).
- [199] I. D. Lawrie, Nucl. Phys. B [FS] **200**, 1 (1982).
- [200] P. Arnold and L. G. Yaffe, Phys. Rev. D **49**, 3003 (1994), err. ibid **55** 1114 (1997).
- [201] P. Ginsparg, Nucl. Phys. B [FS] **170**, 388 (1980).
- [202] S. Hikami, Prog. Theor. Phys. **60**, 226 (1979).

- [203] J. T. Chayes, L. Chayes, D. S. Fisher, and T. Spencer, Phys. Rev. Lett. **57**, 2999 (1986).
- [204] A. Aharony, A. B. Harris, and S. Wiseman, Phys. Rev. Lett. **81**, 252 (1998).
- [205] K. E. Newman, E. K. Riedel, and S. Muto, Phys. Rev. B **29**, 302 (1984).
- [206] This behavior is observed for theories with continuous order parameters. For the Potts model, the situation is different since large numbers of states favor first order phase transitions.
- [207] The symmetry of the full Hamiltonian H is the space group of the triangular lattice. However, as we are most of the time interested in Hamiltonian densities — for instance when the continuum limit has been taken —, the relevant symmetry is C_{3v} .
- [208] Let us emphasize that for other realizations of the Ising universality class, such as demixion or liquid-vapor phase transitions, where the scaling domains extend on three to four decades of reduced temperature, the corrections to scaling are indeed necessary to fit the data on the whole range of temperature. The problem comes from the region of high reduced temperature.
- [209] The values of γ and ν found in $\text{CsMn}(\text{Br}_{0.19}\text{I}_{0.81})_3$ are very small compared with all known values in spin systems as well as what is expected from scaling relations and from numerical simulations (see Table V). The authors of [141] argue that the randomness of the magnetic anisotropy and of the exchange interaction in the c-plane existing in their sample is responsible for these small values. Although it is very difficult up to now to have definitive statements about disordered systems, it seems probable for both randomly diluted systems and systems with random fields that ν obeys the constraint $\nu > 2/d$ where d is the space dimension, see [203, 204] and references therein. Thus, it is far from being straightforward that disorder is responsible for the smallness of ν .
- [210] This result would be almost unchanged if the numerical error bar — and especially the one quoted in [143] — was largely underestimated since it would surely be much less than the theoretical one.
- [211] From the relation $\int d^d \mathbf{y} A(\mathbf{x}, \mathbf{y}) A^{-1}(\mathbf{y}, \mathbf{z}) = \delta(\mathbf{x} - \mathbf{z})$, we deduce the relation in the reciprocal space: $\int d^d \mathbf{p}' A(\mathbf{p}, \mathbf{p}') A^{-1}(-\mathbf{p}', \mathbf{p}'') = (2\pi)^{2d} \delta(\mathbf{p} + \mathbf{p}'')$. With this definition, if $A(\mathbf{x}, \mathbf{y}) = \tilde{A}(\mathbf{x} - \mathbf{y})$, then $A(\mathbf{p}, \mathbf{q}) = (2\pi)^d \delta(\mathbf{p} + \mathbf{q}) \tilde{A}(\mathbf{q})$, where $\tilde{A}(\mathbf{q})$ is the Fourier transform of $\tilde{A}(\mathbf{x})$. Moreover, $A^{-1}(\mathbf{p}, \mathbf{q}) = (2\pi)^d \delta(\mathbf{p} + \mathbf{q}) / \tilde{A}(\mathbf{q})$.
- [212] Note that our factors $(2\pi)^d$ in Eqs. (99) and (100) are unusual. They come from our definition of the Fourier transform: $A(x) = \int \frac{d^d q}{(2\pi)^d} \tilde{A}(q) e^{iqx}$ and from our definition of $\Gamma_k^{(2)}(\mathbf{q}, \mathbf{q}')$ as the second derivative of Γ_k with respect to $\phi(\mathbf{q})$ and not as the Fourier transform of $\Gamma^{(2)}(x, y)$. These factors $(2\pi)^d$ always cancel in the β functions of the coupling constants with the $(2\pi)^d$ coming from their definitions, see for instance Eqs. (111) or (112).
- [213] Let us emphasize that this $O(4)$ fixed point has nothing to do with that of the Heisenberg system around $d = 2$, see Section V A.
- [214] We could also add the q -state Potts model which is known to have $q_c = 4$ in $d = 2$ and probably $2 < q_c < 3$ in $d = 3$. The existence of a critical value of q corresponds also to a collapse of fixed points [205]. Note however that the Potts model has a discrete symmetry and thus cannot be analyzed as the systems with a continuous order parameter for which Mermin-Wagner theorem applies in $d = 2$.